Austrian Journal of Technical and Natural Sciences

№ 5–6 2019
May– June

PREMIER
Publishing

Vienna
2019

Austrian Journal of Technical and Natural Sciences

Scientific journal

№5–6 2019 (May– June)

ISSN 2310-5607

Proofreading Kristin Theissen

Cover design Andreas Vogel

Additional design Stephan Friedman

Editorial office Premier Publishing s.r.o.
Praha 8 – Karlín, Lyčkovo nám. 508/7, PSČ 18600

E-mail: pub@ppublishing.org

Homepage: ppublishing.org

Austrian Journal of Technical and Natural Sciences is an international, German/English/Russian language, peer-reviewed journal. It is published bi-monthly with circulation of 1000 copies.

The decisive criterion for accepting a manuscript for publication is scientific quality. All research articles published in this journal have undergone a rigorous peer review. Based on initial screening by the editors, each paper is anonymized and reviewed by at least two anonymous referees. Recommending the articles for publishing, the reviewers confirm that in their opinion the submitted article contains important or new scientific results.

Premier Publishing s.r.o. is not responsible for the stylistic content of the article. The responsibility for the stylistic content lies on an author of an article.

Instructions for authors

Full instructions for manuscript preparation and submission can be found through the Premier Publishing s.r.o. home page at:
http://ppublishing.org.

Material disclaimer

The opinions expressed in the conference proceedings do not necessarily reflect those of the Premier Publishing s.r.o., the editor, the editorial board, or the organization to which the authors are affiliated.

Premier Publishing s.r.o. is not responsible for the stylistic content of the article. The responsibility for the stylistic content lies on an author of an article.

Included to the open access repositories:

ULRICHSWEB™ GLOBAL SERIALS DIRECTORY

Typeset in Berling by Ziegler Buchdruckerei, Linz, Austria.
Printed by Premier Publishing s.r.o., Vienna, Austria on acid-free paper.

Section 1. Mathematics

Bilan Igor Yuryevich,
Freelancer analyst
E-mail: mathbilan@gmail.com
Bilan Andrey Yuryevich,
Freelancer analyst
E-mail: mathbilan@ukr.net
Zhuk Vladimir Alexandrovich,
Freelancer analyst
E-mail: mathbilanandc@gmail.com

SOME ASPECTS OF NP-COMPLETE TASKS

Abstract. The aim of this paper is to prove the following: if NP is P then we cannot investigate this fact in detail, if NP is not P then also we cannot investigate this fact in detail, if Navier-Stokes equations have solutions then we cannot investigate this fact in detail, if Navier-Stokes equations have not solutions then also we cannot investigate this fact in detail.

Keywords: Goedel, incompleteness, Godel, NP versus P, Navier-Stokes equations.

The idea of proving this and other results, see [1]. Some results were obtained by Yu. Zhaurova.

Definition 0.1. $i \in \boldsymbol{N}$; i is an index. $C_i \in \boldsymbol{Z}$; C_i are constants in polynomials. $j \in \boldsymbol{N}$; j is an index; $p_{j,i} \in \boldsymbol{N}$; $p_{j,i}$ are degrees of variables. $k \in \boldsymbol{N}$; k is an index $x_k \in \boldsymbol{N}$; x_k are variables in polynomials.

Definition 0.2. $P(x_l)$ is polynomial of many variables assembled from elements of definition 0.1.

Definition 0.3. $\forall x_s \; \exists P(x_l) \neq 0$ and there is no proof of this fact [2; 3; 4].

Definition 0.4. Let such polynomials of no proof be $\underline{P(x_l)}$ We can say nothing about $\underline{P(x_l)}$ see [2; 3; 4]. $|\underline{P(x_l)}| = |\boldsymbol{N}|$ see [2; 3; 4].

Definition 0.5. Let L_z be L-machine. L-machine is set of boolean variables and program of logical operations. In any variable of L_z record is made only once. Logical operations of program are: "NOT" z_{i1} "RECORD IN" z_{i2}, z_{i3} "AND" z_{i4} "RECORD IN" z_{i5}, z_{i6} "OR" z_{i7} "RECORD IN" z_{i8}, "TRUE" "RECORD IN" z_{i9}, "FALSE" "RECORD IN" z_{i10}. See [5].

Definition 0.6. Let Turing machine be T_m. Let number of T_m operations be M_{Tm}. Program P_{TmLz} for L_z is equivalent T_m. Let number of P_{TmLz} operations be M_{PTmLz}.

Lemma 0.7. $\forall T_m \; \exists C_{Tm} = const$ and $\exists \; P_{TmLz}$.

Proof. See [5].

Lemma 0.8. $C_{Tm}(M_{PTmLz})^2 < M_{Tm}$

Proof. See [5].

Definition 0.9. $\underline{D}(P(x_l), d_{l,s}) = 0$ if $P(x_l) \in \underline{P(x_l)}$ and $\forall l \forall s \forall x_s < d_{l,s}$ and $Q \in \boldsymbol{N}$ and $\forall d_{l,s} = Q$

Definition 0.10. $\underline{D}(P(x_l), d_{l,s}) = 1$ if $P(x_l) = 0$ and $\exists l \exists s \exists x_s < d_{l,s}$ and $\exists Q \in \boldsymbol{N}$ and $\exists d_{l,s} = Q$

Definition 0.11. Let $\underline{S_1}(P(x_l), d_{l,s})$ be logic equations system for $\underline{D}(P(x_l), d_{l,s}) = 1$

Definition 0.12. Let $\underline{S_0}(P(x_l), d_{l,s})$ be logic equations system for $\underline{D}(P(x_l), d_{l,s}) = 0$

Logic equations system is NP-complete tasks, see [5].

Lemma 0.13. We can build $\underline{S_1}(P(x_l), d_{l,s})$ for $\underline{D}(P(x_l), d_{l,s}) = 1$. We can build $\underline{S_0}(P(x_l), d_{l,s})$ for $\underline{D}(P(x_l), d_{l,s}) = 0$.

Proof. We can use binary number system for calculating the value $V_{\underline{P(xl)}}$ of $\underline{P(x_l)}$ by L_z. If $V_{\underline{P(xl)}} = 0$ then boolean variables of result "OR"$^{d}{}_{1}(z_d)$ = "FALSE".

If $V_{\underline{P(xl)}} \neq 0$ then boolean variables of result "OR"$^{d}{}_{1}(z_d)$ = "TRUE". If we do not record in input boolean variables the data and add "OR"$^{d}{}_{1}(z_d)$ = "FALSE" for boolean variables of result then the program of L_z give us $\underline{S_0}(P(x_l), d_{l,s})$ and $\underline{S_1}(P(x_l), d_{l,s})$. For $\underline{S_1}(P(x_l), d_{l,s})$ we have ∃ solution of a system of logical equations. For $\underline{S_0}(P(x_l), d_{l,s})$ we have not ∃ solution of a system of logical equations.

Theorem 0.14. If NP is P then it is impossible to investigate this fact in detail.

Proof. For ∀ proof of NP is P we have next. We can say nothing about $\underline{P(x_l)}$ see [2; 3; 4]. If we can not prove $\underline{P(x_l)} \neq 0\ \forall x_s\ \forall Q > 0$ then $\exists\ \underline{Q} > 0$ and we have to check $\underline{S_0}(P(x_l), d_{l,s})$ for this $\underline{Q}$. $\underline{S_0}(P(x_l), d_{l,s})$ is NP-complete tasks. We can not prove $\forall \underline{S_0}(P(x_l), d_{l,s})$ and $\forall Q > 0$. And we have brute force algorithm that does not rely on the internal structure of the problem.

Theorem 0.15. If NP is not P then it is very hard to investigate this fact in detail.

Proof. We can say nothing about $\underline{P(x_l)}$ see [2; 3; 4]. That is, proof must be clean of $\forall \underline{S_0}(P(x_l), d_{l,s})$. But, we can say nothing about $\underline{P(x_l)}$ and $\forall \underline{S_0}(P(x_l), d_{l,s})$.

Theorem 0.16. If Navier-Stokes equations is smoothness then it is impossible to investigate this fact in detail.

Proof. If we can say nothing about NP vs P like Theorems 0.14 and 0.15 then if we can make $\forall T_m$ then ∀ initial conditions of the problem the proof is impossible, that is proof must be for $\forall \underline{S_0}(P(x_l), d_{l,s})$ and $\forall Q > 0$. We can make $\forall T_m$ if we make transistor, resistance, conductor, battery by gas pipes. We have: resistance is narrow gas pipe; conductor is gas pipe; battery is gas cylinders; transistor is laminar or turbulent gas flow if gas inflow from an external gas pipe. Transistor is variable adjustable flow resistance.

Theorem 0.17. If Navier-Stokes equations is not smoothness then it is very hard to investigate this fact in detail.

Proof. If we can say nothing about NP vs P like Theorem 0.14 and 0.15 then proof must be clean of $\forall T_m$.

Conclusions 1: evidence for these problems is possible only for constructively constructed particular cases.

Lemma 0.18. Author Yu. Zhaurova. NP is equal to P. A group of people with sufficient motivation solves the NP-complete problem in reasonable time. By subsequent specification of input data.

Proof. Proof is impossible, see Theorems 0.14, 0.15.

Conclusions 2: Author Yu. Zhaurova. Let L be laws of physics. Let E be energy conservation laws. Let A be laws of arithmetic. Let O be physical object. From $L \Rightarrow E$. $A \in L$. Use Godel's incompleteness theorem, see [1; 2; 3; 4]. We have: ∃ O and this O not $\Leftarrow L$. We have: $O \in E$ or O not $\in E$.

References:

1. Bilan I., Bilan A., Zhuk V. Some Aspects of NP-Complete Tasks Under GNU GPL v. 3.0. URL: https://dxdy.ru/topic130597.html
2. Survey I., Davis Martin. Diophantine Equations and Computation, Professor Emeritus Courant Institute, NYU, Visiting Scholar UC Berkeley.
3. Jones James P. Undecidable Diophantine Equations, Bulletin (New Series) of the American Mathematical Society – Vol. 3.– No 2.– September 1980.
4. Davis Martin. The Incompleteness Theorem, Notices of the AMS – Vol. 53.– No. 4.

5. Kuznetsov O. P., Adelson-Velskiy G. M. Discrete Mathematics for Engineers Second Edition,– M. Energoatomisdat 1988.

Section 2. Medical science

Ashurmetov Azizbek Mirsagatovich,
Candidate of Medical Sciences,
Central Clinical Hospital No. 1
Main Medical Department at the Presidential
Administration of the Republic of Uzbekistan
E-mail: ashur.az@mail.ru

PARADOXIAL VASOCONSTRICTION OF CAVERNOUS ARTERIES AS A MANIFESTATION OF SYSTEMIC OXIDATIVE STRESS

Abstract

***Objective*:** To assess endothelial dysfunction and the degree of oxidative stress of cavernous arteries in men with cardiovascular diseases (CVD) and cardiovascular risk factors (CVRF).

Material and methods: 102 men with CVD and CFRF were examined. All men underwent a comprehensive examination, and besides, sexual constitution vector was estimated for all the examined individuals. Endothelial function of cavernous arteries was determined using ultrasonic Doppler examination after exposure to an infrared emitter.

***Results*:** Erectile dysfunction (ED) was detected in 98 (96.1%) men. Endothelial dysfunction (EnD) of cavernous arteries was detected in 93.1% of the examined men. Moreover, in 74.7% of cases, paradoxical vasoconstriction was determined. The sexual constitution vector was within average and weakened average variants in 80.3% of men with ED. Paradoxical vasoconstriction of the cavernous arteries was noted in 57 (69.5%) men with such variants of sexual constitution.

Conclusion: Application of narrow-spectrum IR radiation in diagnosing endothelial dysfunction of cavernous arteries will take a particular place in comprehensive examination of patients with CVD and CVRF. Paradoxical vasoconstriction of cavernous arteries is a local manifestation of systemic oxidative stress. The weakened variant of average and the average variants of sexual constitution in men are a predictor of endothelial dysfunction and weakness of antioxidant protection of blood, organs and tissues.

Keywords: oxidative stress, endothelial dysfunction, terahertz infrared radiation, erectile dysfunction.

It is known that oxidizing (oxidative) stress is involved in pathogenesis of many diseases in humans and animals [1; 2].

Oxidative stress is one of the most common pathological processes, the essence of which is the imbalance in the condition of pro- and antioxidant systems of blood, organs and tissues. This indicates a need for its immediate pathogenetic correction, which can be carried out by means of both specific and non-specific antioxidant therapy.

A large number of studies show that oxidative stress significantly stimulates progression of endothelial dysfunction [3–6].

Numerous studies have confirmed the fact that oxidative stress changes many endothelium functions, affecting vascular tone. Inactivation of nitric oxide (NO) and accumulation of superoxide anion and other reactive oxygen species (ROS) are noted in the presence of arterial hypertension, hypercholesteremia, diabetes, metabolic syndrome, etc.

In a number of laboratory studies on vascular cells researching various enzyme systems, in particular, xanthine oxidase, NADPH/NADPHN oxidase and eNOS, which are capable of producing ROS [7]. ROS are a family of molecules that are formed in all aerobic cells and have a high reactive ability with other biological molecules. Under normal physiological conditions, the production of ROS is balanced by an effective antioxidant system, the molecules of which are able to neutralize them and thereby prevent oxidative damage. Enzymatic antioxidants (superoxide dismutase, glutathione peroxidase, catalase), which are present in tissues, play an important role in conversion of ROS into oxygen and water.

Non-enzymatic antioxidants (fat-soluble vitamins E and carotene, water-soluble vitamin C), which in particular protect plasma lipids from peroxidation and inactivate superoxide anion [8; 9].

In a number of pathological conditions, excessive formation of ROS occurs, suppressing endogenous mechanisms of antioxidant protection, this shift leads to oxidation of biological macromolecules (DNA, proteins, carbohydrates and lipids), having a detrimental effect on functions of cells and tissues.

The presence of risk factors for cardiovascular diseases contributes to progression of oxidative stress [8]. Oxidative stress, in its turn, is involved in pathogenesis of a number of cardiovascular diseases, including arterial hypertension, hypercholesterolemia, atherosclerosis, diabetes mellitus and heart failure [10; 11].

With excessive formation of ROS, endogenous antioxidant defense mechanisms are suppressed, which contributes to oxidation of biological macromolecules (DNA, proteins, carbohydrates and lipids), having a detrimental effect on functions of cells and tissues.

For example, intracellular accumulation of free radicals contributes to lipid peroxidation, resulting in formation of new lipid radicals. Lipid radicals produced in this chain accumulate in cell membranes and can have a large number of undesirable effects, including disruption of plasmolemma integrity and dysfunction of membrane-binding proteins.

Under conditions of oxidative stress, low-density lipoprotein molecules (LDL) are easily oxidized. Oxidized LDL have a damaging effect on vascular intima, leading to production of foam cells involved in formation of atherosclerotic plaques [12; 13].

The first methods of assessing endothelial function were invasive. NO release inducing drugs (acetylcholine, methacholine, papaverine, etc.) were administered intracoronary, and then the degree of vasodilation was measured. In their experiments, P. L. Ludmer et al. found that administration of acetylcholine, when performing coronary angiography, causes endothelium-dependent vasodilation in healthy individuals, while paradoxical vasospasm was detected in the presence of atherosclerotic lesions, indicating endothelial dysfunction [14]. However, due to high cost and complexity of its implementation, the invasive method of research is not currently widely used. To date, the "gold standard" for assessing the functional state of endothelium is non-invasive determination of flow-mediated vasodilation (FMD). The technique described by D. S. Celermajer et al. in 1992, consists in the study of the brachial or radial artery with ultrasound scanning. Due to its availability, simplicity of execution, reliability, high sensitivity and specificity, it has become widespread and is currently used in fundamental scientific research [8]. Essentially, the method relies on the fact that after cessation of pressure in the cuff blood flow rate increases. With an increase in blood flow velocity in the brachial artery, shear stress increases,

affecting the endothelium, resulting in increased synthesis of NO by endotheliocytes, which leads to local vasodilatation. As a result, a flow-dependent vasodilation of the artery is recorded by ultrasound. The degree of vasodilation is directly proportional to the amount of NO produced, which characterizes the function of endothelium [8, 15]. Another way to assess the state of endothelium in a non-invasive way is to examine pulse wave velocity when performing photoplethysmography. There is a method of peripheral arterial tonometry or finger plethysmography, which is actually a modified Celermajer test. Laser Doppler-flowmetry also refers to non-invasive methods for diagnosing endothelial function, the essence of which consists in optical sensing of tissues and analyzing the signal reflected from red blood cells, which quantifies blood flow in microvessels [8]. Assessment of endothelial function is also possible using positron-emission tomography, which gives the opportunity to assess the coronary perfusion reserve, but this method is expensive, so conducting such a study is not possible in every clinic.

There is a well-grounded data on the use of a narrow spectrum of the far-range (from 8 to 50 μm) infrared (IR) radiation in medicine and biology [16–18]. Living organisms for communication and control use the considered range of electromagnetic waves, while living organisms themselves emit millimeter-wave oscillations. Waves excited in the body, when exposed to infrared radiation of terahertz range, imitate, to a certain extent, the signals of internal communication and control (information communication) of biological objects.

The terahertz frequency range of electromagnetic waves is located between extremely high frequencies and optical infrared (IR) ranges (Fig. 1) on the scale of electromagnetic waves and is interesting, first of all, because molecular emission and absorption spectra of various cellular metabolites (NO, CO, reactive oxygen species, etc.) belong to this range.

Purpose of the study. To assess endothelial dysfunction and the degree of oxidative stress of the cavernous arteries in men with cardiovascular diseases (CVD) and cardiovascular risk factors (CVRF).

Material and methods

We examined 102 men, aged between 32 and 74, with CVD and CVRF. All men underwent a comprehensive examination, which included collection of general medical and sexological history, general examination, body mass index (BMI) was determination, waist circumference, blood pressure were measurement, and performing biochemical blood tests. In addition, the level of total testosterone and prostate-specific antigen, the lipid spectrum and blood glucose were determined. All patients were surveyed using IIEF-5 (International Index of Erectile Function) and examined for determining their sexual constitution vector (SCV).

Alongside this, all men were examined for endothelial function of cavernous arteries, using ultrasound study of diameter changes (ultrasound) after exposure to narrow-spectrum (long-range) IR emitters (Fugure 1).

The study of endothelial function of penis cavernous arteries was performed according to the original method. In the position of the patient lying on his back, linear sensor LA 523 10–5 was placed longitudinally along the ventral surface of the penis at a distance of 2–3 cm from the root. The diameter of cavernous arteries was assessed at least twice, by measuring the distance between the opposites walls of each vessel, and mean values were used for calculations. In addition, the following indicators were determined – peak systolic velocity (PSV), peak diastolic velocity (PDV), reactivity index (RI), pulse index (PI). Then, an infrared emitter was applied to the ventral surface of the penis at a distance of 10–12 cm from the root with 5 minutes of exposure (Fugure 2). After the exposure, a re-ultrasound was performed for measurement of the cavernous arteries diameter in the same place. We used the largest diameter values obtained with the repeated study for calculations.

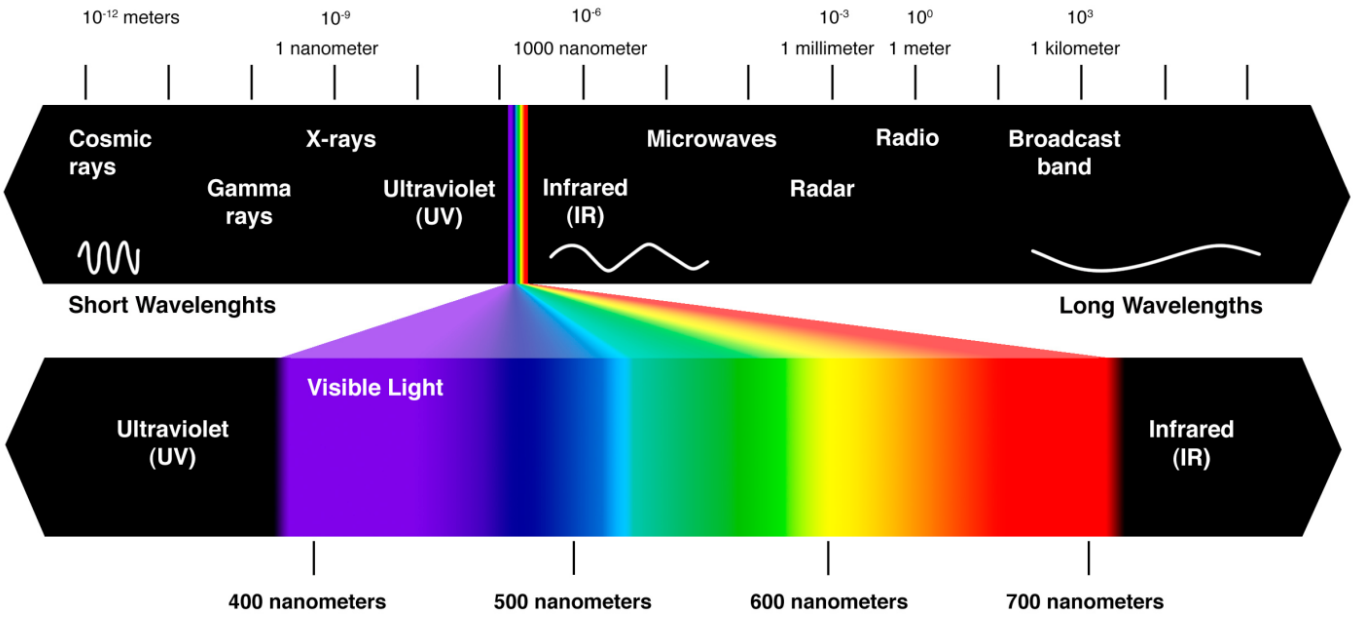

Figure 1. Spectrum of electromagnetic radiation

Figure 2. Far-range infrared emitters

The Percentage of Cavernous Arteries Diameter Increase (PCADI) was calculated by the formula:

$$PCADI = 100\% \times (D2 - D1)D1$$

where D1 is the mean diameter of both cavernous arteries before irradiation with an infrared emitter;

D2 is the mea diameter of both cavernous arteries after irradiation.

All studies were conducted in the morning and by the same ultrasound diagnostics specialist. Before the study, patients were asked to refrain from smoking and taking any medications that affect cardiovascular system. The threshold PCADI value for distinguishing endothelial dysfunction from the norm was 30%.

Results

Manifestations of erectile dysfunction (ED) were detected in 98 (96.1%) patients. According to IIEF-5: mild erectile disorders were detected in 31 (31.6%) men; moderate degree of impairment in 58 (59.2%) men; severe – in 9 (9.2%); signs of ED were absent in 4 (3.9%).

Figure 3. The technique of IR emitter application on cavernous arteries

During the study of endothelial function of cavernous arteries, endothelial dysfunction was detected in 95 (93.1%) patients. Paradoxical vasoconstriction was diagnosed in 71 (74.7%) patients (PCADI < 0%). In 24 (25.3%) patients, PCADI was detected at a level of less than 30% and made up, on average, 16.5%, indicating a dysfunction of cavernous arteries endothelium. In 7 (6.9%) men, endothelial function of cavernous arteries was within the normal range (PCADI > 30%).

Analysis of patients with a paradoxical reaction of the cavernous arteries to narrow-spectrum infrared radiation showed that in 49.3% of cases PCADI = 0%, and in 50.7% of cases PCADI < 0%. Absence of endothelium reaction and manifestations of cavernous arteries spasm were regarded by us as paradoxical vasoconstriction.

The scale for determining the sexual constitution vector revealed the following: 52 (50.9%) men had a weakened variant of the average constitution; the average variant was identified in 27 (26.5%); the stronger average variant – in 12 (11.8%); weak sexual constitution was found in 7 men (6.9%) and a very weak variant of sexual constitution was found in 1 (0.98%) men. In 3 (2.9%) men, a strong variant of sexual constitution was identified.

In 80.3% (n = 82) of men with ED, the sexual constitution vector was within average and weakened average variants. In 57 (69.5%) men with such variants of sexual constitution, paradoxical vasoconstriction of cavernous arteries was noted.

Discussion

It is known that free radical processes and the activity of antioxidant systems in all living organisms form a single whole – oxidative metabolism, which is one of the basic components of metabolism and is supported by appropriate homeostatic mechanisms [1; 2; 19]. Under normal state of body, functioning the rate of free-radical reactions of cell membrane lipids peroxidation and lipoprotein peroxidation is relatively low due to low levels of initiator-radicals formation and action of a balanced antioxidant defense system. However, in the process of inflammatory diseases emergence and development this balance is disturbed, the production of initiator-radicals increases sharply and inactivation of the antioxidant defense system is observed, thus, develops the so-called oxidative stress.

Oxidative stress is one of the links in the chain of pathogenetic changes formation in the body [20]. An increase in oxidative stress and a decrease in antioxidant protection lead to mitochondrial DNA damage and depletion of adenosine triphosphate

(ATP) [21]. Nowadays, the role of oxidative stress in the development of endothelial dysfunction has already been proven [22].

The antioxidant system of each individual, as well as the type of sexual constitution, is formed under the influence of hereditary factors and conditions of development in prenatal period as well as by early ontogenesis.

The paradoxical vasoconstriction of cavernous arteries, which was revealed by us in 74.7% of patients, indicates inactivation of the antioxidant system of endotheliocytes and smooth muscle cells. This requires use of corrective measures for improvement and restoration of endothelial function.

We assume a possible mechanism of paradoxical vasoconstriction in case of endothelial dysfunction of cavernous arteries under the influence of narrow-spectrum (far-range) IR radiation.

The action of infrared radiation, with a frequency corresponding to the molecular emission and absorption spectra of NO and ROS, activates blood phagocytes (monocytes) and endothelial cells. This leads to release of NO and ROS, which increases oxidative stress of the endothelium. In addition, excessive NO can bind with superoxide radicals with formation of one of the strongest oxidizing agents – peroxynitrite. This leads to endothelial dysfunction, depletion of ATP and increased production of endothelin-1 vasoconstrictor.

Unlike infrared radiation, mechanical vibrations, after elimination of compression (according to Celermajer), are converted into electromagnetic oscillations with a frequency that does not correspond to molecular emission and absorption spectra of NO and ROS. Consequently, there is no release of ROS and no increase in the level of NO in phagocytes (monocytes) of blood and endothelial cells.

Conclusion

Therefore, the paradoxical vasoconstriction of the cavernous arteries is a local manifestation of systemic oxidative stress.

The use of narrow-spectrum infrared radiation in the diagnosis of endothelial dysfunction of the cavernous arteries is able to determine the severity of oxidative stress. This suggests the need for immediate pathogenetic correction and inclusion of specific and nonspecific antioxidant therapy into the complex of ED treatment.

Weak, weakened variant of average and average variants of sexual constitution in men are predictors of endothelial dysfunction and weakness of antioxidant protection of blood, organs and tissues.

References:

1. Зенков Н. К., Ланкин В. З., Меньщикова Е. Б. Окислительный стресс. Биохимические и патофизиологические аспекты.– М.: Наука, 2001.– 340 с.
2. Меньщикова Е. Б., Ланкин В. З., Зенков Н. К., Бондарь И. А. с соавт. Окислительный стресс. Прооксиданты и антиоксиданты.– М., 2006.– 556 с.
3. Keaney J. F., Vita J. A. Atherosclerosis, oxidative stress, and antioxidant protection in endotheliumderived relaxing factor action. Prog. Cardiovasc. Dis. 1995; 38: 129–54.
4. Heitzer Th., Schlinzig T., Krohn K. et al. Endothelial dysfunction, oxidative stress, and risk of cardiovascular events in patients with coronary artery disease. Circulation. 2001; 104: 2673–8.
5. Taddei S., Ghiadoni L., Virdis A., Versari D., Salvetti A. Mechanisms of endothelial dysfunction: clinical significance and pre ventive non-pharmacological therapeutic strategies. Curr. Pharm. Des. 2003; 9: 2385–402.
6. Ross R. Atherosclerosis: an inflammatory disease. N. Engl. J. Med. 1999; 340: 115–26.
7. Forstermann U., Sessa W. C. Nitric oxide synthases: regulation and function. Eur. Heart J. 2012; 33: 829–37.

8. Esper R. J., Nordaby R. A., Vilarino J. O., Paragano A. Endothelial dysfunction: a comprehensive appraisal. Cardiovasc. Diabetol. 2006; 54: 1475–2840.
9. Givertz M. M., Sawyer D. B., Colucci W. S. Antioxidants and myocardial contractility. Illuminating the "dark side" of `-adrenergic receptor activation. Circulation. 2001; 103: 782–3.
10. Cai H., Harrison D. G. Endothelial dysfunction in cardiovascular diseases: the role of oxidant stress. Circ. Res. 2000; 87: 840–4.
11. Sharma A., Bernatchez P. N., Haan J. B. Targeting endothelial dysfunction in vascular complications associated with diabetes. Int. J. Vasc. Med. 2012; ID750126. 12.
12. Janeway C. A., Jr., MedzhitovR. Innate immune recognition. Ann. Rev. Immunol. 2002; 20: 197–216.
13. Peiser L., Mukhopadhyay S., Gordon S. Scavenger receptors in innate immunity. Curr. Opin. Immunol. 2002; 14: 123–8.
14. Ludmer P. L., Selwyn A. P., Shook T. L., Wayne R. R. et al. Paradoxical vasoconstriction induced by acetylcholine in atherosclerosis coronary arteries. N. Engl. J. Med. 1986; 315: 1046–51.
15. Уразовская И. Л. Взаимосвязь функционального состояния эндотелия и течения острого инфаркта миокарда с подъемом сегмента ST: дис. … канд. мед. наук.– М.; 2010: 118.
16. Бецкий О. В., Девятков Н. Д., Кислов В. В. Миллиметровые волны низкой интенсивности в медицине и биологии // Биомедицинская радиоэлектроника. 1998.– № 4.– С13–29.
17. Баграев Н. Т., Клячкин Л. Е., Маляренко А. М., Новиков Б. А. Терагерцевая кремниевая наноэлектроника в медицине. Инновации., № 10 (156), 2011; 105–119.
18. Гареев Г. З., Лучинин В. В. Применение терагерцевого излучения в биологии и медицине. Наноиндустрия. № 6 (52), 2014; 34–45.
19. Казимирко В. К., Мальцев В. И., Бутылин В. Ю., Горобец Н. И. Свободнорадикальное окисление и антиоксидантная терапия.– К.: Морион, 2004.– 160 с.
20. Xu X. J., Gauthier M-S., Hess D. T., et al. Insulin sensitive and resistant obesity in humans: AMPK activity, oxidative stress, and depot-specific changes in gene expression in adipose tissue. J Lipid Res. 2012; 53(4): 792–801. doi: 10.1194/jlr.P022905.
21. Goossens G. H. The role of adipose tissue dysfunction in the pathogenesis of obesity-related insulin resistance. Physiol Behav. 2008; 94(2): 206–218. doi: 10.1016/j. physbeh.2007.10.010.
22. Wenceslau C. F., McCarthy C. G., Szasz T., et al. Mitochondrial damage-associated molecular patterns and vascular function. Eur Heart J. 2014; 35(18): 1172–1177. doi: 10.1093/eurheartj/ehu047

Slyvka Nataliia Oleksiivna,
PhD, professor's assistant,
Higher State Educational Establishment of Ukraine
"Bukovinian State Medical University", Chernivtsi, Ukraine
E-mail: slyvkanataliia@gmail.com

ADVANTAGES OF TERLIPRESSIN VERSUS DOPAMINE IN THE TREATMENT OF HEPATORENAL SYNDROME

Abstract. This research is aimed to compare the efficacy of vasoconstrictors used for the treatment of hepatorenal syndrome, such as dopamine and terlipressin. The study enrolled 92 patients, which were divided into 2 groups and examined in the dynamics of treatment. The results have shown that dopamine administration in "renal doses" did not lead to any improvement in kidney function – rates of GFR, serum urea and creatinine, serum ions didn't change significantly ($p > 0.05$) and didn't increase patients survival, despite the obvious temporary improvement of the hemodynamics and dieresis. Terlipressin has demonstrated much better correction of kidney function and decreased the mortality rate ($p > 0.05$). Thus, terlipressin can be considered as the treatment of choice for patients with hepatorenal syndrome.

Keywords: hepatorenal syndrome, alcoholic liver cirrhosis, terlipressin, dopamine.

Introduction. The number of patients with alcoholic liver cirrhosis (ALC) remains consistently high now days. One of the most dangerous complication of ALC is the hepatorenal syndrome (HRS) – renal dysfunction along with the increase of intoxication and a deterioration of patients survival prognosis [1].

HRS develops in patients with ALC, severe liver failure and portal hypertension. HRS manifests with the impaired renal function, arterial circulation failure and high activity of the endogenous vasoactive system. Pronounced vasoconstriction in kidneys, leading to the decrease of glomerular filtration rate (GFR) is the main pathophysiological mechanism of HRS. Arterial vasodilation prevails in the extrahepatic blood flow, leading to the reduction of total vascular resistance and arterial hypotension [2].

The pathogenesis of HRS is not clearly understood yet, but there are evidences of hemodynamic disturbances leading to the decrease in renal blood flow, activation of sympathetic nervous system and increased synthesis of humoral and renal vasoactive mediators [7].

Changes of blood circulation manifest with the hyperdynamic syndrome because of vasodilation in most patients with ALC and HRS [1]. The circulatory disorders in HRS are explained with an increase of deposition of blood in the internal organs associated with severe peripheral vasodilation [6].

To maintain effective kidney blood supply the systolic blood pressure (sBP) has to exceed 85 mm Hg. It is possible to achieve this range by means of volume expanders and vasopressors, such as vasopressin, ornipressin, octreotide, terlipressin or dopamine [9].

The use of dopamine in patients with HRS is based on its ability to inhibit the synthesis of aldosterone, to increase the renal blood flow and GFR.The clinical studies in patients with ALC and HRS have shown that low doses of dopamine (1.5 mcg/kg/min) lead to an increase in renal blood flow by 31% with unchanged GFR. Opinions about the effectiveness of dopamine in patients with HRS are controversial. It is reported that low-dosage of dopamine doesn't increase the diuresis and doesn't decrease serum creatinine level in patients with ALC and HRS [7].

There are also positive effects of dopamine to renal function. At the same time, it is noted that the effect of dopamine is short-lived and manifests itself only during the first week since the onset of treatment [10].

Terlipressin is a synthetic analogue of vasopressin (H-triglycyl-8-lysine), which has a longer half-life and more favorable safety profile as compared to ornipressin. The use of terlipressin in combination with albumin can reduce the activity of renin-angiotensin system, increase sBP, improve the systemic blood flow, and normalize level of the serum creatinine and GFR[3; 9; 10].

Material and methods. This study analyzes the results of a comprehensive examination of 92 patients (64 men and 28 women) with ALC and HRS in the dynamics of treatment. The age of patients ranged from 28 to 73 years, the majority of them were between 41–60 years.

HRS was diagnosed by the criteria of EASL Clinical Practice Guidelines for the management of patients with decompensated cirrhosis [4; 5]:

1. Liver cirrhosis with ascites.

2. Serum creatinine concentration more than 133 mmol/l (1,5 mg/dl).

3. Absence of positive dynamics in the level of serum creatinine (<133 mmol/l) for 2 days after discontinuation of diuretics and volume expansion with albumin (1 g/kg body weight, maximum 100 g/kg).

4. No signs of shock.

5. No history of administration of nephrotoxic drugs.

6. No history of parenchymal kidney disease, manifested by proteinuria more than 500 mg/day, hematuria more than 50 cells in the high power field and/or changes during ultrasound examination.

All enrolled patients with ALC and HRS were prescribed albumin (Albumin-Biopharm 20%; OOO Biopharma Plasma Ukraine) intravenously (i/v), 1 g/kg per day on the first day of treatment and 20–40 g/day – in the next few days. They were divided into two groups: Group 1 (control group) (n = 27) – received dopamine (Dopamine-Darnytsa, 5 mg/ml) in the "renal dose" – 5 mg/kg/min for 7 days; Group 2 (study group) (n = 23) received terlipressin (Remestip 0.1mg/ml, Ferring-Lechyam a.s., Czech Republic) was initially administered at the dose of 3 mg/24 hours by continuous intravenous administration for 7 days. The response to treatment was evaluated every 48 hours, in case if serum creatinine decreased by less than 25% from baseline, the dose was gradually increased to 12 mg/24 hours.

The risk of short term mortality (within the first 29 days) was prognosed by MELD score (Model for End-Stage Liver Disease) [8]. MELD score uses the patient's values for serum bilirubin, serum creatinine, and the international normalized ratio for prothrombin time (INR) to predict survival. It is calculated according to the following formula:

$$MELD = 3.78 \times \ln[\text{serum bilirubin (mg/dL)}] + 11.2 \times \ln[\text{INR}] + 9.57 \times \ln[\text{serum creatinine (mg/dL)}] + 6.43$$

In interpreting the MELD score in hospitalized patients, the 3 month observed mortality is: 40 or more – 71.3% observed mortality; 30–39–52.6% observed mortality; 20–29–19.6% observed mortality; 10–19–6.0% observed mortality; < 9–1.9% observed mortality [8].

Statistical processing of the study results was carried out using the program package STATISTICA 15.0. To assess the difference between groups, Student's t-test for independent samples was used. To measure the degree of linear dependence between the values of the indices in the groups, the Pearson correlation coefficient (r) was used for parametric values, and the chi-square criteria (χ^2) for nonparametric ones. The assessment of patients' survival was performed using the Kaplan Meier method. The statistics are given in the format $M \pm \sigma$. The level $p < 0.05$ was accepted as statistically significant.

Results. Symptoms of chronic hepatic and acute renal failure prevailed in all patients before the treatment has started. Initially, patients of both groups were noted the tendency to hypotonia and tachycardia, which is typical for patients with ALC and HRS.

In patients of Group 1 the symptoms of liver failure were combined with the symptoms of renal failure: low GFR, oligouria, edema, ascites, hyperkalemia, hyponatremia, high levels of serum urea and creatinine. Administration of dopamine at a dose of 5 mg/kg/min was accompanied by an increase of sBP, on the 7–8th day it was 84.7 ± 9.2 mm Hg. ($p < 0.05$) in comparison with the initial level) and reached normal values, while an unreliable increase in the heart rate was recorded. These results can be considered as a hemodynamic stabilization in patients with ALC and HRS. However, sBP has decreased to the baseline values by the 30th day (dopamine was administered only for the first seven days). On the 7–8th day, the examined parameters did not differ from the initial values, the amount of diuresis also did not increase. Thus, dopamine administration in "renal doses" did not lead to any improvement in kidney function – rates of GFR, serum urea and creatinine, serum ions didn't change significantly ($p < 0.05$). By the 30th day, a progressive hyperkalemia along with increase of serum creatinine and urea were observed. The diuresis rate also did not increase.

In Group 2 the terlipressin therapy has significantly improved the indicators of water-electrolyte metabolism and toxins elimination. On the 7–8th day, a significant decrease of serum urea and creatinine occurred in comparison with the initial values up to 17.5 ± 1.9 mmol/l and 165.6 ± 18.9 mmol/l ($p < 0.05$). At the same time, an increase sodium ions and a decrease of potassium were observed ($p < 0.05$). A positive phenomenon was also an increase of the volume of diuresis, observed on the 7–8th day in patients of the Group 2. The clinical effects of the terlipressin therapy were to reduce the degree of overhydration and the symptoms of ascites.

In Group 1 within the first 7–8 days of treatment 5 patients died, and another 18 died by the 30th day – the mortality rate composed 21.8% and 78.3% respectively. Mortality in this group corresponded to the predicted level by MELD score before the start of treatment. In Group 2 within the first 7–8 days of treatment 2 patients died, and another 11 died by the 30th day – the mortality rate composed 7.4% and 40.7% respectively, which was much less than in Group 1 ($p < 0.05$) and less, than the level predicted by MELD score before the start of treatment. The results indicate that the inclusion of dopamine in the therapy of patients with HRS does not reduce their mortality.

Conclusions. The results of the study show that vasopressor therapy according to the scheme of terlipressin + albumin is more effective compared to the scheme of dopamine + albumin – both for the normalization of kidney function, and for the survival of patients with hepatorenal syndrome on the background of alcoholic liver cirrhosis. Thus, terlipressin in combination with albumin can be considered as the treatment of choice for such patients.

References

1. Angeli P., Merkel C. Pathogenesis and management of hepatorenal syndrome in patients with cirrhosis // J. Hepatol. 2018.– No. 48 (Suppl. 1).– P. 93–103. doi: 10.1038/nrneph.2011.96.
2. Arroyo V., Gines P., Gerbes A. et al. Definition and diagnostic criteria of refractory ascites and hepatorenal syndrome in cirrhosis // International Ascites Club. Hepatology. 2016.– No. 23.– P. 164–176. doi: 10.1002/hep.510230122.
3. Boyer T., Sanyal A., Garcia-Tsao G., et al. Predictors of response to terlipressin plus albumin in hepatorenal syndrome (HRS) type 1: relationship of serum creatinine to hemodynamics // J. Hepatol. 2015.– No. 55.– P. 315–321. doi: 10.1016/j.jhep.2010.11.020.
4. EASL clinical practice guidelines on the management of ascites, spontaneous bacterial peritonitis, and hepatorenal syndrome in cirrhosis // J. Hepatol. 2010.– No. 53.– P. 397–417. doi: 10.1016/j.jhep.2010.05.004.

5. EASL Clinical Practice Guidelines: Management of alcohol-related liver disease // Journal of Hepatology. 2018.– No. 69.– P. 154–181. doi: 10.101.j.jhep.2018.03.018
6. Gines P., Schrier R. Renal failure in cirrhosis // N. Engl. J. Med. 2018.– No. 361.– P. 1279–1290. doi: 10.1056/NEJMra0809139.
7. Gluud L., Christensen K., Christensen E., Krag A. Systematic review of randomized trials on vasoconstrictor drugs for hepatorenal syndrome // Hepatology. 2010.– No. 51.– P. 576–584. doi 10.1002/hep.23286.
8. Kartoun Uri, Corey A., Kathleen E, Simon A., et al. The MELD–Plus: A generalizable prediction risk score in cirrhosis // PLoS ONE2017.– No. 12(10): e0186301. URL: https://doi.org
9. Neri S., Pulvirenti D., Malaguarnera M., et al. Terlipressin and albumin in patients with cirrhosis and type I hepatorenal syndrome // Dig. Dis. Sci. 2008.– No. 53.– P. 830–835. doi: 10.1186/s40064–015–1625-z.
10. Sanyal A., Boyer T., Garcia-Tsao G., et al. A randomized, prospective, double-blind, placebocontrolled trial of terlipressin for type 1 hepatorenal syndrome // Gastroenterology. 2008.– No. 134.– P. 1360–1368. doi: 10.1053/j.gastro.2008.02.014.

Section 3. Technical sciences

Jabborova Dilafruz Raupovna,
Majidov Kakhramon Halimovich,
Bukhara Engineering-Technological Institute
E-mail: zhabborova84@inbox.ru

INFLUENCE OF MOISTENING OF WHEAT GRAIN IN AQUEOUS FERTILIZER SOLUTION ON THE YIELD OF FLOUR

Abstract. The effect of hydrothermal treatment on the quality indicator and the yield of flour during the processing of wheat grains of various grades is researched. Hydrothermal treatment carried out with sodium bicarbonate solutions of different concentrations. It has been established that 1.0% aqueous solution of sodium bicarbonate provides improved quality and high yield of flour during processing the wheat grains of various grades.

Keywords: Grain of different grades, moisture and grain yield, hydrothermal treatment, technological indicators.

The selection of mineral fertilizers in the agrotechnical processing of wheat grain grown in the field conditions on the yield obtained from these grain products is important. In the literature there is evidence of work performed in this area [1,4]. However, in the well-known research, not enough attention was paid to the influence of the selection of target fertilizers on the process of obtaining flour and product yield. In this regard, this work is aimed at studying the influence of the process of moistening of wheat grains in a water solution of fertilizers on the yield of flour.

The efficiency of grinding of grain and grain products on mills, in addition to the kinematic and geometric parameters of machine grinding, is also influenced by the methods of flour grinding, the technological properties of grain (humidity, glassiness and their uniformity) and the load on the surface of rollers of mill machines.

In the grinding process, the structural and mechanical properties of the grain (strength, hardness, elasticity, and grinding properties) are also significant. According to the structural and mechanical properties, the grain is divided into soft and hard types [5]. Hard wheat grains are characterized by a high yield of intermediate products in the form of cereals and cereal flour, while soft wheat grains are characterized by a low cereal yield and soft flour.

Humidity of grain has a great technological importance for the formation of structural and mechanical properties (strength) of grain [6].

It has been experimentally proved that with an increase in grain moisture increases its resistance to separation and the energy consumption for its grinding, which was explained by an increase in the elasticity property of the grain. At the same time, according to the results of the experiments, the appearance of a largely elastic strain in the shell parts of the grain and their large resistance to grinding

For a full assessment of the effectiveness of the grinding process, an effectiveness criterion was adopted [7] that takes into account not only the overall

separation rate N (%), but also the decrease in the ash content of the ground products relative to the ash content of the products entering the grinding machine, which is expressed by following formula:

$$E = N \cdot \Delta Z = N \cdot \frac{Z_0 - Z_1}{Z_1} \quad \%$$

where: N – separation rate, %;

Z_0 – ash content of the products entering the grinding machine,%;

Z_1 – ash content of product separated after grinding machine,%;

It was defined that the greater the value of the efficiency criterion, the higher the degree of the grinding process.

To research the effect of moistening on the flour yield, an experiment was conducted with the weighing of flour from a MLU-202 laboratory mill [8]. To determine the flour content of the grain, 2 kg of the sample from samples of the grain moistened with different methods was put inMLU-202 laboratory mill. The results of the experiment are shown in (table 1).

Table 1.– The influence of methods of moistening on the flour yield at grinding the graded flour (ash content of wheat grades 1.83 and 1.76% respectively)

Method of moistening the grain	Grade of wheat grain	Hydrothermal treatment time, hours	Flour yield,%	Ash content of flour,%	Efficiency criterionE,%
Cold air conditioning	Krasnodar-99	24	70.1	0.92	69.2
	Starshina	24	70. 15	0.88	69.5
Aqueous solution of sodium bicarbonate, 0.5%	Krasnodar-99	15.4	70.18	0.93	67.9
	Starshina	15.4	70.14	0.91	65.5
Aqueous solution of sodium bicarbonate, 1.0%	Krasnodar-99	15.4	71.08	0.91	71.9
	Starshina	15.4	71.12	0.879	71.3
Aqueous solution of sodium bicarbonate, 1.5%	Krasnodar-99	15.4	70.4	0.91	71.2
	Starshina	15.4	70.36	0.877	70.8

As we can see from the results of the experiment (Table 1), in the case of moistening with cold conditioning method and hydrothermal treatment for 24 hours, the efficiency criterion of flour yield in the Krasnodar-99 and Starshinagrades was 69.2–69.5%, respectively. At the moistening the grain in a 1.0% aqueous solution of sodium bicarbonate and hydrothermal treatment for 15.4 hours, the flour yield efficiency criterion for the Krasnodar-99 and Starshinagrades was 71.9: 71.3%, respectively, and by comparison with the above results, it was determined experimentally the increase of efficiency criterion by 2.7: 1.8%, respectively. Comparison with the results of experiments using a 1.5% aqueous solution of sodium bicarbonate showed an increase in the value of the efficiency criterion by 0.7–0.5%, respectively.

References:

1. Egorov G. A. Control of technological properties of grain. VSU – Voronezh, 2009.– 348 p.
2. Egorov G. A. Technological properties of grain.– M: "Agropromizdat", 1985.– 334 p.
3. Naumov I. A. Improving the conditioning and grinding of wheat and rye.– M: "Kolos", 1975.– 175 p.
4. Kozmina N. P. Grain and evaluation of its quality.– M.: Selxozizdat, 2012.– 427 p.

5. Kazakov E. D., Kretovich V. L. Biochemistry of grain and products of its processing – M.: "Agropromizdat", 1989–368 p.
6. Egorov G. A. Technology of grain processing. Textbook 2nd ed. – M.: Kolos, 1997. – 376 p.
7. Kurdin V. N., Lichko N. M. Practical training sessionon storage and processing of agricultural products. Textbook, 2nd ed., Revised and supplemented – M.: Kolos, 1992. – 176 p.
8. Kutyga O. N., Vostrikova O. V. Laboratory Workshop on Biochemistry. – Tutorial. – Volgograd, 2011.

Qayimov Fazliddin Samiyevich,
MajidovKahramonHalimovich,
Professor, Bukhara Engineering-Technological Institute
E-mail: fqayimov@bk.ru

USING THE METHODS OF PULSE ELECTRIC FIELD IN THE TECHNOLOGY OF EXTRACTION OF COTTON OILCAKE

Abstract. The influence of the intensity of a pulsed electric field on the extractability of cotton cake is studied. Experimental studies have established that the process of extraction of the extracted material depends on the frequency and parameters of the extraction process using a pulsed electric field. To improve the technological processes of oil extraction and ensure the reduction of material and technological costs.

Keywords: cotton cake, pulse electric field, electrical conductivity, solvent temperature, field intensity.

The technology of extraction of oily substances is a necessary stage of production ofoil in the processing of various oilseeds [1; 2]. Cottonseeds are characterized by a peculiar quality and physical-chemical characteristics [3]. Extraction of oil from cottonseeds is carried out in two main stages: prepressing and extraction [4]. Duringprepressing of cottonseedjam in the resulting cake there remains 8–13% of vegetable oil, which must be extracted by the extraction method. Existing methods of cotton cake extraction are associated with certain difficulties and disadvantages. Therefore, recently considerable attention has been paid to the use of methods for the electric-physical treatment of oil-containing raw materials of the extracted reaction mass or the solvent used [5].

In order to intensify the technological processes of extraction of cotton cakes, the technology of extraction of oil-containing raw materials using pulsed electric field methodswas researched in the work.

Experimental studies were carried out using cotton cakes obtained in the prepressing shop of Kogon-Yog Extract JSC. To create a pulsed electric field, an installation (Fig. 1) mounted in the experimental laboratory of the enterprise was used.

Experimental studies were carried out at the following technological modes and ranges of electrical parameters of a pulsed electric current:

- electric field strength –1, 3, 5, 6 and 7 kW/cm;
- pulsefollow rate –0.5, 1.5, 5, 10 and15 Hz;
- solvent content –10, 20, 30, 40 and50 mass%;
- time of processing –10, 30, 60, 90 and 120 sec;
- pulseduration-10, 20, 30, 40 and 50 sec.

Studies have established the dependence of the electrical conductivity of crushed cottonseeds at a frequency of 100 Hz on the value of the inverse temperature in the range from 25 to 60 °C. The data obtained are presented in (Table 1).

Table 1.– Dependence of specific conductivity on inverse temperature (K^{-1})

Specific conductivity, cm/m 10^{-4}	**Inverse temperature, $1/T\ 10^2$, K^{-1}**
0	0
1	0.335
2	0.320
3	0.315
4	0.313
5	0.309
6	0.305
7	0.301
8	0.300

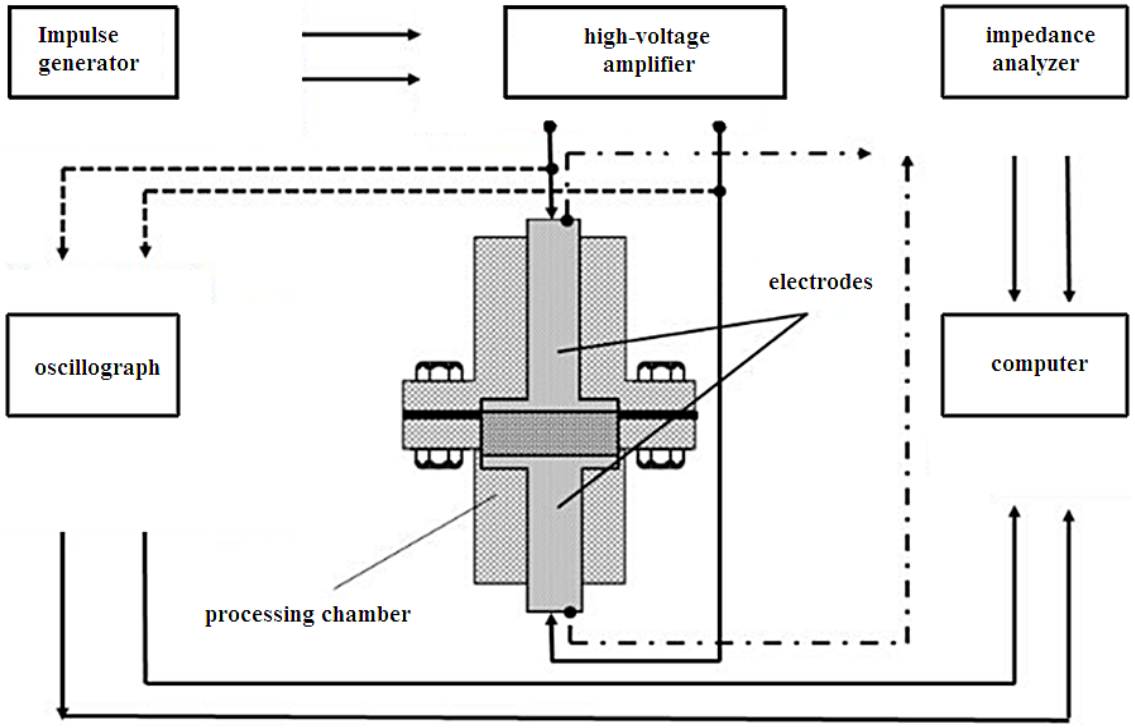

Figure 1. Schematic diagram of the experimental equipment of processing with pulsed electric field

Similar dependences of value of the electrical conductivity were obtained for samples with a 40% mass content of solvent (extraction gasoline) (Fig. 1).

Table 2. – The dependence of specific conductivity on the mass ratio of solvent

Mass content of the solvent,%	Specific electrical conductivity, См/м.10^{-4}
0	Ø
10	Ø,4
20	6
30	13
40	20
50	25
60	27

Studies have obtained data on the dependence of the specific electrical conductivity of the material on the mass content of the solvent (Table 2), which is in the range from 4 to 28 mkCm/M, which made it possible to determine the necessary energy loads and strength parameters at processing by a pulsed electric field.

Based on mathematical processing and planning of experimental results by the known method [5], the maximum yield of extractive substances for 48.2% was established.

To determine the effect of electrical parameters on the yield of extractive substances the following equation was used [5]:

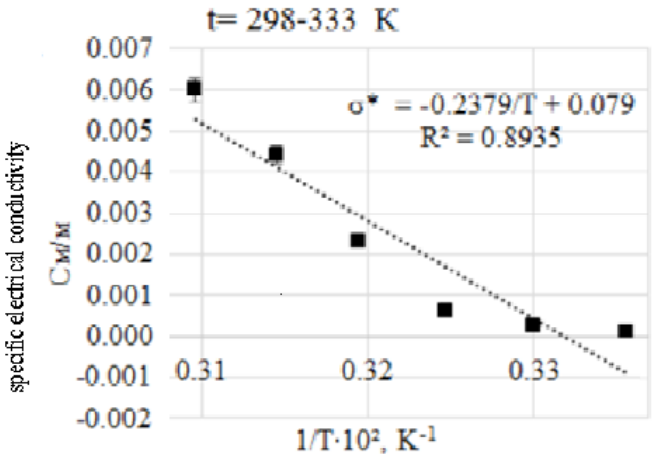

Figure 2. The dependence of the specific conductivity on the inverse temperature (solvent content is 40%)

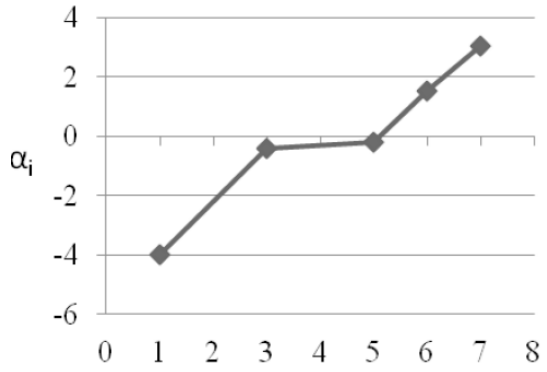

a) Strength, kW/cm

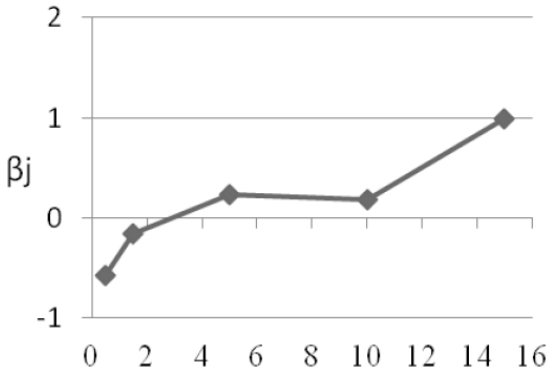

b) Frequency, Hz

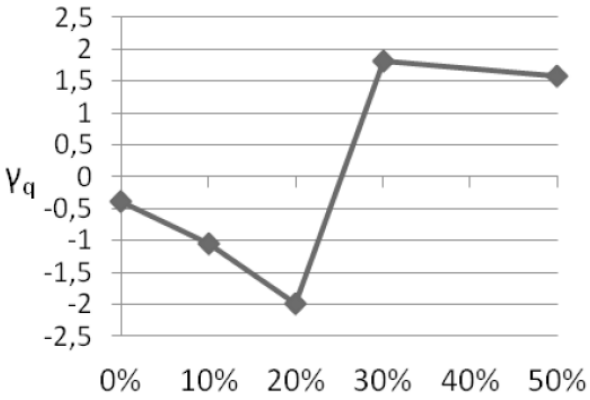

c) Solvent content, mass.%

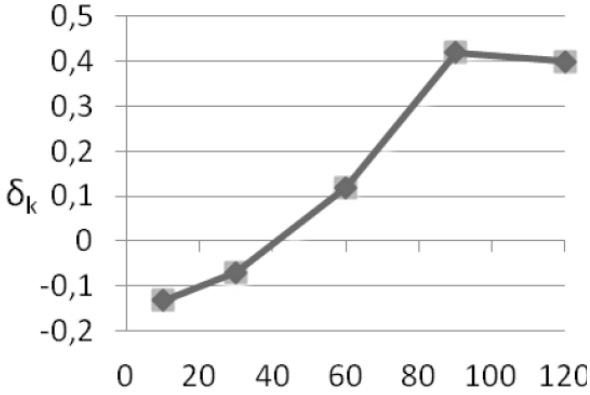

d) Time of processing, sec

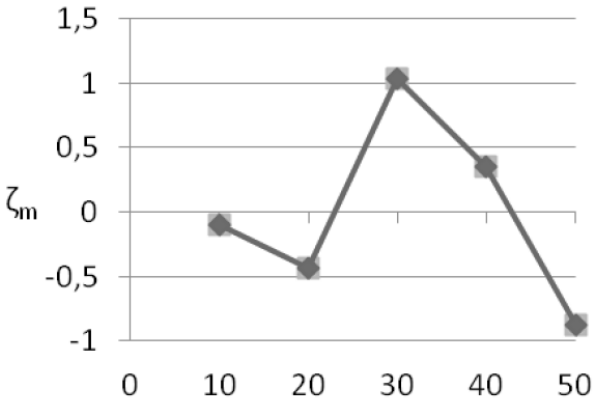

e) Duration of impulse, microsec

Figure 3. Effect of field strength (a), processing frequency (b), solvent content (c), processing time (g) and pulse duration (e) on the yield of extractives

$$K = \frac{c_0 - c}{c_0 - c_m} = \frac{1}{1+\beta} - \sum_{n-1}^{\infty} A_n \exp(-\mu_n^2 Dt / R^2) \quad (1)$$

where:

K – yield of extractive substances;

c, c_m, c_0 – extractant concentrations;

β – frequency of a pulsed electric field;

A_n; D – diffusion coefficient;

t – time;

The coefficients indicated in the equation are determined by the data shown in (Fig. 3).

Experimental studies have established that the process of extraction of the extracted material depends on the frequency and parameters of the extraction process using a pulsed electric field.

The proposed rational technical solution of the process of extraction of oil from cottonseed cake using processing with a pulsed electric field with electrical-physical effects at the stage of preparing the material for extraction allowed to improve the technological processes of oil extraction and to reduce material and technological costs.

References:

1. Kopeykovsky V. M. Technology of production of vegetable oils.– M.: Food Industry, 1982.– 410 p.
2. Shcherbakov V. G. Technology of production of vegetable oils.– M.: Kolos, 1992.– 207 p.
3. Ataullaev A. X., Sultanbekova D. M. and other. Technological properties of cottonseeds // Food industry, 1989.– No. 4.– P. 49–52.
4. Beloborodov V. V. The main processes of the production of vegetable oils.– M.: Food Industry, 1966.– 478 p.
5. Rogov I. A. Electrophysical methods of food processing.– M.: IN "Agropromizdat". 1988.– 272 p.

Sukhonos Maria,
Doctor of technical sciences, Professor,
Vice-Rector on scientific work, Professor
of the Department of project management
in municipal services and building
O. M. Beketov National University
of urban economy in Kharkiv
E-mail: Sukhonos.maria@gmail.com

Shevetovsky Valentyn,
Postgraduate, Department of project management
in municipal services and building
O. M. Beketov National University of urban economy in Kharkiv
E-mail: VVShevetovsky@gmail.com

Starostina Alona,
Candidate of technical science, head of the research center,
Associate Professor of the Department
of project management in municipal services and building
O. M. Beketov National University of urban economy in Kharkiv
E-mail: Alenastarostina2010@gmail.com

DEVELOPMENT OF A MATERIAL MANAGEMENT METHOD FOR AN INDUSTRIAL CONSTRUCTION PROJECT

Abstract. The paper deals with the problem of providing material resources for industrial projects. The proposed material management method based on the integration of plans integration and storage of resources, which allows to get the most rational savings from purchases at wholesale prices.

Keywords: project management, material resource, industrial facility, construction.

The construction of new industrial facilities today is the key to the successful and promising development of the production sectors of the economy in any country. The development of industrial infrastructure contributes to an increase in the number of jobs, wage growth, which increases the level of well-being of the population, and also, due to the innovative component of new industrial facilities, the level of competitiveness of the industry and the state as a whole grows.

In connection with the increasing relevance of the issues of creating new industrial facilities, there is a need for science-based and economically viable methods for building industrial enterprises. This forms the purpose of this paper, which is to develop a method for managing the material resources of industrial construction projects.

Industrial construction projects (ICP) have an unconventional life cycle [1, 11]. First of all, this is due to their promising type of activity, since it is on what type of innovative production the company will choose and the unique equipment that will ensure the output depends. As a rule, this equipment is made to order, has a long production time, and is purchased under prepaid contracts, payments for which are made even before the start of the start-up

schedule. These projects are also distinguished by scale and, depending on the functional purpose of an industrial facility, consist of a complex of design (planning) and construction works of separate structures: industrial buildings, workshops and factories (main and auxiliary); energy buildings (CHP, boiler, transformer substations); transport and storage buildings and structures (warehouses, terminals, locomotive depots); administrative and household buildings (engineering, laboratory buildings of industrial enterprises); plumbing installations for the maintenance of water supply and sewage (pumping, water towers). That is, many both specific and unified (of the same type) resources, which are acquired at different times and under different conditions, is required for the implementation of ISP, which requires special attention when planning purchases and coordinating their volumes [1, 12].

Many studies are devoted to procurement logistics management issues, among which [2–5], but all of them are tied to the production process, which is cyclical in nature, and not to the project activity, which is unique and has known time constraints. That requires the refinement of existing procurement logistics methods in terms of their applicability to meet the requirements of ISP.

To ensure the implementation of ISP appropriate to use the software. Now, the most widely used in construction has been the Microsoft Project software, which is recommended by the authors of the paper. Thus, for the classification of project resources, it is proposed to use the structure presented in [6, 20], namely, to allocate labor, cost and material resources. Due to the specificity of the resource base, it is necessary to introduce additional gradation for material resources, namely, to divide them into unique, specific and unified resources. The first group consists of unique resources, as mentioned above, they are manufactured for a long time, made to order, have a high cost, are prepaid before the start of the project. Specific – it provides resources that can be made to order, but, as a rule, have several alternatives and different payment systems. Unified – this kind of resources is available in large quantities, at any time, from any suppliers and under different contracts. What forms a large pool of alternative scenarios for the procurement of material resources. As a rule, when purchasing unified materials in large quantities, the price per unit of production decreases, which creates an additional source of savings. However, there is not always a place to store purchased resources in enough quantities. The way out of this situation is the use of the stream construction method and the use of the erected sections of facilities for storage facilities.

Thus, we present the steps of the proposed method for the management of material resources of the ISP. The first step is to determine milestones of the PCP, the delivery and installation dates of unified and specific resources, and also to add them to the Gantt chart in Microsoft Project. The next step, based on the obtained milestones, is the ISP network schedule. A pool of necessary resources is formed, and resources are assigned to tasks. After the appointment, a resource schedule is formed, that is, the required daily amount of each type of resource is determined.

To use the construction site for the needs of storage of resources, it is necessary, as the next step, to divide the area into sections, then determine which sections for which needs and for which period can be used. Based on these data, a calendar schedule of available storage areas at the construction site is formed, with an indication of their qualitative and quantitative characteristics.

The next step in the ISP material management method is the allocation of those resources, the purchase of which cannot be moved in time and the volumes are changed. It is also necessary, if necessary, to "book" in the calendar schedule a place on the construction site for these resources.

It then reviews the remaining storage sites and the remaining resources. Resources are ranked depending on the size of the savings that 1 m^3 of space brings when purchasing this resource at a wholesale price.

The next step is to fill the storage areas at the construction site in such a way as to, firstly, ensure the uninterrupted supply of the necessary resources for construction. Secondly, to ensure the purchase and storage of the maximum amount of resources, with the greatest savings of 1 m^3 of space. And, thirdly, to reduce as simple as possible the plots that can be used for the needs of storing material resources for ISP after the materials from this site have already been used for construction. When distributing purchases in this way, it is also advisable to pay attention to the possibility of moving non-critical project tasks, which allow for a more flexible use of the material resources of the ISP.

The finally stage of the method is the formation of a unified plan for the procurement and storage of material resources for the implementation of ISP based on the received calendar data on their purpose, procurement, delivery and use.

Thus, the paper describes the ISP material management method, which, unlike the existing methods, is based on the specifics of the life cycle of these projects, takes into account the gradation of material resources to specific, unique and unified, includes an analysis of the construction site sections from the point of view of its use for storage needs material resources and has a basic outgoing document a single plan for the procurement and storage of material resources for the implementation of ISP.

The advantage of this method is the integration of the ISP base plan – the project procurement plan for material resources and the storage plan for these resources. Also, the priorities of the method include the possibility of choosing the optimal variant of ISP at cost due to the purchase of standardized products at a wholesale price.

The disadvantages of the method include many stages strictly regulated in the order of implementation, which, subject to lack of information in one of them, reduces the quality of the results. Also, a negative fact is the impossibility of performing operations in one software product, which leads to the need to import large amounts of data, which increases the possibility of various kinds of errors.

Further study and refinement require the classification of construction sites, with the aim of grading them according to the storage conditions of various types of material resources, developing a change management method related to providing ISP material resources, as well as automating the proposed method to increase the number of obtained potential ISP implementation scenarios by reducing the time to implement the steps of the method and simplify data import processes.

References:

1. Сухонос М. К. Модель життєвого циклу проектів будівництва промислових об'єктів / М. К. Сухонос, В. В. Шеветовський, А. Ю. Старостіна // Науково-технічний збірник «Комунальне господарство міст». Серія: технічні науки та архітектура. 2017.– № 193 – С. 10–14.
2. El Khayyam Y. Integrated production and logistics planning / El Khayyam Y., Herrou B. // International Journal of Online Engineering. 2018.– Vol. 14.– Iss. 12.– P. 84–96.
3. Díaz-Madroñero M. A mathematical programming model for integrating production and procurement transport decisions / M. Díaz-Madroñero, J. Mula, D. Peidro // Applied Mathematical Modelling. 2017.– No. 52 – P. 527–543.
4. Absi N. The multi-item capacitated lot-sizing problem with setup times and shortage costs / N. Absi, S. Kedad-Sidhoum // European Journal of Operational Research. 2008.– No. 185(3) – P. 1351–1374.
5. Prostean G. Logistics scenario for wind turbine assembly based on ERP / G. Prostean, C. Vasar, A. Badea // Advances in Intelligent Systems and Computing. 2018.– No. 634 – P. 194–200.
6. Богданов В. В. Управление проектами в Microsoft Project 2017. Учебный курс(+CD) – СПб.: 2018.– 595 с. с ил.

Section 4. Chemistry

Ergasheva Saodat,
Kurbanbaeva Sanobar,
Badriddinova Farida,
Kadirov Baxodir,
Tashkent Chemical-technological institute
E-mail: Ulug85bek77@mail.ru

SYNTHESIS OF CU: ZN-HEDP AND COMPOSITIONS WITH A BIOCIDE ACTIVITY BASED ON THEM

Abstract. For the normal functioning of technological schemes with a closed water circulation, it is necessary to prevent not only corrosion and scaling, but also biofouling. It should be in view of the fact that the problem of biofoulingis considered as such and as a problem of microbiological corrosion. Thus, the reaction of obtaining inhibitors with universal properties based on HEDP and CFR, in the ratio of initial reagents CFR: HEDP: Cu: Zn = 0.5: 2: 0.25: 0.75 ÷ 0.5: 2: 0.75: 0.25. It has been established that when using CFR as a synergistic component, it is possible to increase the effectiveness of corrosion inhibition of copper-zinc complexes of HEDP by 2–4 times, which explains the advantage of synergistic efficiency.

Keywords: normal functioning, obtaining inhibitors, universal properties, synergistic component, corrosion inhibition.

Introduction. For the normal functioning of technological schemes with a closed water circulation, it is necessary to prevent not only corrosion and scaling, but also biofouling. It should be in view of the fact that the problem of biofoulingis considered as such and as a problem of microbiological corrosion.

Biological impurities – algae, mold, fungi penetrate with water into heat exchangers and pipelines, contaminating their surface. The contamination reduces the efficiency of heat exchange; contribute to the development of corrosion, which, in turn, reduces the service life of the water-cooling system. To eliminate these phenomena, bactericides of directional action are used. Both oxidizing and non-oxidizing agents are used. The most common bactericides-oxidants include chlorine and bromine. These substances in most cases provide a high level of protection against microorganisms.

Currently, more effective drugs are being developed with fewer restrictions on application. However, for certain specific cases, special compositions are offered. Thus, the authors [1; 2] consider the composition content containing NTF and or HEDP, polyacrylamide (PAA) and Zn^{2+} as a corrosion inhibitor for structural steels in neutral aqueous solutions as well as biocidal. A biocidal composition for suppressing the vital activity of sulfate-reducing bacteria is offered, containing a synergistic mixture of the preparation, obtained by the interaction of hexamethylenetetramine with a light fraction of waste

production of glycerol ("Bactericide LPE-11B") and formalin at ratios of 1: 9–9: 1. It is indicated that the minimum effective concentration of a biocide is 270 mg/l [3]. The use of the product of the interaction of hexamethylenetetraamine and monochloroacetic acid as a reagent to suppress the growth of microorganisms [4].

Isothiazolone is used as biocides in the new multi-component compositions – citric acid / PF (HEDP) / polymer acrylate. It is shown that a new inhibitor can reduce corrosion, prevent scaling and growth of microbes in the tested conditions [5].

Along with sisothiazoline, quaternary phosphonium salts, dichloroiso- and trichloroisocyanuric acids, glutaraldehyde are also used to reduce the problems of biofouling of circulating systems [6]. Scale inhibitors include NTF, PBTC, polyacrylic acid, phosphono-sulfuric acid; corrosion – HEDP, phosphinosulfonic acids, etc.

Company Nalco suggests using natural products as a biocide, in particular, oils extracted from eucalyptus and the growth of tea crops. The composition contains a mixture of oils, and in specific versions of the preparation can be applied in concentrations from 1 to 250 mg/l [7]. For the same purpose, it is offered to dose reagents such as ammonium salts of polydimethyldiallyl chloride, polydimethyldiallyl-bromide, polydecyldimethyl-halides, etc. into water. It is indicated that the molecular weight does not have a noticeable effect on the effectiveness of preparations, the preferred area is from 10.000 to 3.000.000, the concentration in water can reach 1000 mg/l [8]. It was established that when trichloroisocyanurate (1) is used as a biocide, active oxidizing agents in the form of OH^-, HO^- and active oxygen, destroying bacteria, algae, etc. are formed in water. In the experiments, the bacteria content in water was 105–106 ml; under the influence of (1) and exposure for 12 hours, complete inactivation was observed. Also, the authors found that (1) and phosphonates are compatible preparations [9].

NTF compositions with Zn (2+) and various additives as synergistic fragments are used as scale inhibitors and corrosion inhibitors. As an additive to Zn-NTF, the following are used: N'-eran-N,N1,N-trimethyl ammonium bromide (CTAB) [10]; EDTP, aminoethylidenediphosphonic acid [11]; phthalic anhydride [12; 13].

Another biocide and biodegradable dispersant includes alkyl dimethyl- benzyl ammonium chloride, dialkyldimethylammonium chloride, propylene glycol [14].

To prevent the formation of bacterial deposits [15], for example, in the paper industry, it is offered to introduce into the water cationic polyelectrolytes - 1,1-oxybis (2-chloroethane) and / or epichlorohydrin with amines, N-methylmethanamine or ammonia. The preferred concentration of the composition is 0.5–50 mg/l.

Currently, the literature describes several thousand chemical compounds with biocide properties, however, in practice, for security reasons, only hundreds of them are used. Every year, dozens of biocide preparations are removed from production due to low antimicrobial activity or high toxicity.

Experimental part.

The method of obtaining zincate-HEDP. The technique is carried out in the following sequence: the water in the calculated amount is poured in the reactor - a heat-resistant glass, and 1g of glycerin is add. The mixture is stirred for 1–2 minutes. Then 2/3 of the calculated amount of HEDP is add. The temperature at the same time should be 30–35 °C. After that, zinc oxide is sent to the reactor, stirred until complete dissolution and obtaining a clear liquid. Then, the calculated amount of finely-ground sodium hydroxide is added to the reaction mixture and vigorous agitation is continued.

At the same time the temperature is controlled in the range of 20–25 °C. Then, the remaining 1/3 part of HEDP is added to the reactor. The solution, losing white color, gradually becomes transparent. The finished product is cooled to room temperature for

stabilization and stored under these conditions for 30–60 minutes. The yield is 98.2%.

The method of obtaining the copper complex HEDP. A calculated amount of 110.0 ml of water, 1.0–3.0 g of glycerin (or citric acid), 1.0–3.0 g of extraction phosphoric acid is poured into a glass, mixed and the calculated amount of copper oxide is added, heated up to 50–75 °C until complete dissolution of copper oxide. In a separate beaker, 15 g of HEDP is dissolved in 21.0 ml of water and 4.5 g of hydroxycine is added. The reaction is carried out at room temperature. The reaction mass is maintained for 20–30 minutes.

Then, with intensive transfer, the solution prepared in the first glass is added to the reaction mass. A clear blue solution is obtained in quantitative yield. Obtaining an inhibitor with biocide activity. The suggested method of obtaining a multipurpose inhibitor is carried out in three stages: stage No. 1, obtaining Cu-HEDP; stage No. 2, production of Zn-HEDP and stage No. 3 of preparation of a mixture of Cu-HEDP with Zn-HEDP ("ICSB-UNI-1") and preparation of a composition with the addition of synergistic activity of the component - carbamide-formaldehyde resin (CFR).

The composition and structure of the obtained product "ICSB-UNI-1" is established by various physical-chemical methods of analysis.

ICSB-UNI-1 was analyzed on an "Agilent Technology" chromatography-mass spectrometry GC / MS AT 5973N using the "DRUGSP-SHORT.M" method using a 30 m × 0.25 mm capillary column with 5% phenylmethylsiloxane at an injector temperature of 280 °C, sample size 1 ml. Comparison with the basic data of the device proves that the obtained "ICSB-UNI-B" has high purity. The infrared spectrometer "ICS-UNI-B", which was taken on an Agilent Technology FTIR-640 instrument with a recording range of 4000–400 cm^{-1} and the number of scans is 12, a band is present at 1250–1300 cm^{-1} related to localized bond P = O; the band at 2500–2700 cm^{-1} refers to the stretching vibrations of the group of the fully deprotonated PO_3 group; there are also bands at 1180–1240 and 2500–2700 cm^{-1} related to the stretching vibrations of the P – O (H) bond of the protonated phosphate groups, which indicates that the complexes are partially protonated; the intense band at 1042 cm^{-1} refers to the stretching vibrations of the Cu – O bond; the band at 650–750 cm^{-1} to the stretching vibrations of the C – P bond, the intense band at 570–550 cm^{-1} to the stretching vibrations of the Zn – O bond; the absorption bands at 480–460 cm^{-1} to the deformation vibrations – O – P – O. This allows us to conclude that the coordination of the PO_3 group with the Zn atom occurs with the localized π-bond P = O, the oxygen atoms in the PO_3 group do not equal rights.

Results and discussion. As was shown earlier, multipurpose reagents can be created on the basis of organophosphonates. However, due to the relatively high cost of such products, as well as the lack of raw materials for the production of products of this type in our republic, the possibility of overcoming this situation is to create a relatively inexpensive, most effective composition containing organophosphonates in the amount of 30–40% from the total mass of the reagent.For this purpose, compositions obtained on the basis of the copper-zinc complex HEDP with the addition of CFR were studied. Inhibiting properties of the composition are presented in (table 1 and 2).

Table 1. – The influence of the composition «ICSB-UNI-1» and CFR on the corrosion rate of steel grade St. 3, water hardness 8.9 mg/l

№	Inhibitor components	Inhibitor concentration, g/l	Average mass loss, g	Corrosion velocity, g/m²·an hour	Protective effect,%
1	*2*	*3*	*4*	*5*	*6*
1.	Without inhibitor	–	0.0390	0.750	–

1	*2*	*3*	*4*	*5*	*6*
2.	"IKSB-UNI-1": CFR (1:1)	4.0 6.0 8.0 10.0	0.0097 0.0086 0.0054 0.0038	0.249 0.221 0.138 0.097	75.1 77.9 95.1 97.9
3.	"IKSB-UNI-1": CFR (2:1)	4.0 6.0 8.0 10.0	0.0075 0.0056 0.0016 0.0008	0.148 0.112 0.034 0.017	80.3 85.1 95.5 97.7
4.	"IKSB-UNI-1": CFR (3:1)	4.0 6.0 8.0 10.0	0.0073 0.0054 0.0015 0.0008	0.172 0.151 0.091 0.075	77.0 79.9 87.8 90.0

From the data presented in (table 1 and 2), it can be seen that with the addition of CFR to the composition "ICSB-UNI-1", the efficiency of the initial reagent as a corrosion inhibitor can be significantly increased. The protective effect against steel corrosion when using reagents "ICSB-UNI-1" and CFS is more than 97% in water of hardness 8.9 mg/l and more than 94% in water of hardness 12.9 mg/l.

Table 2. – The influence of the composition "IKSB-UNI-1" and CFR on the corrosion rate of steel grade St. 3, water hardness 12.9 mg/l

№	**Inhibitor components**	**Inhibitor concentration, g/l**	**Average mass loss, g**	**Corrosion velocity, g/m²·an hour**	**Protective effect,%**
1.	Without inhibitor	–	0.0390	0.750	–
2.	"ICSB-UNI-": CFR (1:1)	4.0 6.0 8.0 10.0	0.0121 0.0061 0.0050 0.0034	0.310 0.156 1.282 0.087	68.9 84.3 87.1 91.2
3.	"ICSB-UNI-": CFR КФС (2:1)	4.0 6.0 8.0 10.0	0.0110 0.0048 0.0032 0.0023	0.282 0.123 0.082 0.058	71.7 87.6 91.7 94.1
4.	"ICSB-UNI-": CFR (3:1)	4.0 6.0 8.0 10.0	0.0109 0.0047 0.0031 0.0023	0.279 0.120 0.079 0.058	62.8 87.9 92.0 94.2

Experiments on the inhibition of the vital activity of microorganisms (biofouling) were carried out on the basis of standard algological requirements in the following order: objects of experience (or research) were carried out in microalgae Chlorella vulgaris, as well as in E. Clara cultures belonging to the Euglena Ehr family. Experiments were performed in standard living food conditions for cultures. Table 3 shows the results of the same cultures grown in a tough food environment.

Table 3.– The biological effect of preparations on the growth of E. Clara in a hard food environment

Reagent dose	Lysis area sizes (sm)	
	"ICSB-UNI-": CFR(1:1)	"ICSB-UNI": CFR (2 : 1)
0.1	0.42 ± 0.03	0.23 ± 0.04
0.3	0.60 ± 0.05	0.67 ± 0.03
0.5	0.90 ± 0.07	0.98 ± 0.05
0.7	0.96 ± 0.08	–
Control	–	–

The results of the experiment show a dramatic effect of any amount of the preparation applied to the column of cultures planted in a hard food environment. Here, a separate indicator is *"ICSB-UNI-1"*, in which the concentration acts lethally at 0.5 m. When analyzing these results, the inhibitory effect of these preparations up to 92–96% *"ICSB-UNI-1"* on algae development that it is shown the presence of formaldehyde residues in the composition of this product is explained.

The effect of biomass formation was studied by conducting the same experiments on Scenedesmusoblianus cultures (Fig. 3). A certain concentration of "IKSB-UNI-1" is significantly reduced by 4–5 days of growing the biomass of these crops.

This is a result of the negative effects of the preparation, this decreases the vitality of the cells and destroys the main breeding cells.

In the control variant in the opposite position for 18–19 days of cultivation, the vitality of the cells was at the level of the proposed requirements, and the preservation of certain sizes of biomass was observed.

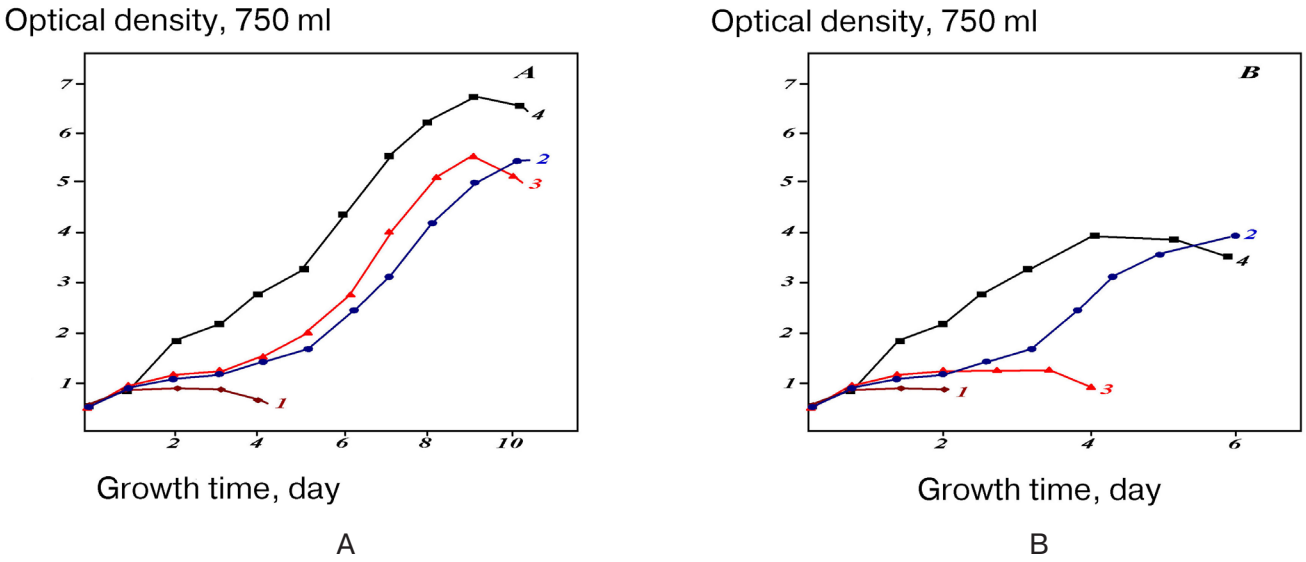

Figure 1. Performance of "ICSB-UNI-1"+CFR by different concentrations at the growth of Chlorellavulgaris cell: A – control, B – experiment, (1–0.1 ml/l, 2–0.3 ml/l, 3–0.5 ml/l, 4–0.7 ml/l)

It has been established that compositions containing only zinc in their composition are not a biocide and are not capable of suppressing the growth of microorganisms; the increase in the composition of the proportion of copper compared with the molar fraction of zinc increases the biocidal effectiveness of the composition (100% of the dead microorganisms), which confirms the role of copper in the compositions obtained.

Conclusion. Thus, the reaction of obtaining inhibitors with universal properties based on HEDP and CFR, in the ratio of initial reagents CFR: HEDP: Cu: Zn = 0.5: 2: 0.25: 0.75 ÷ 0.5: 2 : 0.75: : 0.25. It has been established that when using CFR as a synergistic component, it is possible to increase the effectiveness of corrosion inhibition of copper-zinc complexes of HEDP by 2–4 times, which explains the advantage of synergistic efficiency. At the same time, "ICSB-UNI-1", taken with Cu: Zn in 0.25: 0.75 ratios, effectively suppresses the vital activity of microorganisms and, accordingly, biofouling.

References:

1. Pat. CN1772656A KHP. Manufacture of composite antiscale – corrosion in hibitor for treating recirculated cooling water / Gong Qiuming, Zhao Yanhui et al. Опубл. 17.05.2006; C.A. 2006.– V. 145.– 195062 p.
2. Pat. CN1781858A KHP. Low-phosphine composite inhibitor for carbon steel material in water / Wang Fengyun, Lei Wu, Xia Mingzhu. Опубл. 07.06.2006, C.A. 2006.– V. 145.– 362799 p.
3. Pat. CN1804123 AKHP. Scale and corrosion inhibitor for carbon steel / Du Min, Gao Rongjie et al. Опубл. 19.07.2006. C.A. 2006.– V. 145.– 475641 p.
4. Pat. DE19853561 Al Германия, МКИ C02F 005–14. Scale and corrosion inhibitor for water / R. Kleinstueck, Ch. Holzner, A. Spaniol. Заявл. 20.11.1998. Опубл. 25.05.2000. C.A. 2000.– V. 133.– 8818 p.
5. Rajendran S. et al. // Anti-Corros. Methods Mater. 1998.– V. 45.– No. 4.– P. 256–261.
6. Role of citrate ions in the phosphonate-based inhibitor system for mild steel in aqueous chloride media / Gunasekaran G., Dubey B. I. et al // Defence Science J. 2005.– V. 55.– No. 1.– P. 51–62.
7. Schmith G. et al. / 8th Eur. Symposium. 1995. C.A. 1996.– V. 124.– 121487 b p.
8. Study on synergistic effect of molybdate / Tang Yongming, Yang Wenzhong, Lu Huifeng, Ju Bin // Nanjing Huagong Daxue Xuebao, Ziran Kexueban. 2001.– V. 23.– No. 2.– P. 64–66. C.A. 2001.– V. 135.– 9754 p.
9. Synergistic effect of ethyl phosphonate and Zn^{2+} in low chloride media / Ra- jendran S., Apparao B. V., Palaniswamy N. // Anti-Corros. MethodsMater. 1998.– V. 45.– No. 6.– P. 397–402. C.A. 1999.– V. 130.– 69499 p.
10. Synergistic effect of molybdate and Zn^{2+} on the inhibition of corrosion of mild steel in neutral aqueous environment / Rajendran S., Apparao B. V., Palaniswamy N. // J. Electrochem. Soc. India. 1999.– V. 48.– No. 1.– P. 89–93.
11. Pat. CN1715216 AKHP. Manufacture of stable scale and corrosion inhibitor / Shen Zhichang. Опубл. 04.01.2006. C.A. 2006.– V. 145.– 50597 p.
12. Kompleksowa ochrona ukladow wodnych inhibitor amiopartyminazwiaz – kach fosfonowych / FalewiczP. //race Naukowe Institutu Technologii Nieorganiczneji Nawozow Mineralnych Politechniki Wroclawskiej. 2002.
13. Synergistic effect of NTMP, Zn^{2+} and ascorbate in corrosion inhibition of carbon steel / Rao B. V. Appa, Rao S. Srinivasa, Babu M. Sarath // Indian J. of Chem. Technology. 2005.– V. 12.– No. 6.– P. 629–634.
14. Synergistic effect of molybdate and Zn^{2+} on the inhibition of corrosion of mild steel in neutral aqueous environment / Rajendran S., Apparao B. V., Palaniswamy N. // J. Electrochem. Soc. India. 1999.– V. 48.– No. 1.– P. 89–93.
15. Synergistic effect of NTMP, Zn^{2+} and ascorbate in corrosion inhibition of carbon steel / Rao B. V. Appa, Rao S. Srinivasa, Babu M. Sarath // Indian J. of Chem. Technology. 2005.– V. 12.– No. 6.– P. 629–634. C.A. 2006.– V. 145.– 107452 p.

Juraev Vays Narzullaevich,
Independent conpetitor, senior teacher
of Tashkent Chemical-technological institute
Boborajabov Bakhodir Nasriddin ogli,
Independent conpetitor, assistor
of Tashkent Chemical-technological institute
Vapaev Murodjon Dusummatovich,
doctorant of chair"Technology of plastmasses
and high-holecular compounds"of Tashkent
Chemical-technological institute
Ibadullaev Akhmadjon,
d.t.sci., professor, chief of chair
"Chemical technology of oil and gas processing"
of Tashkent Chemical-technological institute
E-mail: Ulug85bek77@mail.ru

MODIFICATION OF BITUMEN BU WASTE OF GAS-PROCESSING, GASO-CHEMICAL AND RUBBER INDUSTRIES

Abstract. In this article influence of combinated modification of road bitumen on the complexe of properties of the polymer-bitumen composition has been considered. It was shown increasingof working temperature interval and improvement of the physico-chemical properties of composition and also optimal composition of rubber-bitumen composites for car roads of sharply continental climate was elaborated.

Keywords: bitumen, gasopyrolysed resin, resin crumb, modified carbon, liquid rubber, composition, technology, road bitumen.

Introduction. In road branch the road bitumen is integral part. It is used for bondind and cohesion of mineral materials, introducing in tire-coverof car roads. In process of expluatation tire-covers didn't always can to preserve integrity during ofdemanded period of time owing insufficient quality of bitumen [1]. By this reason numerous investigations have been carried out with aim of perfection of base-physico-chemical indixes of road oil bitumen. Actual task in this direction is drawing in the industrial production of road materials home waste and also by-productsof different manufactures.

Objects and methods of investigation. The most perspective method of modification of oil bitumen concluded inusing of waste of gaso-processing, gaso-chemical and rubber industries as modifiers owing their low cost in comparasion with polymer modificators. Also one of important factors of utilization of waste at bitumen modification is ecological factor namelly decreasing of unused industrial waste.

In thisworkpossibility of using gaso-pyrolysis resin (GPR), rubber crumb (RC) and modified carbon (MC), which is a secondary raw material at acetylene production, in modification of composition of bitumen compositions has been investigated.

Gaso-pyrolysis resin – solid substance of black colour without odour, it's composition didn'tstable and has depended onpyrolysis raw material (Table 1).

Table 1.– Chemical composition of gaso-pyrolysed resin

Number of carbon	Akcanes	Dienes	Olephynes	Cycloalcanes	Arenes	Inall
5	0.8	0.89	4.91	0.19	0	6.79
6	0.22	0.41	3.87	0.41	32.94	37.85
7	0.25	0.14	0.84	0.45	11.23	12.91
8	0.12	0.08	0.18	0.48	9.75	10.61
9	0.04	0.1	0.04	0.15	7.56	7.89
10	0.03	0.11	9.07	0.4	5.23	14.84
11	0.18	0.69	2.95	0	0.47	4.29
12	0	0.15	1.84	0	0	1.99
Bcero	1.64	2.57	23.7	2.08	67.18	97.17

Rubber crumb – is strong zeduce to fragments rubberfractions of which in process of processing can differ by form and dimensions of particles. Howeverin final result, all these fractions have preserved the base characteristics of initial material: elasticity and molecular structure. For obtain of rubber crumb tire – covers unfit for usinghave been used as raw materials.

Modified carbon – carbon-containing secondary raw materials which has differedby chemical composition from nown sorts of low-structural technical carbon, T 900, T 701, T 705, P 803 (table 2) namely by high content of oxygen and hydrogen.

Table 2.– Elemental composition of MC and some sorts of technical carbon

Name of index	Content,%				
	MC	T 900	T 701	T 705	P 803
Carbon	88–90	96–99	96–98	96–98	97–99
Hydrogen	3–4	0.3–0.5	0.4–0.6	0.6–0.8	0.4–0.6
Oxygen	6–7	0.1–0.2	0.3–0.5	0.3–0.5	0.1–0.2
Sylfer	–	0.1	0.3	0.3	0.2
Ash content	0.8–0.9	0.1–0.2	0.4–0.6	0.4–0.5	0.4–0.5

Investigation of extraction products of carbon-containing secondary raw materials has witnessed about presence 12% of organical compounds apretizated on surface of carbon particles. Following element composition has been determined (%): C-92.11; H-5.70 and O-2.19. The formula of the extract is $C_{54}H_{40}O$.

Average-numeral molecular mass of thisraw-material is equaled 700 according to data by gel-chromatography. IR-spectroscopical invitigation has shown that products of extraction are combination of condensated aromatical and paraffino-naphthene hydrocarbons and also oxygen-containing carbonyl compounds. On this in particularappearance of characteristical bands of absorption in ranges of 3050 sm^{-1} (valent vibrations of C-H – bonds of aromatical ring), 2860, 2930 and 2975 sm^{-1} (valent vibrations of C-H – bonds of methyl and methylene groups) has been indicated and also bands of absorption at 1710 sm^{-1} (> C = O) in carbon chain.1730 sm^{-1} (in resins of asphaltenes); in range1500–1600 sm^{-1} correspond to valent vibrations of > C = C < bonds forming at thermal cyclization and oligomerisation of acetylene. PMR-spectrums have indicatedon the presence of protons at d = 6.70; 6.85 and 7.10 ppm, typical for aromatic structures and their derivatives.

Extragatedproduct has given narrow individual signal of EPR with concentration PMC = $1 \cdot 10^{14}$ spin/g. It is necessaryto note that results of mass-spectrometricalinvestigation also have confirmed the proposed composition of extractionproducts. Carring out investigationhasshown that carbon-containing secondary raw-material is anMC surface of which has microcapsulated by oligomerical oxygen-containing compounds. Thickness of oligomeric cover calculated by values of specific geometrical surface was equiled 50–60 E.

MC is characterized by higher value of oil and iodine numbers, what is conected with roughness of surface (S = 25–30 m^2/g) and presence of polyconjugated systems. Also it is necessaryto note a high degree of dispersion.

Electronno-microscopicalinvestigationhaswitnessed that structure of particles of MChas different insome degreefrom particles of initial technical carbon: characteristical for technical carbon clear borders of spheroidal form of particles are absented.

However after thermotreatment at 1573 K during 1 hour (in nitrogen atmosphere) it's structure has approachedtostructure of technical carbon and at thismiddle surface diameter of particles has decreased from 30.6 to 21.5 nm. Increasing ofspecific geometric surface from 20.3 to 29.3 m^2/g was observed what isconnectedwith process of dispergation of more large particles owing to evaporation moisture and othersaccompaining compounds in process of thermotreatment.

By comparision of results of rontgeno-graphical investigation of initial and MC it was determined that for they is typical presence of impuritiesof crystalline phasewhatcan beattributed to hydrocarbons containing in iheircompositions (12%). The base phase of MCwas phase having typical turbostrated structure what is proved by typical characteristical asymmetrical profile of diffractional bands. Diffractogramof MC is differencedfromsuch of technical carbon by low regulation of turbostratedbundles of layers about which value J_{002}/J_{002} has witnessed.Degree of regulation of MC (parameter J_{002}/J_{002}) has increased athigh-temperature (973–1573 K) treatment. Dimensions of ranges of cogerated distance of amorphous phases have been determined; dimentionsof layers are in limites 15–20 E.

Carring out investigations have allowed to suppose that structure of MCis probably is middle stage of process of formating soot structures. It is possifle to suppous that using of carbon filler appretirated by oligomeric cover consisting from systems ofconjugation has allowed to developein principle new approach for creation polymer-bitumen compositions with improvment properties.

Bitumen oil-roading (BOR) of marks 40/60 and 50/70 has been used in this investigation and their initial characteristics are presented in (table 3).

Table 3.– Initial characteristics BOR40/60 andBOR50/70

Mark	Temperature of softing by "Ring and Ball", °C	Temperature of fragility by Fraasy, °C	Penetration at 0 °C	Penetration at 25 °C	Duration at 0 °C, sm	Duration at 25°C, sm	Elasticity at 0 °C,%	Elasticity at 25 °C,%
BOR40/60	59.35	–22.4	12.5	40	7.6	24	21.05	33.3
BOR50/70	58.5	–24.8	31	50	10.4	30.7	5.7	18.6

The base characteristics of prepared samples of bitumen astringent havebeen analysed by following methods: thermal heat capacity – by method "Ring and Ball"; low temperature properties – by the method of determination of fragility temperature – by method Praasy, index of penetration – by method ofdetermination of depth of needle penetration; plasticity – by method ductiality; reduction –by method of determination of elasticity; adgession of bitumen – by method passive cohesion with mineral materials.

Obtained results and their discussion. Samples of modified bitumen were prepared; base characteristics of bitumen were determined and on this base optimal values of it'sindexes of qualityby two samples of bitumen compositions were take away (table 4). From data of table 4 it is shown that modifining additionshave im-provemen the base index of heat-stability–the softening temperature. Introduction of modificators has decreased index of penetration bothat 25 °C and 0 °C, owing towhichchangingof mark of initial bitumen was carried out. Temperatureof fragility is one of the important index of low-temperature properties of compositions. It was determined that only for first sample (3% GPS + 5% liquid rubber) improvement of this index has been observed what can be explained by presence of polymer in common with GPS in modified addition.

Table 4.– Basical properties of modified samplesof bitumen

Samply	Temperature of softing, °C	Temperature of fragility, °C	Penetration at 0 °C	Penetration at 25 °C	Duration at 0 °C, sm	Duration at 25 °C, sm	Elasticity at 0 °C,%	Elasticity at 25 °C,%
BOR40/60+3% GPS+3% liquid rubber	61.05	–26.3	12	23	6.7	16	11.76	42.18
BOR50/70+20% of rubber cruimb	60.85	–19.3	25	36	6.6	14	10.6	21.7
BOR50/70+7% MU	60.2	–21.4	27	38	6.1	12	8.3	21

Index of tensilityfor all samples was lower than forinitial bitumen what can be explained by an increasingof viscosity of bitumen composition at introduction of additions. Improvementof index of elasticity at 25 °C and 0 °C for all samples was observed but however thisindex wasbest at using GPS, liquid rubber jointly with GPS and MC in a modified addition.

Also in this work it was carried out determination of adhesium by method of "passive cohesion". Investigationhas shown that compositions with modified additions has corresponded to GOST by full cover of surface of mineral material by bitumen film after exposition of sample in boiling distilled water during 30 min. and alsoall samples of bitumen bindings have carried out tests on cohesionwith mineral materials.

Republic of Uzbekistan is characterized by charp continentaly climate, high solar activity in the summer period and low temperatures in wintry period. By this reason at the same time with data presented earlierthe frost-resistance of materials is also very important characteristic. Obtainedresults have shown that samples undergoneto testing after 30 cycles of freezing and thawing have decreased strength at pressing on value 14% and lest from initial. At inspection destruction of samples wasn't observed. Coefficient of frost-resistance at thiswasequaled from 0.80 to 0.95. These data havewitnessed about sufficient frost-resistance of testing samples of asphalt-concrete.

It is necessary to note that used regimeof testing on frost-resistance was more hard in comparison with realregime of covers exploitation. Didn't exclude that destruction effect from charpchanging of temperature of samples can bedisplay in higher degree than at work in real conditions of exploitation.

Carring out investigationshave witnessed a considerable heat-frost resistance of asfalto-concrete on the base ofrubber-bitumen composites of following composition: BOR40/60 (BOR50/70) – 7%, GPS – 1–3% from mass of bitumen, liquid rubber – 1–3%

from mass of bitumen and rubber crumb – 20–25% from total volume and also mineral additions.

Resume. Thus in work possible using of waste gas-processing, rubber industry and liquid rubber as modifying additives to bitumen BOR40/60 and BOR50/70 has been determined. These modifiers haveallowedto increase work temperature interval of bitumen and also it's elasticity but at thisthey have decreased index of penetration changing markof initial bitumen. According to carring out investigatons the optimal composition of rubber-bitumen composites for car roadsof charp continental climate has been elaborated.

References:

1. Vapaev M. D., Boborazhabov B. N., Teshabaeva E. U., Ibadullaev A. S. Road compositions based on modified bitumens // Austrian Journal of Technical and Natural Sciences No. 9–10.2018.– P. 34–37.
2. Boborazhabov B. N., Vapayev M. D., Akhmadzhonov S. A., Ibadullayev A. S. Issledovaniye svoystv dorozhnykh bitumov, modifitsirovannykh kombinirovannymi dobavkami // Tosh DTU khabarlari Ilmiy-tekhnikaviy va amaliy jurnal – No. 3.– Toshkent, 2018.– P. 167–172.
3. Ibodullayev A. S., Seydabdullayev Y. A. O. Issledovaniya uglerodistogo materiala i yego vliyaniya na svoystva kabel'nykh rezin // Jurnal "Kompozitsionnyye materialy".– Tashkent, 2015.– No. 3.– P. 25–28.

Vafaev Oybek Shukurlaevich,
Doctor of Philosophy (PhD), Senior Research Associate,
LLC Tashkent Scientific Research Institute of Chemical Technology
E-mail: vafaev.oybek@mail.ru
Tadjikhodzhaev Zokirkhodzha Abdusattorovich,
Doctor of Technical Sciences, Professor,
leading research associate,
LLC Tashkent Scientific Research Institute of Chemical Technology
Djalilov Abdulahat Turapovich,
Director, Academician of ANRUZ, Dr. Chem. Sciences, Professor,
LLC Tashkent Scientific Research Institute of Chemical Technology
E-mail: a.t.djalilov@mail.ru

INFLUENCES OF DEPRESSOR ADDITIVE ON QUALITY INDICATORS OF DIESEL FUEL

Abstract. The possibility of decrease in temperature of hardening of diesel fuel by means of the depressor additives synthesized on the basis of secondary polymeric waste is shown in article. Depressor efficiency of additives depending on a ratio of their components is studied. It is shown that for decrease in temperature of freezing of diesel fuels by the most effective are introduction of depressor additives.

Keywords: depressor additiv, temperature of hardening, diesel fuel, efficiency of additives.

In the works on development of depressor additives, various by the nature, which are carried out by us earlier the factors influencing efficiency of their action on low-temperature properties, such as compatibility of a depressor with diesel fuel, size of its concentration, temperature of introduction of a depressor to fuel, presence of water and some other indicators have been investigated.

From the depressors synthesized by us for further experiments the most effective additive DP3 capable at concentration of 0.2% is defined to lower fuel hardening temperature on average on 12–180 °C depending on its hydrocarbonic structure.

Often diesel fuels differ on hydrocarbonic structure, i.e. in different consignments of run diesel fuel paraffin of a normal structure (N paraffin), isoparaffin, aromatics and others therefore the research of hydrocarbonic composition of fuels and his influence on efficiency of the depressor additive DP3 is of a certain interest can prevail. For this purpose we into three samples of fuel in equal concentration entered a depressor of DP3 (tab. 1).

Table 1.– Influence of concentration of a depressor on temperature hardenings of fuel, ˚C

Fuel	Concentration of a depressor,%			
	0	**0.05**	**0.1**	**0.2**
sample 1	–14	–23	–25	–26
sample 2	–11	–	–25	–27
sample 3	–7	–7	–9	–9

From (tab. 1) it is visible that efficiency of action of a depressor on temperature of hardening of fuel is various. It can be explained, from our point of view, with various hydrocarbonic composition of fuel (tab. 2).

Table 2. – Hydrocarbonic structure of the studied samples diesel fuels, %

Group structure	Diesel fuel		
	sample 1	sample 2	sample 3
N paraffin, from them	25	30	40
C_5–C_{14}	12	15.5	19.5
C_{15}–C_{18}	7	8	13
C_{19}–C_{25}	6	6.5	7.5
Isoparaffin	47	49	30
aromatic hydrocarbons, from them	10	10	8
monocyclic	5	5.8	5.8
Naftena	14	9.5	12
unsaturated hydrocarbons	4	1.5	10

Apparently from the (tab.) the 2nd samples of diesel fuels 1 and 2 considerably differ from a sample 3 on the group hydrocarbonic structure. The obtained data on dependence of efficiency of a depressor on hydrocarbonic composition of fuel well will be coordinated with references from which follows that generally hydrocarbons can be located in the following row on decrease of a susceptibility to depressors:

N paraffin & gt; aromatic hydrocarbons & gt; isoparaffin and naftena.

The good susceptibility of N paraffin to depressors is caused by the mechanism of effect of these additives which interact with the crystallizing paraffin. However N paraffin have high temperatures of hardening, their presence sharply worsens low-temperature properties of fuels. At optimum concentration of N paraffin in fuel action of depressors is shown best of all.

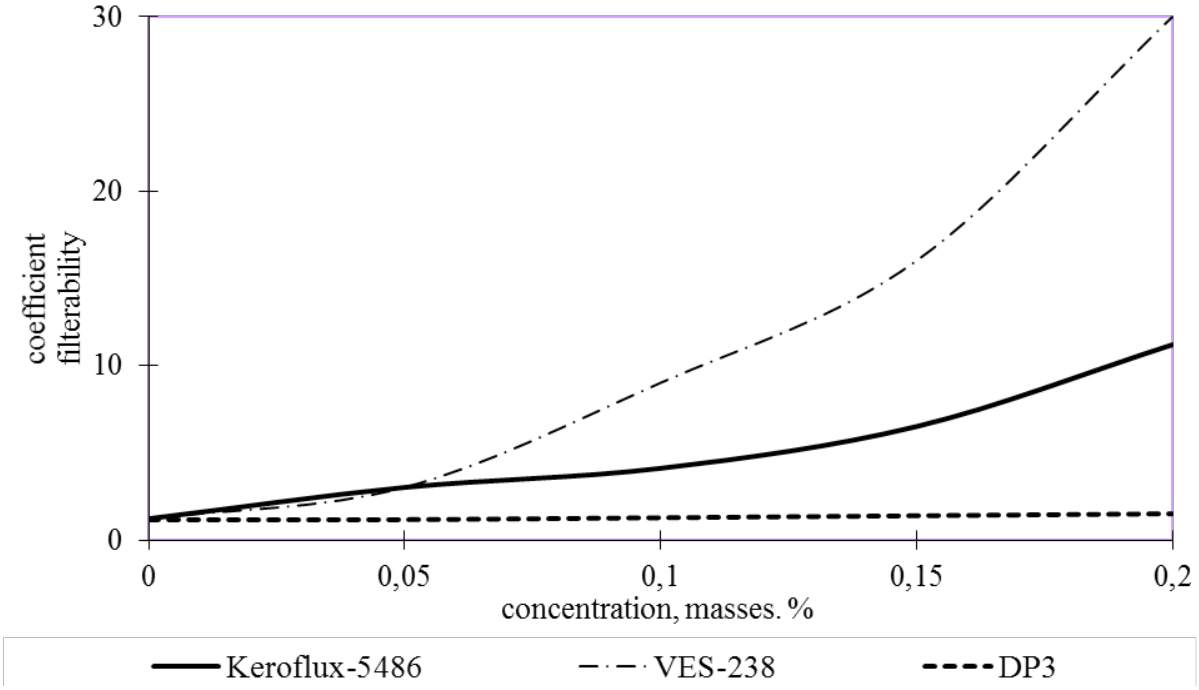

Figure 1. Influence of concentration of additives on coefficient of filterability of diesel fuel

From aromatic hydrocarbons those which contain side paraffin chains are more susceptible. With increase in number of rings and reduction of length of side chains their susceptibility to depressors decreases [2].

From literature it is known that in some cases presence of depressor additives can negatively influence certain indicators of quality of fuel. So, at introduction of 0.2% of the additive VES-238 the coefficient of filterability of fuel of a summer grade increases to 30, then at a hrakneniye goes down a little, but all the same remains rather high concerning the normalized value equal 3, and sostavklyat 4–5. Increase in coefficient of filterability is observed also when using a depressor of Keroflux-5486. At test of the depressor of DP3 synthesized by us his insignificant influence, in comparison with the known analogs, on this indicator (fig. 1) is established.

Introduction of 0.2% of the additive VES-238 affects also increase in an indicator "the actual pitches" [3].

Tests by definition of influence of the developed additive DP3 on initial indicators of diesel fuel are carried out according to GOST 305–82 on a fuel sample 2 (tab. 3). At researches depressor additive with the concentration equal of 0.2% has been used.

Table 3. – Influence of a depressor on quality indicators diesel fuel

Name of an indicator	**Normalized in accordance with GOST 305–82**	**Actual for fuel before introduction of a depressor**	**Actual for fuel from 0.2% of a depressor**
1	***2***	***3***	***4***
Cetane number, not less	45	47	47
Fractional structure: 50% are overtaken at a temperature, °C, not above	280	265	265
96% are overtaken at a temperature (the end of distillation), °C, not above	360	342	342
Kinematic viscosity at 20 °C, mm^2/with, (cSt)	3.0–6.0	4.2	4.2
The flash temperature for diesels of general purpose determined in the closed crucible, °C, not below	40	52	52
Mass fraction of sulfur,%, no more	0.20	0.17	0.17
Mass fraction of merkaptanovy sulfur,%, no more	0.01	be absent	
hydrogen sulfide content	be absent		
Test on a copper plate	Stand		
Content of water-soluble acids and alkalis	be absent		
Concentration of the actual pitches, mg on 100 cm^3 of fuel, no more	40	3	3
Acidity, mg the GAME on 100 cm^3 of fuel, no more	5	1.26	1.26
Iodic number, of iodine on 100 g of fuel, no more	6	0.5	0.5

1	*2*	*3*	*4*
Ash-content,%, no more	0.01	be absent	
Koksuyemost of the 10% rest,%, no more	0.20	0.028	0.028
Filterability coefficient, no more	3	1.5	1.5
Density at 20 °C, kg/m^3, no more	860	810	810

From (tab. 3) it is visible that additive Dp3v introduction diesel fuel doesn't affect filterability coefficient, content of the actual pitches and other indicators.

Thus, the conducted researches have shown that efficiency of the additive DP3 considerably depends on hydrocarbonic composition of fuel and doesn't worsen his quality indicators. Considering depressor efficiency and climatic conditions of the Republic of Uzbekistan, the developed additive, at rational selection of hydrocarbonic structure of a summer grade of diesel fuel, can be quite used for improvement of its low-temperature properties at operation of automotive vehicles during the winter period.

References:

1. Vafayev O. Sh., Tadzjikhodzjayev Z. A., Djalilov A. T. Republican scientific and practical conference "Urgent Problems of Chemical Science and Innovative Technologies of Her Training". 2016.– Tashkent.– P. 88–89.
2. Englin B. A. Use of motor fuels at low temperatures.– M.: Chemistry. 1980.– 208 p.
3. Danilov A. M. Use of additives in fuels.– M.: World. 2005.– 189 p.

Vu Minh Thanh,
Institute of Chemistryand Material,
E-mail: vmthanh222@yahoo.com

REMOVAL OF Cr(III) FROM AQUEOUS SOLUTION BY LOW-COST Fe_3O_4/TALC NANOCOMPOSITE

Abstract. The Fe_3O_4/Talc nanocomposite was synthesized by using the chemical co-precipitation method. The reaction was carried out under a nonoxidizing oxygen-free environment. The Cr^{3+} adsorption by Fe_3O_4/Talc nanocomposite was carried out in batch conditions. The kinetic data of the adsorption reactions were described by pseudo-first-order and pseudo-second-order equations and intraparticle diffusion models. Results showed that the pseudo-order was fitted to the kinetic data. The isotherms of adsorption were also studied using Langmuir and Freundlich equations in linear forms. It found that the Langmuir equation showed better linear correlation with the experimental data than the Freundlich. The maximum monolayer coverage, q_{max} at 297 K were found to be 54.35 mg/g.

Keywords: nanocomposite, Langmuir and Freundlich equations, cleaning of drains.

1. Introduction

Heavy metal ions pollutants exis in the aqueous has increased over the last some decades due to industrial. In which, Cr is widely used in industry as plating, alloying, tanning of animal hides, inhibition of water corrosion, textile dyes and mordants, pigments, ceramic glazes, refractory bricks, … [1]. Due to this wide anthropogenic use of Cr, the consequential environmental contamination increased and has become an increasing concern in the last years [2]. The toxic ions enter the food chain and then the human body [3]. Water pollution by heavy metals is one of the most serious threat to public health and the environment. Because heavy metals are non-biodegradable and are more difficult to remediate [4]. Some in place treatment technologies are mainly based on physicochemical, electrochemical or advanced oxidation processes. Physicochemical processes include membrane filtration, chemical precipitation, ion-exchange, and adsorption. Electrocoagulation, electroflotation, and electrodeposition are categorized under the name of electrochemical methods [5]. Recently, nanotechnology is a practical approach in treating wastewaters, too. Among all these possible methods, those with cost-effective, environment-friendly and no further pollutants features are the favorites [6].

In recent years, the use of natural compounds [7], agricultural waste material [8], industry [9], it is inexpensive to make adsorbent materials to remove heavy metals of interest. Such as, Talc $[Mg_3Si_4O_{10}(OH)_2]$, is a natural compound widely used in the form of a fine powder in several industrial products. The structure of talc is the well-known 2:1 (T–O–T) layer configuration consisting of an octahedral magnesium (Mg) coordinated sheet (O) sandwiched between two tetrahedral silicon (Si) coordinated sheets (T) [10]. Talcum powder (30–50 μm) for preparing the nanocomposite was supplied by Talcum powder Phu Tho – Viet Nam. Talc-based materials have been synthesized and applied as adsorbent materials for removing toxic agents such as heavy metals [11], wastewater containing organic dyes [12].

In this work, the adsorption isotherm, kinetic of Cr^{3+} ion onto Fe_3O_4/Talc nanocomposite produced from Talc (Phu Tho – Viet Nam) were studied.

2. Experiments

2.1. Fe_3O_4/Talc nanocomposite

The material is synthesized by the co-precipitation method on the talc layers in an inert atmosphere, with the 1:2 ratio of Fe^{2+}/Fe^{3+}. The synthesis process is carried out as document [13] with talc

powder of Vietnam (particle size ≤ 50 μm; density 2.4 g/cm^3; main components include: SiO_2: 56.8%; MgO: 31.5%; Fe_2O_3: 3.5%).

The materials structure was determined by Field Emission Scanning Electron Microscope method (FESEM, Jeol 6610LA, Japan). Nitrogen adsorption-desorption isotherms were performed at 77 K in Tristar 3000-Micromeritics equipment, USA, using static adsorption proceduce. Samples were degassed at 80°C and 10^{-6} Torr for minimum 12 h prior to analysis. BET surface areas were calculated from the linear part of BET plot according to IUPAC recommendation. Pore size distributions of the samples were calculated via the conventional BJD model and magnetic properties by measuring with a vibrating-sample magnetometer.

2.2. Studying the adsorption of Cr^{3+} ion by Fe_3O_4/ Talc nanocomposite

The process of adsorption of Cr^{3+} ion in aqueous solution is carried out in interrupted conditions at a temperature of 297 K. Stirring speed of 200 v/min, the initial concentration of Cr^{3+} is varied within 10–200 ppm. The solution's pH was surveyed from 4–7, the volume of Cr^{3+} solution was 50 ml, the amount of adsorbent used was 0.1g. The concentration of before and after Cr^{3+} adsorption is calculated by oxidizing the sample to determine the total Cr concentration and subtracting Cr (VI) concentration, in which Cr (VI) is determined by colorimetric method. when chelating with 1.5-Diphenylcarbazide, the total Cr was determined by FAAS method on the ContrAA 700 device of Analytikjena at a wavelength of 359.34888 nm; Acetylene/air stream; 50 mm lamp height.

Adsorption capacity of Fe_3O_4/Talc nanocomposite is calculated by the formula [14]:

$$q = \frac{(C_o - C_t).V}{m} \quad (1)$$

Where, V is the volume of solution (l); m is the mass of adsorbent (g); C_0, C_t are Cr^{3+} concentrations in the initial solution and at time t respectively (mg/l);

inetics of the adsorption process is studied by basing on the pseudo-first-order adsorption kinetics equation (B_1) in linear form: $\ln(q_e - q_t) = \ln(q_e) - k_1.t$ (2), where: k_1 (min^{-1}) is the rate constant of the pseudo-first-order adsorption kinetics process; q_e, q_t are the adsorption capacities at the equilibrium time and time t. The pseudo-second-order adsorption kinetics equation in linear form: $\frac{t}{q_t} = \frac{t}{q_e} + \frac{1}{k_2.q_e^2}$ (3), Where: k_2 (mg/g.min) is the rate constant of the adsorption kinetics process [15; 16]. Diffusion kinetics equation: $\ln(q_t) = \ln(k_D) + 0.5.\ln(t)$ (4), where: k_D (mg/g.(min)$^{0.5}$) is the diffusion coefficient [17]. Elovich equation: $q_t = \frac{1}{\beta}\ln(\alpha\beta) + \frac{1}{\beta}\ln(t)$ (5) where: α and β are constants of Elovich – type equation [18].

3. RESULTS AND DISCUSSION

3.1. Properties of Fe_3O_4/Talc nanocomposite

The surface properties, porosity or pore size is one of the factors to evaluate the adsorption capacity of the material. Figure 1 is the FESEM image of Fe_3O_4/Talc nanocomposite.

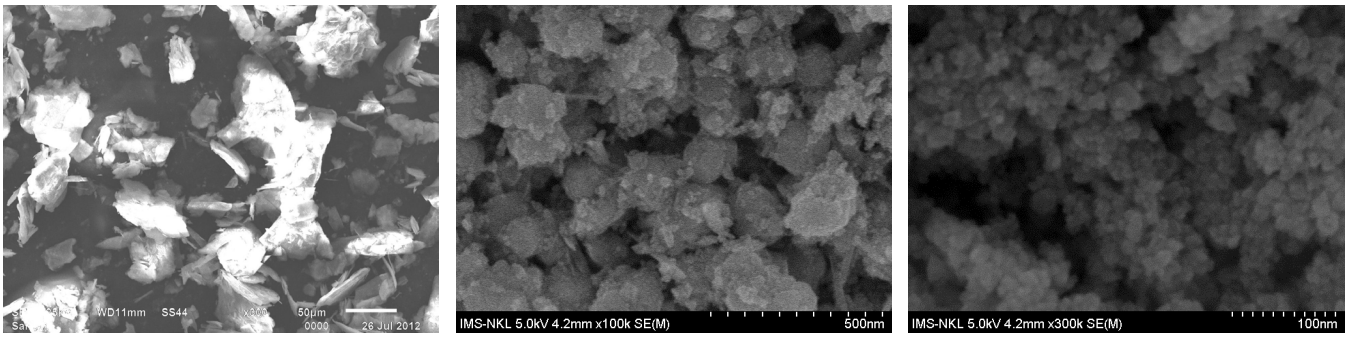

(a) (b) (c)

Figure 1. Scanning electron microscopy image of Talc (a) and the synthesized Fe_3O_4/Talc (b, c)

From the results of (Figure 1), it is shown that Talc surface material has particle sizes in the range of 30–50 nm, cubic particles are less uniform and have smooth surface. Nanocomposite materials at different magnifications (Fig. 1.b, 1.c), had distribution of Fe_3O_4 nanoparticles with dimensions less than 30 nm. Then, the synthetic nanocomposite material will give a larger surface area than the base material, which will be shown through the measurement of specific surface area by BET.

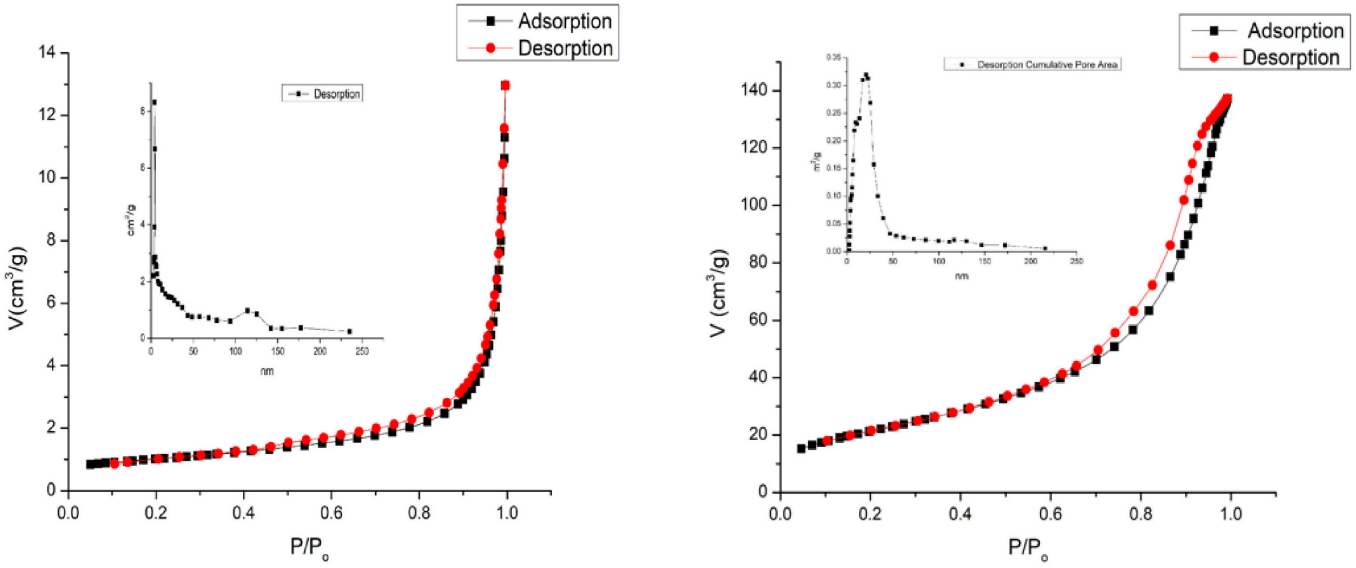

Figure 2. Nitrogen adsorption – desorption isotherms and Barrett-Joyner-Halenda (BJH) pore-size distribution for Talc, Fe_3O_4/Talc nanocomposite at 77K

From the results in (Figure 2), it is shown that the talc surface material has adsorption-desorption isotherm of the intermediate form between III and IV with the appearance of H_3 hysteresis loop, Fe_3O_4/Talc nanocomposite samples give adsorption-desorption isotherm of type IV and H_3 hysteresis loop, rod-shaped and letter-shaped according to IUPAC classification [19]. This allows the prediction that synthetic nanocomposite materials contain both large pores and medium pore, in which the medium pores are more numerous. The specific surface area of talc surface material is 3.45 m^2/g which is much smaller than that of the nanocomposite material, which reachies 78.95 m^2/g. In particular, large pore area of the nanocomposite Smacro = SBET – SBJH, ads – Smicro = =8.27 m^2/g; the pore diameter averages 11.8 nm.

The magnetic properties of materials are assessed by the method of vibrating-sample magnetometry. The results for a material sample with near zero magnetic coercivity, with a saturation magnetization of 32.4 emu/g, this indicates that the survey sample is superparamagnetic, iron oxide particles is distributed with nano size on the soluble surface. Therefore, the material is convenient to separate from the aqueous solution after adsorption with the help of external magnetic fields [20].

3.2. Adsorption process of Cr^{3+} on Fe_3O_4/Talc nanocomposite

Effects of pH: The temperature is 24 °C for 60 minutes. Filter and determine the concentration of Cr^{3+} in the solution after adsorption.

The results in (Figure 3) show that when pH gradually increases, the adsorption capacity of lead increases, so the ability to treat lead contamination in water depends on the environmental pH. However, the survey process was carried out from pH = 4 to pH = 7 because, at points of pH less than 4, the dissolution of Fe_3O_4 nanoparticles occurs, in addition, at lower pH, the adsorbate solution will be positively charged thus making H^+ ions compete effectively

with Cr^{3+} cations, which may reduce lead adsorption [21], with pH greater than 7, the hydrolysis of chromium occurs. Therefore, subsequent surveys will be chosen with a pH value = 6.5.

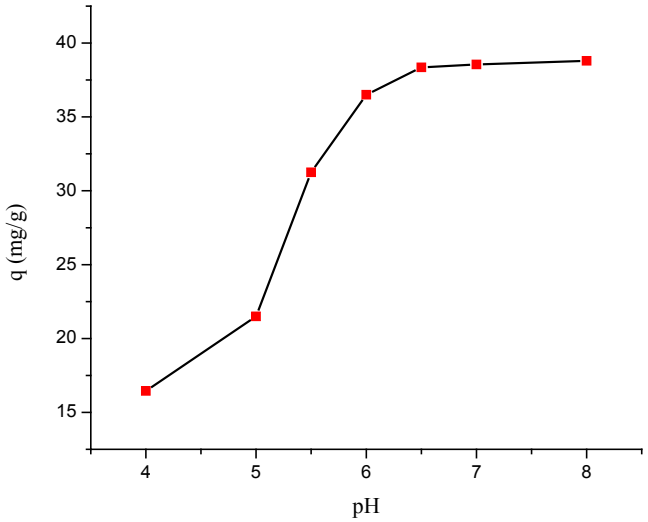

Figure 3. Effect of pH on adsorption of Cr^{3+} onto Fe_3O_4/Talc(50 ml of Cr^{3+} 98.6 mg/l, 0.1 g sorbent)

Determining the time to reach adsorption equilibrium:

The Cr^{3+} survey solution has a concentration of C = 106.5 mg/l, adjusting solution's pH to pH = 6.5. Proceed on a magnetic stirrer at a speed of 140 rev/min, a temperature of 24 °C during the time periods in turn: 5 to 120 minutes. Then, filter and collect the filtrate for survey.

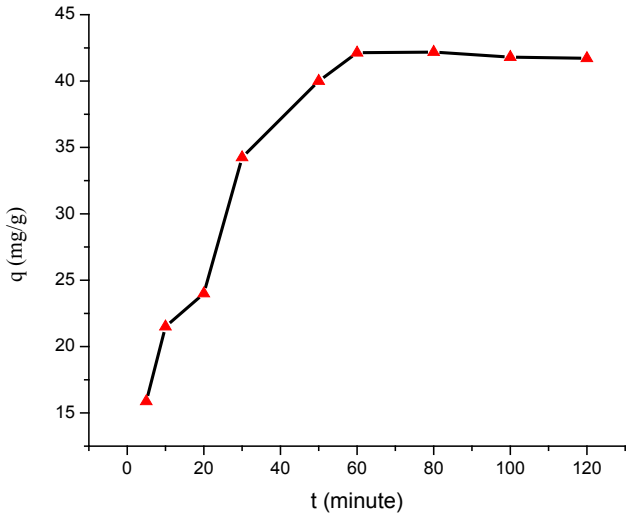

Figure 4. Effect of contact time on adsorption Cr^{3+} onto Fe_3O_4/Talc (50 ml of Cr^{3+} 106.5 mg/l, 0.1 g sorbent)

Survey results show that, in the range of 5–60 minutes, the adsorption capacity of materials increases with adsorption time. After 60 minutes, the adsorption capacity is almost unchanged, so the time to reach adsorption equilibrium 60 minutes.

Isothermal adsorption kinetics:

The isothermal adsorption kinetics of the material is studied with two models of Langmuir and Freundlich Fe_3O_4/Talc. The survey solution contains Cr^{3+} and 0.1 g of material to be stirred at a speed of 140 rev/min, a temperature of 24 °C for a period of 60 minutes. The isothermal adsorption model is given in (Figure 5).

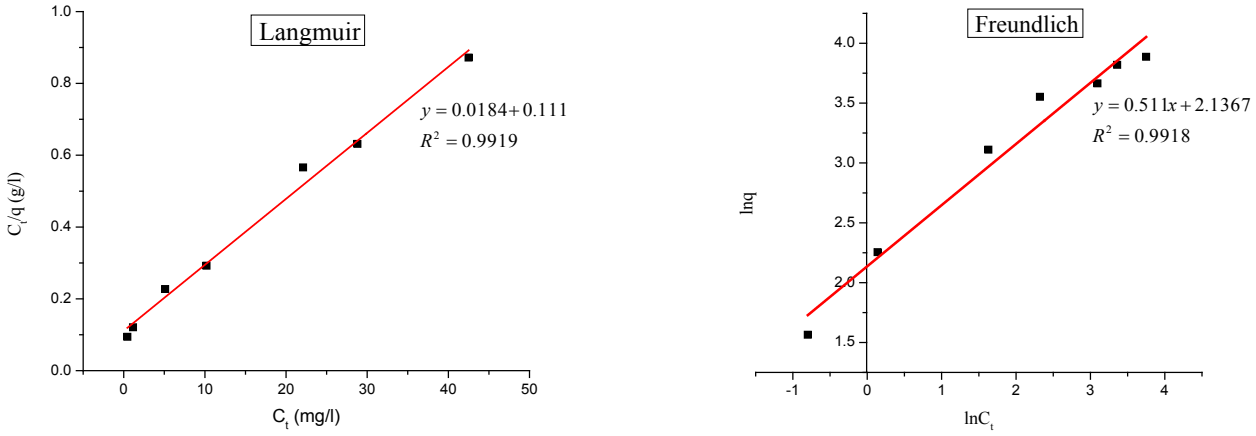

Figure 5. Cr^{3+} adsorption isotherm on Fe_3O_4/Talc fitted to Langmuir and Freundlich

Table 2.– Langmuir and Freundlich isotherm constants for the adsorption of Cr^{3+} ion by Fe_3O_4/Talc

Freundlich isotherm				Langmuir isotherm		
1/n	n	K_f mg/g	R^2	Q mg/g	K_L L/mg	R^2
0.511	1.9566	8.4720	0.9918	54.3478	K=0.1658	0.9919

From the survey results fitted to Langmuir and Freundlich adsorption models, it is shown that the adsorption process of Cr^{3+} by Fe_3O_4/Talc nanocomposite is more suitable with Langmuir model, however, with the absorption process also complies with the Freundlich isothermal equation. This shows that the synthetic material has adsorption centers with nearly the same surface energy. This shows that the lead adsorption process of Fe_3O_4/Talc nanocomposite conforms to the Langmuir model in theory, but the empirical data also obeys the Freundlich model, which is due to the range of studied concentrations lies within the linear distribution range according to Freundlich model.

3.3. Survey of adsorption kinetics

The linear regression equations of $\ln(q_e - q_t)$ on t for first-order kinetic model, $\frac{t}{q_t}$ on t for second-order kinetic model and $\ln(q_e)$ on $\ln(t)$ for diffusion kinetics model, q_t on ln t for Elovich model are shown in (Figure 5). From the value of the slopes and the intercepts of the straight line equations, it is possible to calculate the respective kinetic equation constants given in (table 3), (figure 6).

From the results in (Table 3), it is shown that the quadratic equation of type 2 has a correlation coefficient of approximately 1, furthermore, the values of the k constant are almost unchanged, which indicates that the speed constant does not depend on concentration. This proves that the adsorption process depends on the number of adsorption centers on the surface and the adsorbate is the Cr^{3+} ion.

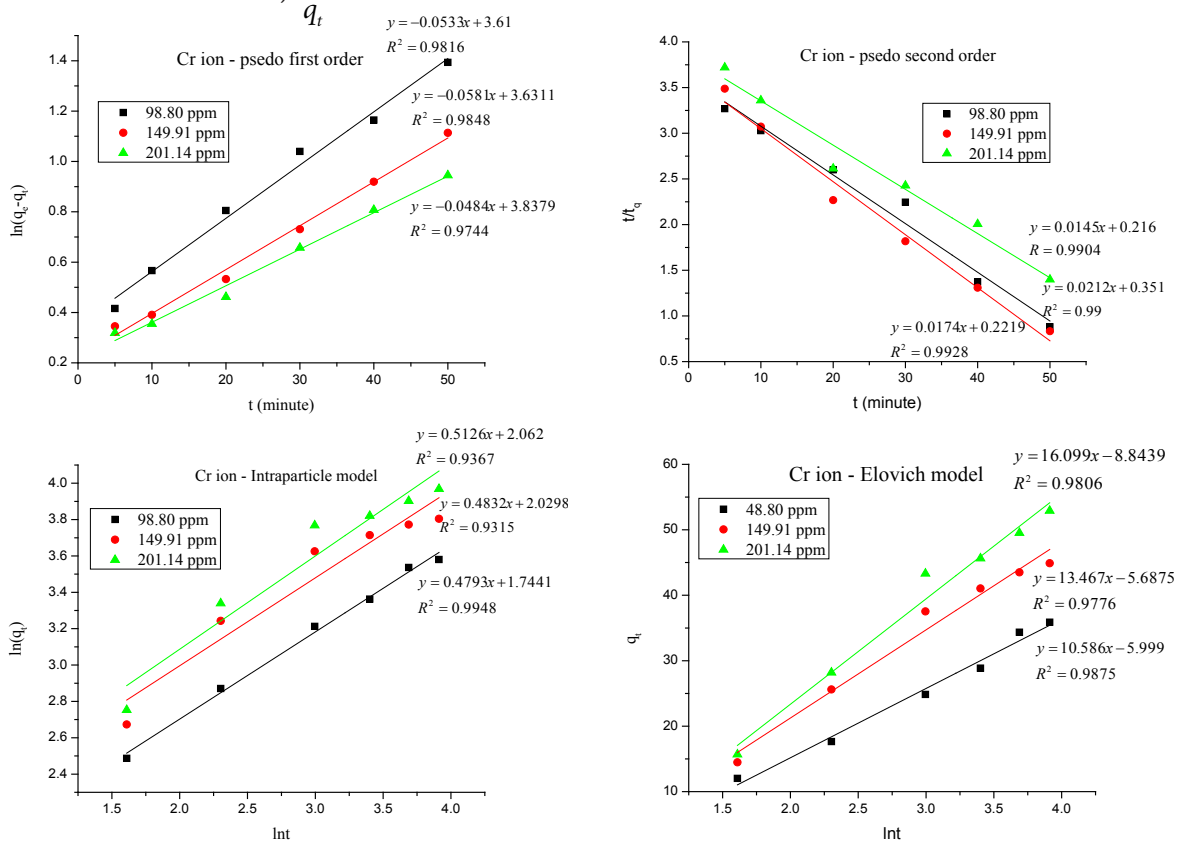

Figure 6. The kinetic models of adsorption of Cr^{3+} ion on the Fe_3O_4/Talc

Table 3.– Kinetic parameters for the removal of Cr^{3+} onto Fe_3O_4/Talc

Co (ppm)	Pseudo 1st order		Pseudo 2st order		Intraparticle diffusion		Elovich model		
	R^2	k_1	R^2	k_2	R^2	K_D	R^2	α	β
98.80	0.9816	0.0533	0.990	0.00128	0.9948	5.7208	0.9875	–0.0149	–0.1667
149.91	0.9848	0.0581	0.9928	0.001364	0.9315	7.6126	0.9776	–0.0193	–0.1758
201.14	0.9744	0.0484	0.9904	0.000973	0.9367	7.8618	0.9806	–0.0013	–0.1131

3. Conclusion

The Fe_3O_4/Talc nanocomposite was synthesized with the Talcum powder Phu Tho – Viet Nam by the chemical co-precipitaiton method. The reaction was carried out under a nonoxidizing oxygen-free. The surface area of the nanoparticles was determined to be 78.95 m^2/g with an average diameter of 11.8 nm and the saturation magnetization of 32.4 emu/g.

The experimental results indicate that the Fe_3O_4/Talc nanocomposite is an effective adsorbent of Cr^{3+} ion from the aqueous solution. The adsorption equilibrium data fitted very well to the Langmuir and Freundlich adsorption isotherm models. The kinetic data showed that the adsorption process followed the pseudo-second order kinetic model.

The maximum adsorption capacities of 53.35 mg/g occurred at pH 6.5 and 298 K. These results permit us to conclude that Fe_3O_4/Talc nanocomposite is a promising low-cost adsorbent for Cr^{3+} removal from wastewater and can be applied in a magnetically-assisted water treatment technology.

References:

1. Zayed A. M. and Terry N. Chromium in the environment: factors affecting biological remediation, Plant and Soil, 2003.– Vol. 249.– No. 1.– P. 139–156.
2. Helena Oliveira. Chromium as an environmental pollutant: Insights on induced plant toxicity, 2012. Journal of Botany, ID375843.
3. Grimm J., Bessarabov D., Sanderson R. Review of Electro-assisted methods for water purification, Desalination, 1998. 115,– P. 285–294.
4. Reena Singh, Neetu Gautam, Anurag Mishra, Rajiv Gupta. Heavy metals and living systems: An overview. Indian Journal of Phamacology, 2011.– Vol 43. 3,– P. 246–253.
5. Arezoo Azimi, Ahmad Azari, Mashallah Rezakazemi, Meisam Ansarpour. Removal of heavy metals from industrial wastewaters: A review. ChemBioEng, 2017. 4,– No. 1.– P. 1–24.
6. Giusy Lofrano, Giovanni Libralato, Jeanette Brow. Nanotechnologies for Environmental remediation: Applications and Implications, Spinger, 2017.
7. Abu Zayed M. Badruddoza and et al. Fe_3O_4/cyclodextrin polymer nanocomposites for selective heavy metals removal from industrial wastewater. Carbohyrated polymers, 91, 2009.– P. 322–332.
8. Fanuel J Ligate, James E. G. Mdoe, Removal of heavy metal ions from aqueous solution using rice husks-based adsorbents. 2015. Tanz. J. Sci.– Vol. 41.– P. 91–102.
9. Amit Bhatnangar and etc. A review of the use of red mud as adsorbent for the removal of toxic pollutants from water and wastewater, Journal Environmental technology, 2011.– Vol 32. 3,– P. 231–249.
10. Marco Bruno, Mauro Prencipe, Giovanni Valdre. Ab initio quantum-mechanical modeling of pyrophyllite $[Al_2SiO(OH)_2]$ and talc $[Mg_3Si_4O_{10}(OH)_2]$ surfaces. Phys Chem Minerals, 2006. 33,– P. 63–71.

11. Katayoon Kalantari and et al. Rapid adsorption of heavy metals by Fe_3O_4/Talc nanocomposite and optimization study using response surface methodology. Int. J. Mol. Sci. 2014. 15,– P. 12913–12927.
12. Liu Wenlei, Zhao Shanlin, Cui Shuang, Zhang Jinhui, Li Ping & Yang Shuangchun. Adsorptive characteristics of modified talcum powder in removing methylene blue from wastewater, Chemical Speciation and Bioavailability, 2014. 26(3),– P. 167–175.
13. Katayoon Kalantari, Mansor Bin Ahmad, Kamyar Shameli, Roshanak Khandanlou. Synthesis of talc/Fe_3O_4 magnetic nanocomposites using chemical co-precipitation method. International Journal of Nanomedicine, 2013. 8,– P. 1817–1823.
14. Wan Ngah W. S., Fatinathan S. J. of Environmental Management. 2010. 91,– P. 958–969.
15. Yuh-Shan Ho. Citation review of Lagergren kinetic rate equation on adsorption reactions, Scientometrics, 2004.– Vol. 59.– No. 1.– P. 171–177.
16. Ho Y. S. Adsorption of heavy metals from waste streams by peat, Ph. D. Thesis, University of Birmingham, 1995. U.K.
17. Ping Ge, Fenfting Li, Kinetics and Thermodynamic of heavy metal Cu (II) adsorption on mesoporous silicates, Polish J. of Environ.Stud, 2011. 20(2),– P. 339–344.
18. Abbas Sabah Thạeel, Isotherm, kinetic and thermodynamic of adsorption of heavy metal ions onto local activated carbon, Aquatic Science and Technology, 2013.– Vol. 1.– No. 2.– P. 53–77.
19. Matthias Thommes and et al. Physisorption of gases, with special reference to the evaluation of surface area and pore size distribution (IUPAC Technical Report), Pure Appl. Chem. 2015. 87(9–10): – P. 1051–1069.
20. Xinhua Xu et al., Nanoscale Zero-Valent Iron (nZVI) assembled on magnetic Fe_3O_4/graphene for Chromium (VI) removal from aqueous solution, Journal of Colloid and Interface Science, 2014. 417,– P. 51–59.
21. Mahmood Iram, Chen Guo, Yueping Guan, Ahmad Ishfaq, Huizhou Liu. Adsorption and magnetic removal of neutral red dye from aqueous solution using Fe_3O_4 hollow nanospheres. Journal of Hazardous Materials. 2010. 181,– P. 1039–1050.

Erkaeva Nazokat Aktamovna,
Doctoral student of Tashkent Institute of Chemical Technology
Shokirova Dildora Ilhomovna,
Master of the Tashkent Institute of Chemical Technology
Erkaev Aktam Ulashevich,
Doctor of technical sciences,
Professor, Tashkent Institute of Chemical Technology
Sharipova Habiba Teshaevna,
Candidate of engineering sciences,
Associate Professor, Tashkent Institute of Chemical Technology
Kaipbergenov Atabek Tulepbergenovich,
Doctor of technical sciences,
Head of the Department of the Nukus State Pedagogical Institute
E-mail: atabek2004@mail.ru

INFLUENCE OF TECHNOLOGICAL PARAMETERS ON PROPERTIES OF LIQUID SYNTHETIC DETERGENTS

Abstract. To obtain gel and liquid synthetic detergents, various mixtures were prepared containing surfactants, sodium chloride and carboxyl methylcellulose. The rheological properties of these mixtures were studied depending on the mass ratio of the initial reagents and temperature. Determined that to obtain a gel and liquid detergents must vary within the following ranges of content of initial components in detergent compositions, mass.%: surfactants 5–30, starches 0–2, Na CMC 0.5–2, NaCl 0.5–4, alkalis 1–7.

Keywords: synthetic detergents, component, ratio, density, viscosity, detergency, solution.

Synthetic detergents (SD) along with high detergency should be characterized by high biodegradability in water bodies, high economical production, consumption, good presentation and stability of quality indicators, non-toxicity for people, animals and aquatic organisms [1; 2]. They are multicomponent compositions used in aqueous solutions to intensify the removal of contaminants from various hard surfaces – fabrics, fibers, metals, glass, and ceramics. In a narrower sense, synthetic detergents are commonly understood as household detergents for washing clothes and washing dishes [3; 4].

Accelerated development of the chemical industry has allowed in recent years to significantly expand the range of domestic SD and increase their production. Analysis of the consumption of technical detergents in our country shows that for the degreasing of various surfaces instead of alkalis, surfactant aqueous solutions and compositions with active additives are increasingly used.

The development of the production of SD technical purpose in our country should be aimed at the creation of alkaline detergents that can eliminate the use of flammable and toxic solvents.

Studying of rheological behavior of pulps is very important question as if the pulp is very viscid and not transportable, then it will be impossible to carry out further technological processes.

The mixes prepared by mixture of a feed stock in various mass ratios were exposed to a research. The composition of the mixes used for receiving SD is given in table 1 and 2. Density and viscosity of mixes measured in temperature range from 20 to 60 °C. Density of a pulp was determined by a piknometer method, and for viscosity test used VPJ viscosimeter – 1 [5; 6].

For studies were prepared sodium lauryl ether sulfate (SLES) containing solutions with a ratio of SLES: H_2O in the range of 10: 90–30: 70.

It has been established (Table 1) that with an increase in the mass ratio of SLES in a SLES: H_2O solution from 10: 90 to 30: 70, the density of solutions decreases from 1.093 to 0.945 g/cm^3, respectively.

Table 1.– Influence of technological parameters on rheological properties SLES containing solutions

Composition solution		Density, g/cm^3			Viscosity, cP		
		Temperature, °C			Temperature, °C		
		20	40	60	20	40	60
1.	SLES: H_2O = 10:90	1.093	1.091	0.910	20.47	9.72	6.87
2.	SLES: H_2O = 20:80	0.948	0.939	0.934	27.86	12.28	7.59
3.	SLES: H_2O = 30:70	0.945	0.938	0.931	50.37	22.41	8.68
4.	NaCl: SLES: H_2O = 0.5:20:79.5	0.948	0.939	0.927	29.27	13.01	5.23
5.	NaCl: SLES: H_2O = 2:20:78	0.953	0.948	0.939	205.25	46.30	7.98
6.	NaCl: SLES: H_2O = 4:20:76	0.973	0.969	0.976	268.7	184.94	113.28
7.	Urea: H_2O = 1:20:79	0.941	0.936	0.928	28.97	13.42	5.04
8.	Corn starch: H_2O = 5:20:75	0.946	0.939	0.935	28.30	13.40	4.39
9.	Potato starch: H_2O =10:20:70	0.949	0.941	0.937	28.62	13.74	4.40

The addition of NaCl to the solution in the amount of 0.5% led to a slight increase in the density to 0.948 g/cm^3 at a temperature of 20 °C. A further increase in the amount of added NaCl to 4% led to the formation of a thick mass.

The addition of urea to the solution containing SLES in the amount of 1, 5, 10% did not significantly affect the density of the solution and this indicator of these solutions varied from 0.941 g/cm^3 to 0.949 g/cm^3.

We studied the density of solutions of corn and potato starch, as well as the density of various solutions of gelatin (Table 2).

Table 2.– Rheological properties of solutions containing starch and gelatin

№	Composition solution	Density, g/cm^3			Viscosity, cP		
		Temperature, °C			Temperature, °C		
		20	40	60	20	40	60
1	*2*	*3*	*4*	*5*	*6*	*7*	*8*
1.	Corn starch: H_2O = 2:98	0.928	0.923	0.915	11.72	8.36	2.57
2.	Corn starch: H_2O = 4:96	0.937	0.932	0.923	13.20	8.97	2.66
3.	Corn starch: H_2O = 8:92	0.945	0.944	0.941	13.89	7.05	3.86
4.	Corn starch: H_2O = 16:84	0.975	0.961	0.953	15.43	7.23	3.52
5.	Potato starch: H_2O = 2:98	0.926	0.921	0.916	16.95	8.14	2.45
6.	Potato starch: H_2O = 4:96	0.935	0.932	0.927	17.63	6.34	2.25
7.	Potato starch: H_2O = 8:92	0.945	0.941	0.935	17.75	7.05	2.51

1	*2*	*3*	*4*	*5*	*6*	*7*	*8*
8.	Potato starch: H_2O = 16:84	0.971	0.964	0.961	17.89	8.13	3.63
9.	Gelatina: H_2O = 10:90	0.945	0.937	0.924	7.83	2.68	1.98
10.	Gelatina: H_2O = 15:85	0.963	0.952	0.943	22.53	20.33	1.54
11.	Gelatina: H_2O = 20:80	1.057	1.023	1.019	388.3	275.9	156.0

It has been established that an increase in the concentration of corn starch solution in a mixture from 2 to 16% led to an increase in the density of these solutions at 20 °C from 0.928 to 0.975 g/cm^3, respectively.

The study of the density of various solutions of potato starch showed that the densities of these solutions practically do not differ from density of corn starch solutions and their values at 20 °C range from 0.926 to 0.971 g/cm^3.

To study the rheological properties at temperatures from 20, 40, 60 °C, gelatin solutions of 10, 15, 20% concentration were prepared. It was established that an increase in the concentration of the gelatin solution from 10 to 20% at a temperature of 20 °C led to an increase in the density from 0.945 g/cm^3 to 1.057 g/cm^3, respectively.

In order to determine the possibility of using carboxyl methylcellulose (CMC) as one of the initial components of gel SD, the effect of CMC grade and temperature on the rheological properties of solutions of various CMC concentrations was studied.

The concentration of CMC solutions varied from 1 to 2 and 4%. With an increase in the concentration of the CMC solution, the density of the solution increases (Table 3). For example, a 1% solution of $CMC_{1000/1300}$ at 20 °C has a density of 0.924 g/cm^3. Increasing the concentration of the $CMC_{1000/1300}$ solution to 4% led to an increase in this indicator to 0.949 g/ml. The same pattern is observed when using $CMC_{85/600}$ and $CMC_{85/800}$.

As can be seen from the data of (Table 3), the density of the solutions, this indicator does not depend on the concentration.

Table 3.– Changes in the rheological properties of Na CMC solutions as a function of concentration, temperature, and Na CMC grade

№	Composition solution	Density, g/cm^3			Viscosity, cP		
		Temperature, °C			Temperature, °C		
		20	40	60	20	40	60
1.	Na CMC1: H_2O = 1:99	0.924	0.913	0.841	23.83	9.72	3.67
2.	Na CMC1: H_2O = 2:98	0.931	0.924	0.921	582.96	196.80	52.78
3.	Na CMC1: H_2O = 4:96	0.949	0.895	0.883	18566	4022.0	1004.4
4.	Na CMC2: H_2O = 1:99	0.905	0.859	0.847	25.61	12.17	4.22
5.	Na CMC2: H_2O = 2:98	0.934	0.925	0.917	33.72	9.62	3.68
6.	Na CMC2: H_2O = 4:96	0.948	0.931	0.925	94.83	3.6	7.93
7.	Na CMC3: H_2O = 1:99	0.923	0.918	0.908	51.3	18.27	5.49
8.	Na CMC3: H_2O = 2:98	0.931	0.923	0.915	64.92	20.26	5.93
9.	Na CMC3: H_2O = 4:96	0.942	0.931	0.923	107.16	40.73	4.75

Note: Na CMC1$_{1000/1300}$, Na CMC2$_{85/600}$, NaCMC3$_{85/800}$

In order to obtain a gel SD, various mixtures were prepared containing surfactant, sodium chloride and CMC. The rheological properties of these mixtures

were studied depending on the mass ratio of the initial reagents and temperature (Table 4).

It was established that at a temperature of 20 °C the density of mixtures varies from 0.900 g/ml to 0.928 g/ml. The lowest density of 0.900 g/ml has a mixture containing 20% N_1 mixture and 80% N_2. An increase in the mixture rate to 50% led to an increase in the mixture density to 0.901 g/ml. A further increase in the mixture rate to 90% did not affect the density. From the studied mixtures, the N_2 sample consisting of $CMC_{1000/1300}$ and equal to 0.92 g/ml has the highest density of 0.92 g/ml.

Table 4. – The effect of temperature and mass ratio of initial reagents on the rheological properties of mixtures

№	Composition of the solution N_1: N_2	Designation sampling	Density, g/cm³			Viscosity, cP		
			Temperature, °C			Temperature, °C		
			20	40	60	20	40	60
1.	1:0	N_1	0.998	0.995	0.989	16.57	6.45	2.51
2.	0:1	N_2	1.000	0.993	0.985	36.54	16.46	5.66
3.	0.9:0.1	CM_1	1.000	1.000	0.980	16.20	7.07	277
4.	0.5:0.5	CM_2	1.000	1.000	0.980	15.72	4.01	32.92
5.	0.2:0.8	CM_3	1.000	1.000	0.980	17.62	4.39	3.42

Note: N_1–(NaCl : SLES : H_2O) = 4 : 20 : 76), N_2–$CMC_{1000/1300}$: H_2O = 4 : 96)

The study of the effect of the norm of alkaline additives in various standards on mixtures (Table 5) that the addition of NaOH in the amount of 6.24% to CM_2 led to an increase in the density to 0.9964 g/ml. Adding the same amount of NaOH to CM_2 had no noticeable effect on density. The study of the influence of the KOH norm from 16.32 to 6.24% to CM_2 showed that with an increase in the KOH norm, the density increased slightly. Adding 16.32% KOH to CM_3, the density decreased by 0.0469 g/ml.

Table 5. – The effect of alkaline additives and the temperature of the mixture on their rheological properties

№	Type of additive	Quantity of additive, gr	Density, g/cm³			Viscosity, cP		
			Temperature, °C			Temperature, °C		
			20	40	60	20	40	60
When using CM_2								
1.	NaOH	1.63	0.9932	0.9872	0.9764	60.850	28.988	12.697
2.		3.14	0.9952	0.9821	0.9801	100.610	61.600	27.417
3.		6.24	0.9964	0.9784	0.9821	159.221	83.222	50.887
4.	KOH	1.78	0.9604	0.9536	0.9465	134.020	76.164	76.589
5.		3.51	0.9788	0.9708	0.9678	167.064	92.963	44.896
6.		6.78	0.9888	0.9844	0.9796	268.897	184.945	113.288
When using CM_3								
7.	NaOH	1.63	0.9463	0.9339	0.9276	60.666	30.662	15.047
8.		3.14	0.9756	0.9722	0.9644	93.701	56.741	23.045
9.		6.24	0.9951	0.9895	0.9732	151.765	81.439	30.496
10.	KOH	1.78	0.9580	0.9345	0.9278	127.689	71.458	30.478
11.		3.51	0.9592	0.9514	0.9435	161.467	91.288	44.693
12.		6.78	0.9720	0.9644	0.9610	167.477	152.988	95.687

It should be noted that by adding KOH to CM_2, the density of the mixture increases relative to CM_3 · So, if the density of sample 4 where 1.78% KOH is added is equal to 0.9604 g/ml, then with the same KOH standard with CM_3, the density decreased to 0.9580 g/ml, and the addition of 6.78% KOH to CM_2 resulted in increase the density to 0.9888 g/ml. In sample 12, the addition of the same amount of KOH to CM_3 led to a decrease in this indicator to 0.9720 g/ml. It was established that with an increase in temperature from 20 to 60 °C, the density of the mixture decreases in all samples.

Upon receipt of gel products, viscosity of the samples is of great importance. Therefore, the influence of the norm and type of alkaline additive study of the viscosity of mixtures containing SLES, at a temperature of 20 °C showed that this figure varies from 20.47 to 50.37 cP. The addition of NaCl in the amount of 2% led to an increase in the viscosity of the mixture to 205.25 cP. With the addition of 4% NaCl a thick mass was formed.

Adding carbamide to the mixtures containing SLES did not have a significant effect on the viscosity of the solution.

It also has a significant impact on this indicator temperature. For example, an increase in temperature from 20 to 60 °C in sample N_5 lowered the mixture viscosity from 205.25 to 7.98 cP (Table 1). Solutions of corn, potato starch and gelatin have a small viscosity. With an increase in the concentration of corn starch solution from 2 to 8 and 16%, the viscosity increases from 11.72 to 13.89 and 21.43 cP, respectively. The viscosity of solutions of potato starch varies in the range of 12.95–17.9 cP (Table 2).

The study of the effect of gelatin concentration on solution viscosity showed a sharp increase in this indicator with increasing gelatin concentration. So, if 10% gelatin has a viscosity of 7.83 cP at 20 °C, then increasing the concentration to 20% led to an increase in this parameter to 388.3 cP. An increase in temperature to 60 °C led to a sharp decrease in viscosity to 1.98 cP in sample 9 (Table 2). The study of the effect of concentration and grade of CMC on the viscosity of solutions of different concentrations showed that at a temperature of 20 °C the highest viscosity is 18566.67 cP and has a 4% solution of $CMC_{1000/1300}$. An increase in temperature to 60 °C led to a decrease in this indicator by 18.5 times to 1004.40 cP (table 3).

The presence of alkali KOH in the mixture increased their viscosity. As can be seen from table 6, the sample containing CM_2 and 6.24% NaOH has the highest density of 0.9964 g/ml. This sample at a temperature of 20 °C has a viscosity of 159.22 cP. But with a rise in temperature to 60 °C, the viscosity decreased to 50.88 cP.

The addition of KOH to CM_2 in the amount of 6.78% led to an increase in viscosity up to 268.8 cP. But the addition of KOH in CM_3 in the same amount lowered the viscosity of the mixture to 167.477 cP (sample 12) of (table 5).

Thus, the study of the rheological properties of various mixtures at temperatures of 20–60 °C showed that solutions of CMC and KOH increase the density and viscosity of mixtures. But as the temperature rises to 60 °C, the viscosity of mixtures containing CMC decreases sharply, which makes it possible to use it as a raw material for the production of SD.

To evaluate the foaming (foaming ability), it is common to determine the height of the column or the volume of the foam, the stability of the foam. Almost all surfactant solutions have the ability to create foam in certain conditions.

For surfactants characterized by the presence of a certain concentration at which there is an optimal foaming ability. A mandatory condition of the washing action is the surface activity of the compounds, mechanical strength and sufficient viscosity of the hydrated layers of the detergent, as well as the formation of strong hydrated adsorption layers around the contaminants, which prevents their secondary deposition on the fabric. One surface activity is not enough for a substance to possess detergency. Known substances with surface activity, but not pos-

sessing washing ability, as they do not form strong surface films (alcohols, fatty acids).

P. A. Rebinder believed that only surfactants that form solutions with maximum colloidal properties are effective detergents. For the manifestation of the wetting ability, it is also possible to completely cover the surface with an adsorption layer of a surfactant. The surfactant used as a detergent should have the following properties.

1. Ability to wet contaminated surfaces.

2. The ability to effectively remove pollution (for this detergent must overcome the adhesion force between the oil – pollution and the substrate).

3. Ability to prevent contamination from settling back.

To determine the foaming ability of CMC, solutions of various concentrations were prepared,%: 0.5; 1; 5; 10; 20; 30; 40; 50. The stability of the foam was determined within 3600 seconds.

The results of the experiments showed that in the initial period of time (0 seconds) a 10% solution of the mixture (SLES: H_2O-10:90) has a maximum height of 40 cm. With an increase in concentration to 50%, the height of the foam decreases to 19 cm. The stability of the foam is low. So, if the height of the foam 10% solution at the initial moment of time is 40 cm, then after 3600 seconds it decreases to 14 cm. The height of the foam of a 1% solution of the mixture (SLES: H_2O-10:90) after 3600 seconds is 13 cm.

An increase in the mass ratio of SLES: H_2O to 20:80 and 30:70 leads to a decrease in the height of the foam. But even in this case, the 10% solution of the mixture at the initial moment has a maximum height of 31 and 35 cm. After 3600 seconds, it decreased to 5 and 6 cm.

Investigation of the effect of sodium chloride on the foaming ability showed that sodium chloride does not affect the foaming ability. Thus, the addition of 0.5, 2, and 4% sodium chloride in the mixture (SLES: H_2O-20:80) showed that the 10% solution has a foam height of 30, 31, 32 cm at the initial moment of time. But in this case, the stability of the foam is insignificant and after 3600 seconds in this sample the height of the foam was 5, 6, 7 cm, respectively. The use of various grades of starch and CMC as a raw material does not affect the foaming ability of the solution. In this case, in all samples, regardless of the concentration of the solutions and time, the height of the foam did not exceed 0.1 and 1 cm, respectively.

As is known, to determine the optimal parameters for the production of CMC, mixtures of N_1, N_2, N_3 and CM_1 prepared from (N_1+N_2) in a ratio of 90 : 10, CM_2, prepared from a mixture of N_1 and N_2 in a ratio of 50 : 50, as well as CM_3 were prepared, prepared from N_1 and N_2 in a ratio of 20 : 80. From these mixtures were prepared 1 and 5% solutions.

To study the functional properties of the CMC samples, alkaline additives NaOH and KOH were added in various amounts to CM_2 and CM_3.

As can be seen from Table 6, at the initial moment in these samples the height of the foam varied from 25 to 36 cm, and the stability of the foam fluctuated in the intervals of 60–170 minutes. When using NaOH, the height of the foam and its stability is 2–6 cm more and 15–20 minutes, respectively, than when using KOH. This is especially true when using CM_3.

Table 6. – The effect of the amount of alkaline additives on the functional properties of samples

№	Name compositions	Type of alkaline additive	The amount of alkaline additive%	pH	Maximum foam height, cm	Foam stability, min.
1	*2*	*3*	*4*	*5*	*6*	*7*
1.	CM_2	KOH	1.79	10.11	25	60
			3.52	11.09	28	90
			6.78	12.35	30	120
2.	CM_2	NaOH	1.63	11.57	30	80
			3.14	12.29	32	110

1	*2*	*3*	*4*	*5*	*6*	*7*
2.	CM_2	NaOH	6.24	12.50	34	140
3.	CM_3	KOH	1.79	11.16	27	90
			3.51	11.20	29	120
			6.78	12.42	30	150
4.	CM_3	NaOH	1.63	11.96	32	110
			3.14	12.20	34	140
			6.24	12.36	36	170

Adding alkaline additions of KOH to CM_2 and CM_3 showed a low foaming ability of SD. In these samples, the height of the foam is 25–30 cm.

In the studied ranges of variation, the content of the initial components in the detergent compositions, the pH of the samples varied from 10.11 to 12.36. With the same doses of alkali, the pH is 0.1–1.4 more than when using NaOH.

The washing action is characterized by the effectiveness of removing contaminants from the surface of fabrics and solid surfaces and is determined by: the nature of solid surfaces (metal, glass, plastic mass), the condition of the surface being cleaned, the nature and structure of the fabric. the nature and intensity of pollution, the properties of detergents and their concentration, the degree of water hardness, the temperature of the solution, the strength of the mechanical effect on the surface being cleaned, the duration of washing.

The detergency of SD was determined on a 10-point scale.

The results of the experiments showed that the mixture containing SLES, sodium chloride and urea has the best washing ability in the range of 4–8. So, for example, samples containing SLES, sodium chloride and water in a ratio of 10 : 2 : 78 with a concentration of 1.0–5.0% have a detergent action of 5–8 points. The detergent effect of the samples increases slightly with an increase in the content of SLES, and the addition of alkaline components to the composition increases by 1.0–2.5 points.

It is established that changes in the type of additive mixtures containing corn, potato starches and gelatin have virtually no effect on the detergent effect of the composition. The presence of CMC in the mixture increases the detergency of SD.

Thus, taking into account the above, it can be concluded that to obtain gel-like and liquid detergents, it is necessary to vary the content of the initial components in the following intervals, mass.%: surfactant – 5–30, starch – 0–2, NaCMC – 0.5–2, NaCl – 0.5–4, alkali – 1–7.

References:

1. Абилова А. К., Ершова Т. С. Экологические свойства синтетических моющих средств / – М., 2001.– 230 с.
2. Kimyo, neft-gaz qayta ishlashning va oziq ovqat sanoatlarining innovatsion texnologiyalarining dolzarb muammolari / Erkaev A. U., Rambergenov A. K., Ospanova N. S., Toirov Z. K., Burashov N. // – Toshkent – Qo'ng'irot 2010.
3. Ветошкин Ю. С. Прогнозирование производства и потребления СМС и товаров бытовой химии в России до 2010 г. / Бытовая химия. 2007.– № 25.– 16 с.
4. Андерс Е. К. Глобальный и Российский рынок СМС. Состояние, развитие, перспективы / Бытовая химия. 2007.– № 26.– 5 с.
5. ГОСТ 22567.1–77. Метод определения пенообразующей способности.– М.: Изд. Стандартов, 1978.– 6 с.
6. ГОСТ 22567.15–95. Средства моющие синтетические. Метод определения моющей способности.– Минск: Изд. Стандартов, 1999.– 11с.

Narzullaev Akmal Khollinorovich,
Post-graduate student of Tashkent Scientific Research Institute of Chemical Technology
E-mail: akmal.narzullayev.90@mail.ru,
Beknazarov Khasan Soiibnazarovich,
Doctor of engineering, Head Scientist of Tashkent Scientific Research Institute of Chemical Technology
Djalilov Abdulakhat Turapovich,
Doctor of chemistry, Academician of the Academy of Sciences of Uzbekistan, Tashkent Scientific Research Institute of Chemical Technology,

EVALUATION OF INHIBITING PROPERTIES OF IC-DAIR-1 CORROSION INHIBITOR IN AQUEOUS AND SALINE MEDIA

Abstract. The article demonstrates environmental safety and efficiency of the use of developed inhibitors in IC-DAlR-1 systems in aqueous and saline media of water supply and in circulating water, as well as in oil and gas chemical industries.

Keywords: corrosion inhibitors, diethanolamine, oleic acid, zinc adduct, metal corrosion, phosphoric acid, nitrogen/phosphorus-containing inhibitors, amine groups.

Introduction. The inhibitors used are mainly based on chemically pure reagents, which, of course, have an impact on the output product price. The literature describes metal corrosion inhibitors in water, aqueous solutions of acids, alkalis, salts, as well as corrosion inhibitors in atmospheric conditions and in non-aqueous liquid media. In addition to practical recommendations and the results of numerous experimental studies, many literature sources give an overview of theoretical models of the inhibitors mechanism, and study their classification [1].

Given the above, the aim of this article is to obtain new highly efficient, highly molecular corrosion inhibitors containing phosphate and amine groups and study the process of corrosion inhibition. In general, given that the expensive corrosion inhibitors are now fully imported, it seems appropriate to study the development and use of new oligomeric corrosion inhibitors [2].

Phosphorus/nitrogen-containing compounds showed by their protective properties that the most significant molecular fragment, determining their protective properties, is a long-chain hydrocarbon radical, located at nitrogen donor atoms of the amino group or phosphorus of the phosphoryl group [3].

Experiment.

In this article, oligomeric corrosion inhibitors synthesized on the basis of diethanolamine, oleic acid and zinc adduct IC-DAlR-1 were studied.

The reaction was carried out in a 500 ml flask equipped with a reflux condenser for 9 hours at a temperature of 150–200 °C.

Corrosion inhibitor is used in tower cooling systems. One of the most effective corrosion inhibitors in water systems is IC-DAlR-1 inhibitor.

The protection degree of corrosion inhibitors was calculated by the formula

$$Z = \frac{V_{ko} - V_{ki}}{V_{ko}}$$

$V_{\kappa o}$ – is the corrosion rate of samples in non-inhibited medium, g*m^{-2} h

$V_{\kappa i}$ – is the corrosion rate of samples in inhibited medium, g*m^{-2} h

IC-DAlR-1 and Puro-tech 1011 the corrosion rate K_{mass} (mass), is determined by the following formula:

$$K_{mass} = \frac{g_0 - g_1}{S \cdot T}$$

g_0 – is the sample weight in the initial state;

g_1 – is the sample weight after reaction;

S – is the surface under study;

T – is the testing time.

IC-DAlR-1

$$K_{mass1} = \frac{9.6281 - 9.6109}{0.000893 \cdot 24} = 0.8025\ g/m^2h$$

Puro-tech 1011

$$K_{mass2} = \frac{8.0124 - 7.9680}{0.000882 \cdot 24} = 2.0479\ g/m^2h$$

Weight corrosion index is recalculated on a depth index according to the formula

$$P = 8.76 \cdot \frac{Kmass}{\gamma}$$

Where P – is the corrosion depth index;

K_{mass} – is the weight index of corrosion rate.

γ – is the density of metal

IC-DAlR-1

$$P_1 = 8.76 \cdot \frac{0.8025}{7.91 \cdot 10^6} = 0.00000088\ mm/g$$

Puro-tech 1011

$$P_2 = 8.76 \cdot \frac{2.0479}{7.91 \cdot 10^6} = 0.00000226\ mm/g$$

The traditional method for graphic processing of polymerization curves to determine the corrosion rate is the extrapolation in semi-logarithmic coordinates of straight-line portions of cathodic and anodic branches before their mutual intersection. However, despite the obvious simplicity of the method, its practical use is often associated with a number of complications. The tangent construction itself is quite subjective, and a more reliable extrapolation requires an additional precise definition of corrosion potential [4; 5].

Results and discussion. Analysis of the studies has shown that the change in corrosion rate and the inhibitor efficiency depends on the inhibitor concentration. Table 1 shows the efficiency of a corrosion inhibitor in aqueous media.

Experimental evidence to study the corrosion rate of steel plates in IC-DAlR-1 aqueous dispersion, both with and without additives, showed that when the concentration changes, the steady-state electrode potential is shifted to a positive region due to the formation of corrosion protection of a barrier type. This effect is greatly enhanced along with an increase in the concentration of an oligomer inhibitor in aqueous dispersion.

It should be also noted that the character of the inhibitor absorption onto the electrode surface, its efficacy, as well as the belonging of inhibitors to the cathodic and anodic types depend not only on its character, but also to a large extent on the medium potential. Judging by the steady-state potential, when IC-DAlR-1 is added, the protection degree is significantly increased. Moreover, more effective corrosion protection is provided when there is a 0.2% IC-DAlR-1 solution, the protective coefficient of which passes through a maximum.

Table 1.– Protective properties of the oligomeric corrosion inhibitor in aqueous and saline media at 30°C for 200 hours

Sample name	With concentration%	Medium	Sample weight loss $m_1 - m_2$	Protection degree, Z%
1	***2***	***3***	***4***	***5***
dis Watery	–	–	–	–
IC-DAlR-1	0.2	Aqueous	0.0015	96.25
IC-DAlR-1	0.05	Aqueous	0.002	95
IC-DAlR-1	0.001	Aqueous	0.0023	94.25
Puro-tech 1011	0.2	Aqueous	0.0018	95.5
Puro-tech 1011	0.05	Aqueous	0.0021	94.7

1	*2*	*3*	*4*	*5*
Puro-tech 1011	0.001	Aqueous	0.0025	93.75
IC-DAlR-1	0.2	NaCl 3%	0.004	90
IC-DAlR-1	0.05	NaCl 3%	0.0054	86.5
IC-DAlR-1	0.001	NaCl 3%	0.0057	85.75
Puro-tech 1011	0.2	NaCl 3%	0.0049	87.7
Puro-tech 1011	0.05	NaCl 3%	0.006	85
Puro-tech 1011	0.001	NaCl 3%	0.0068	83

The mechanism of this oligomeric corrosion inhibitor is mainly determined by the transition of the surface-protected metal to a stable surface film-type state involving particles of fine additives. However, the inhibitors effect in this case is more complex than in film-formation, and is also associated with the nature of ion adsorption of the surface-active agent [6]. For example, if the electrode surface is positively charged relative to the solution, the oligomer inhibitor, which is anion, will be adsorbed onto, if the inhibitor surface is negatively charged – undissociated molecules.

Therefore, the transition to another condition of the process changes the coatings structure or the steady-state potential of metal. By changing the solution composition or applying external polarization, the nature of absorption and, consequently, the nature and effectiveness of inhibitors based on phosphorus/nitrogen-containing oligomers may change. In general, the oligomeric corrosion inhibitors that were synthesized by us have a sufficiently high efficiency of inhibitory effect.

Conclusion. Inhibitors with substituents near the phosphoryl group are more effective in corrosion protection. The protective effect of nitrogen/phosphorus-containing inhibitors is due to the formation of tightly packed films on the surface of steel.

The protective effect of multi-component polymer-type inhibitors based on industrial waste and local raw materials, exceeding that of imported inhibitors up to 5 percent, has been achieved;

The environmental safety of the use of developed inhibitors in water supply systems and circulating water, as well as in oil and gas chemical industries has been shown, their efficiency of 95.15% has been determined.

References:

1. Изоляция труб, фитингов и арматуры в полевых условиях. Serviurap's pipeline protection system // Water and Waste Treat (Or. Brit.). 2000.– No. 5.
2. El-Etre A. Y., Abdallah M., El-Tantawy Z. E. Corrosion inhibition of some metals using lawsonia extract, Corros. Sci. 47, 2005.– P. 385–395.
3. Khadom A. A., Yaro A. S., AlTaie A. S., Kadum A. A. H. Electrochemical, activations and adsorption studies for the corrosion inhibition of low carbon steel in acidic media, Portug. Electrochim. Acta 27, 2009.– P. 699–712.
4. Тошев М. Э., Умаров А. Н., Кадиров Х. И. Ингибиторы солеотложения для водогрейных котлов и систем теплоснабжения. Международная научно-техническая конференция «Актуальные проблемы инновационных технологий в развитии химической, нефте-газовой и пищевой промышленности». 2016.
5. Кузнецов Ю. И., Казанская Г. Ю., Цирульникова Н. В. Аминофосфатные ингибиторы коррозии стали, «Защита металлов», 2003.– Том 39.– С. 141–145.
6. Кузнецов Ю. И., Казанская Г. Ю., Ингибирование коррозии железа этилендиаминтетраметиленфосфонатными комплексонатами, «Защита металлов», 1997.– Том 33.– С. 234–238.

Tukhtayev Feruz Sadulloyevich,
P.G. student, Tashkent state technical university
Negmatova Komila Soyibjonovna,
doctor of the technical sciences, professor
Tashkent state technical university
Negmatov Soyibjon Sodikovich,
doctor of the technical sciences, professor,
academician of Academy of Sciences
of the Republic of Uzbekistan
Tashkent state technical university
Karimova Dilorom Amonovna,
candidate of the chemical sciences, assistant professor
Navai state pedagogical institute
E-mail: kamalova.di@mail.ru

RESEARCH OF MAGNETIC CHARACTERISTICS ELECTROCONDUCTIVE COMPOSITION POLYMERIC SORBENT (CPS)

Abstract. In article is considered about receiving and characterizing of various forms of the carrying-out polymer-polyaniline. Curve magnetizations of the received forms are investigated. It is revealed that in the oxidized form material shows a magnetic hysteresis at the room temperature. For polyaniline without special alloying with magnetic additives such result is received for the first time.

Keywords: polymer, polyaniline, magnetic properties, electric conductance, magnetics, oxidations, backs.

Organic magnetics (or otherwise molecular magnetics) stopped being exotic at the end of the last century. Rather wide range of organic highly spin materials on the basis of complexes with charge transfer [1] and radicals of a nitroksid was received. Also, as structural elements of organic magnetics aromatic amines were used. Recently magnetic properties of the high-molecular polyinterfaced connections – electroconductive polymers are intensively investigated.

It is shown that representatives of this class – polyaniline, polypirrole, the polythiohair dryer possess intensive spin-spin interaction and are perspective for creation of high-molecular organic magnetics. Development of materials of this type not only is supported by interest in fundamental problems of magnetism, but also is a part of the general process of search of new materials with an unusual combination of the properties providing new opportunities for the equipment and technology. A research object in the real work was the organic semiconductor the polyaniline relating to high-molecular aromatic amines.

Fat points are not coupled electrons which are not participating in covalent communications. Pluses are symbolized by existence of the effective positive charge (hole) localized on nitrogen atom as a result of its oxidation.

The polymeric chain of electroconductive polyaniline (PANI) consists of regularly alternating benzene rings and nitrogen-containing groups (fig. 1). Such structure of a chain provides polyinterface (regular alternation of unary and double communications).

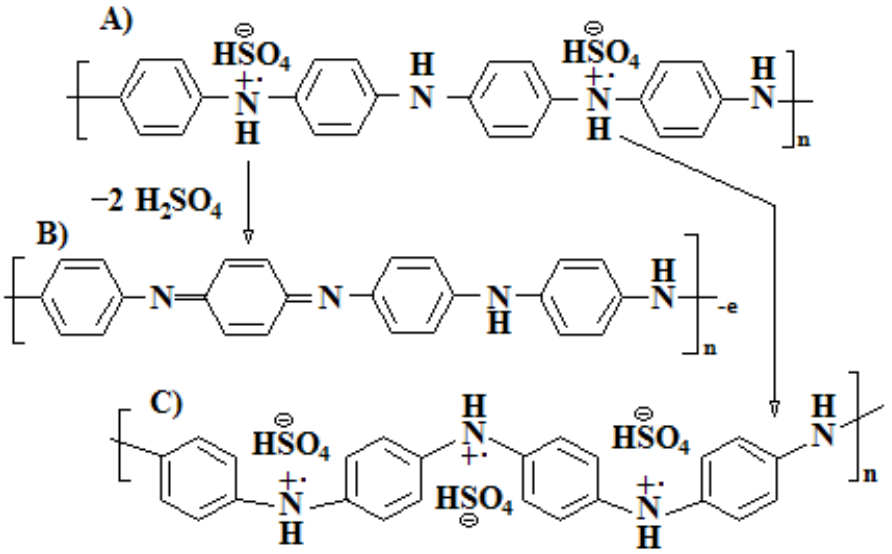

Figure 1. Structural formulas of various forms of polyaniline. The A – protonated emeraldine form containing a half of the oxidized atoms of nitrogen, B – deprotonirovation emeraldine with the smallest concentration of spin, C – the protonated PANI pernigraniline form where more than a half of atoms of nitrogen are in the oxidized state

The polymeric chain forms the zigzag lying in one plane, at the same time clouds of π-electrons are blocked over and under the chain plane. Carriers of a charge are formed in such polymer at its oxidation. As the centers of oxidation of the PANI serve the nitrogen atoms having couple of electrons which is not involved in chemical valent bonds. At oxidation, i.e. withdrawal of one of electrons, in a polymeric chain the positive charge appears. Removal of one of electrons of couple means formation not coupled a back. Existence of such spin in material also results in the PANI uncommon magnetic properties. Content of the oxidized nitrogen atoms in the PANI can change from zero (that corresponds got into condition a leykoemeraldine) almost to unit (the highest oxidation level – pernigraniline). Most the PANI stable form is emeraldine where every second atom of nitrogen (fig. 1) is oxidized.

The positive charge arising at oxidation in the main chain has to be compensated (in chemical terminology it is stabilized) by an antiion. The best stabilizers of carriers of a charge of the PANI are strong acids. Anion of acid is connected by Coulomb interaction with the electronic hole formed at oxidation (i.e. during removal of an electron). Interaction of the PANI with acid is reversible and is called protonation. Removal of the stabilizing acid (deprotonirovation) leads to decrease in conductivity and concentration of not coupled spin.

Processes of oxidation restoration and protonation-deprotonirovation of the PANI are reversible. It creates variety of the forms of polymer having various properties.

In the real work the PANI magnetic properties, the oxidation which underwent various chemical treatment at a post-polymerization stage and being in various states and protonation are investigated.

By preparation of samples much attention was paid to purity of initial reagents, care of carrying out synthesis and the subsequent operations, on purpose not to allow pollution of samples magnetic impurity and not to change morphology of the studied material. It is especially important when studying weak magnetism of the obscure nature. In our opinion, a comparative research of the same initial material which magnetic properties change at the chemical influence which is not bringing impurity and not changing material morphology, most reliably. At

synthesis of the PANI and its post-polymerization processing metal ware and devices were not used. Samples were stored and transported in tight plastic packing.

Polyaniline is received by method of oxidizing polymerization of aniline [2]. Equal volumes of solutions of aniline (0.2 M) in sulfuric acid (0.2 M) and ammonium sulfate peroxide (0.25 M) in water mixed at the room temperature. Within 10 min. in a reactionary flask there was an exothermic reaction which was followed by change of coloring of the reactionary environment and loss of a dense black-green deposit of polymer.

The protonated PANI emeraldine form was the main product of polymerization. Synthesis by-products, sulfate of ammonium and sulfuric acid and also small amounts of oligomer of aniline were removed repeated washing of a deposit in acidic water environments and methanol. An exit of polymer made 95–98%.

The research of the PANI various forms by EPR-analysis methods with use of an organic standard of spin density showed that the maintenance of not coupled spin depends on oxidation level and protonation of polymer [3].

The experimental results received in the real work raise the questions on which there are only presumable answers so far. Is even more problematic to offer an overall picture of the phenomena and interactions shown in an experiment.

In article the possibility of management of magnetic properties of the carrying-out polyaniline by means of chemical treatment of polymeric material is shown. The nature of the influences changing magnetic properties was not connected with introduction of magnetic additives that proves own nature of magnetism of polyaniline. At the same time concerning the mechanisms responsible for magnetism of polyaniline, only the hypothetical assumptions can be made. The bigger number of the parameters necessary for characterization of polymeric material, in comparison with traditional solid-state objects is essential (for example, conformational characteristics of polymeric chains) leaves, in our opinion, an opportunity for many assumptions and demands a further research.

References:

1. Allemand P. M., Khemani K. C., Koch A., Wudl F., Holezer K., Donovan S., Gruner G., Thompson J. D. Science 253, 1991.– 301 p.
2. Stejskal J., Sapurina I., Prokes J., Zemek J. Synth. Met. 105, 1999.– 195 p.
3. Karimova D. A. Studying of structure polymer – polymeric compositions on the basis of polyaniline and various polyacids. "Composite materials". – No. 4. 2011.– P. 12–14.

Fayzullayev N. I.,
Samarkand State University
Rakhmatov Sh.B.,
Bukhara medical institute
E-mail: xurshiduz@yandex.ru

KINETICS AND MECHANISM OF THE REACTION OF THE CATALYTIC OXYCONDENSATION REACTION OF METHANE

Abstract. Internal diffusion retardation in oxycondensation process of methane was analyzed. Effect of diferent factors to the reaction rate of preparation ethylene from methane was studied. Based on experimental results the reaction mechanism for the reaction of ethylene formation from methane was proposed and kinetic equation characterizing the whole process was chosen and its adequacy was tested.

Keywords: methane, ethyele, oxycondensation, mechanism, volumetric rate, kinectic equation, diffusion.

Introduction

Detected reserve of the natural gas deposit of the Republic of Uzbekistan is almost 2 trillion m^3, and the oil is 350 million tons. Currently 31–32% of oil deposits have been mined in the Republic. Only 0.5–2.0% of methane has been processed chemically worldwide. This puts the task to increase products based on methane from the natural gas and to broaden researches focused on researched synthesizing important materials for the national economy. Saving materials and heat-energetic resources is one of the important tasks of modern technique. Development of the energy saving technology is one of the main directions of chemical technology and scientific technical progress. In many chemical processes in industry energy loss is main part of the total extravagance. Moreover development of technology using heat resources (oil, coal, natural gas) are raw materials and energy sources in many chemical syntheses simultaneously is important [1–3].

The only correct way of perspective processing the natural gas is oxycondensation reaction, and the process takes place in one step and at the normal atmospheric pressure.

More than 30 year passed since the oxycondensation reaction of methane was discovered, but stable catalyst with high activity and yield was not developed so far, thus the reaction has not been applied in industry. For this reason development of catalyst and optimization of working parameters of apparatus for the preparation planned products with maximal yield is important [4–10].

Experimental section

Based on the analysis of reactants and products, the following parameters of the process were determined:

1. Hydrocarbon conversion:

$$X_{yB} = \frac{\sum_i c_i^{maxc} \cdot \mathrm{n}_\mathrm{i}^\mathrm{c}}{\sum_i c_i^{maxc} \cdot n_i^c + c_i^{yB}} \cdot 100\%$$

2. Oxygen conversion:

$$\mathrm{X}_{\mathrm{O}_2} = \frac{\left(C_{O_2}^0 - C_{O_2}^i \cdot K_N\right)}{C_{O_2}^0} \cdot 100\%$$

3. Selectivity relative to the reaction products:

$$S_i = \frac{C_i^{maxc} \cdot n_i^c}{\sum_\mathrm{i} \mathrm{C}_\mathrm{i}^{\mathrm{maxc}} \cdot \mathrm{n}_\mathrm{i}^\mathrm{c}} \cdot 100\%$$

4. Yield of the reaction:

$$Y_i = \frac{C_i^{maxc} \cdot n_\mathrm{i}^\mathrm{c}}{\sum_i c_i^{maxc} \cdot \mathrm{n}_\mathrm{i}^\mathrm{c} + C_i^{yB}} \cdot 100\%$$

where C_i^{yB} – concentration of respective hydrocarbon from the reactor (mol.%); C_i^{maxc} – concentrate of the product I from the reactor (mol.%); n_i^c – number of carbon atoms in the product molecule; $C_{O_2}^0$ – concentration of oxygen in initial mixture (mol%); $K_N = \frac{N_2^0}{N_2^i}$ – coefficient related to change of net volume during the reaction, N_2^i – concentration of nitrogen input of the reactor; N_2^i – concentration of nitrogen from the reactor.

The rate of the reaction according to individual components (reactants and products) in the mixture based on the their concentration in mixture was calculated suing the formula below.

$$W_i = V_\Sigma (C_{i,0} - C_i)/\nu$$

ν – catalyst volume; W_i-rate of the depletion of reactant-*i* or formation of product-*i* (mol·s^{-1}·cm^{-3}); V_Σ – sum rate of stream of reaction mixture (normal conditions cm^3/sec); $C_{i,0}$ and C_i – initial and final concentrations of components respectively.

Oxycondensation reaction of methane was studied in stream differential reactor in laboratory conditions. The reactor is made of quarts with the length 650 mm and inner diameter 8 mm. catalyst dimension is 0.25–0.5 mm. Methane: oxygen in 2÷7–1volumetric ratio was sent to the reactor at the rate 1 ÷ 15 l/hour. The temperature was changed from 700 to 850 °C. oxycondensation reaction of methane was carried out in stream differential reactor at the normal atmospheric pressure. Gas products of the reaction was analyzed using GC.

Catalyst with the composition Metanni oksikondensasiyalash reaksiyasi uchun $(Mn_2O_3)_x \cdot (Na_2MoO_4)_y \cdot (ZrO_2)_z$ for the oxycondensation reaction of methane was prepared using the sol-gel method. Phase content was carried out on DRON-4.0 (CuK_α – beam) diffractometer, and particle size was determined on the scanning electron microscope ((JSM-6380 LV) and the transmission electron microscope (EMV-100BR).

Effect of internal diffusion retardation in the oxycondensation of methane was analyzed using the method proposed by Wagner:

$$F_S = \frac{d_z^2 \cdot z}{4 \cdot D_{eff} \cdot c} < 1 \qquad (1)$$

where F_S – Tile modulus; D_{eff} – effective diffusion coefficient of oxygen to the inner shell of catalyst, m^2/s; d_z – diameter of the catalyst particle, m; *g* – maximum rate of the reaction, mol/mol·s; *c* – reactant concentration, mol/mol.

The temperature difference in the interior and exterior of the catalyst granule effect on the rate of reaction was defined using the following equation;

$$\frac{d_z^2 \cdot r \cdot \Delta H}{4 \cdot \lambda_{kat} \cdot T} < \frac{RT}{E_A} \qquad (2)$$

where ΔH – reaction enthalpy, J/mol; λ_{kat} – heat conductivity of the catalyst particle, $Vt(m{\cdot}k)$; T – temperature, K; E_a – activation energy, J/mol; R – Universal gas constant, J/(mol·K).

In order to evaluate effect of external diffusion retardation on the surface of the catalyst the criterion was applied, it resembles the rate of reaction on the surface of catalyst relation to diffusion rate of substances from gas or liquid phase. If the rate of reactants in the stream differs less than 5% from the concentration on the surface, the rate of reaction does not differ more than 5% from the kinetic rate, thus the nonequality fulfills;

$$\frac{r \cdot d_z}{2 \cdot \beta \cdot c} < 0.15 \text{ yok} \qquad (3)$$

$$\frac{d_z \cdot r \cdot \Delta H}{2 \cdot \alpha \cdot T} < 0.15 \frac{RT}{E_A} \qquad (4)$$

where β – mass exchange coefficient, m/s. α – heat exchange coefficient, Vt/(m^2·K).

Calculations show that F_S = 0.35, the left side of equation (2) $1.6 \cdot 10^{-3}$, the right side 0.045; the left side of nonequality (3) 0.03; the left side of nonequality (4) $2.6 \cdot 10^{-3}$, the right side less than $6.7 \cdot 10^{-3}$, thus oxycondensation reaction of methane in a kinetic range.

Results and discussion

In order to study the kinetic law of oxycondensation reaction of methane effect of partial pressure of methane and oxygen on the rate of formation of ethylene at the temperature 700 ÷ 800 °C and volumetric rate 600 ÷ 1200 hour^{-1} was studied.

Effect of partial pressures of reactants on transition the law the partial pressure of one gas was changed while the other gas partial pressure was kept constants. In order to keep the linear rate required amount of argon gas was sent to the reactor. The volume of catalyst was tuned to the experiment conditions to keep the comparative rate constant.

Keeping the linear rate of gas stream at different values of the temperature and volumetric rate, effect of the partial pressure of methane on the oxycondensation process is given in (Table 1).

Table 1.– Effect the partial pressure of methane on different volumetric rates and temperatures (P_{total} = 0.1 MPa, P_{oxygen} = 0.014 MPa)

Volumetric rate of methane, ml/ml.cat.hour	Partial pressure of methane, MPa	Conversion degree of methane to ethylene,%			Selectivity relative to ethylene S,%		
		T=700 °C	T=750 °C	T=800 °C	T=700 °C	T=750 °C	T=800 °C
600	0.017	8.8	14.3	20.6	6.7	8.4	10.6
800	0.017	7.6	11.5	17.4	5.6	7.2	8.8
1000	0.017	6.7	9.1	13.5	5.2	6.4	7.6
1200	0.017	5.8	8.5	9.7	4.8	5.8	6.5
600	0.025	18.4	20.8	2405	7.2	9.5	12.8
800	0.025	15.2	17.6	21.0	6.4	8.2	11.3
1000	0.025	13.0	15.2	18.6	5.6	6.4	10.0
1200	0.025	10.6	12.8	14.4	4.8	5.0	8.1
600	0.033	25.8	27.4	28.6	23.2	34.6	41.8
800	0.033	24.6	30.2	35.8	41.9	54.5	57.8
1000	0.033	23.4	33.2	42.8	64.3	72.8	81.4
1200	0.033	20.8	28.5	39.2	48.8	62.5	75.9

As shown on the table, increase in the partial pressure of methane at different comparative volumetric rates and temperatures, decreases total conversion.

Effect of the partial pressure of oxygen on the kinetic law of the oxycondensation reaction at the temperature 700 ÷ 800 °C and volumetric rate 600 ÷ 1200 hour^{-1} was studied. The partial pressure of oxygen changed from 0.014 MPa to 0.01 MPa, while the partial pressure of methane kept constant (0.033 MPa). Results are given in (Table 2).

Table 2.– Effect the partial pressure of oxygen on different volumetric rates and temperatures (P_{total} = 0.1 MPa, $P_{methane}$ = 0.033 MPa)

Volumetric rate of methane ml/ml.cat.hour	Partial pressure of oxygen, MPa	Conversion degree of methane to ethylene,%			Selectivity relative to ethylene S,%		
		T=700 °C	T=750 °C	T=800 °C	T=700 °C	T=750 °C	T=800 °C
1	*2*	*3*	*4*	*5*	*6*	*7*	*8*
600	0.010	17.2	20.8	24.6	9.8	12.3	14.5
800	0.010	14.8	18.4	21.2	8.2	10.0	11.3
1000	0.010	10.4	14.0	17.8	6.4	8.5	9.8
1200	0.010	7.7	11.2	15.5	4.9	6.0	7.5

1	*2*	*3*	*4*	*5*	*6*	*7*	*8*
600	0.012	20.5	23.8	27.2	15.0	20.4	24.8
800	0.012	18.2	20.0	24.5	13.2	17.5	19.9
1000	0.012	15.8	17.4	21.1	10.7	14.8	16.2
1200	0.012	13.9	16.2	18.7	8.5	11.2	13.8
600	0.014	25.8	27.4	28.6	23.2	34.6	41.8
800	0.014	24.6	30.2	35.8	41.9	54.5	57.8
1000	0.014	23.4	33.2	42.8	64.3	72.8	81.4
1200	0.014	20.8	28.5	39.2	48.8	62.5	75.9

As shown in the table, decrease in the partial pressure of oxygen also decreases the total conversion of methane, and yield of formation and selectivity as well.

Results of kinetic studies show that increase of contact time and elevated temperature the process parameters improve.

Increase in the ration of CH_4 : O_2 decreases the conversion of methane and oxygen. Input of ethane, ethylene, CO and CO_2 also decreases the formation of products. nisbatining ortishi metan va kislorod konversiyasining pasayishiga olib keladi. Increase in the contact time increases conversion of oxygen and methane, and decreases the selectivity relative to ethylene. Elevation of temperature increases conversion of methane, and decreases the selectivity relative to ethane and ethylene. Increase in the methane: oxygen ratio increases selectivity to ethane and selectivity to ethylene stays unchanged.

Increase in the temperature increases the conversion of oxygen. At 700 °C conversion of oxygen reaches 95% for 0.9 sec, at 1000 °C contact time is 0.009 sec.

Increase in the conversion of oxygen decreases the selectivity of the process. Increase in temperature up to 700–800 °C, the selectivity of the process decreases, and later the selectivity increases at 850–9650 °C.

Oxycondensation reaction of methane takes place in homogeneous-heterogeneous mechanism. Activation of methane takes place on the surface of hard oxide catalyst. On the active site of the catalyst one hydrogen atom evolves from methane and methyl radical forms.

Ethylene formation from oxycondensation of methane is one step process and takes place at normal atmospheric pressure. The process can be described using the following (schemes 1):

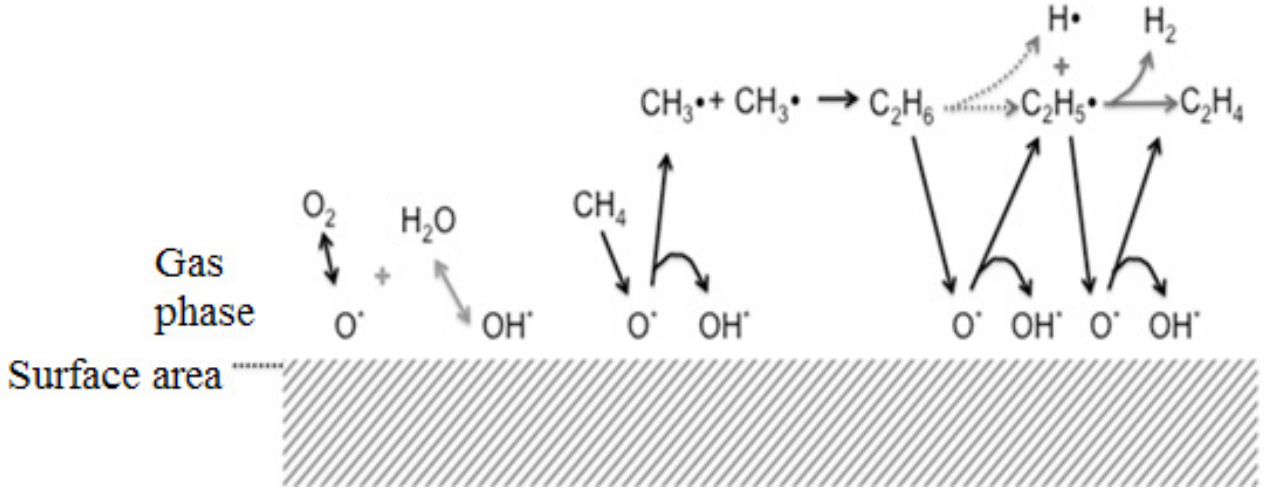

Schemes 1. Methane oxycondensation reaction mechanism to get aimed products

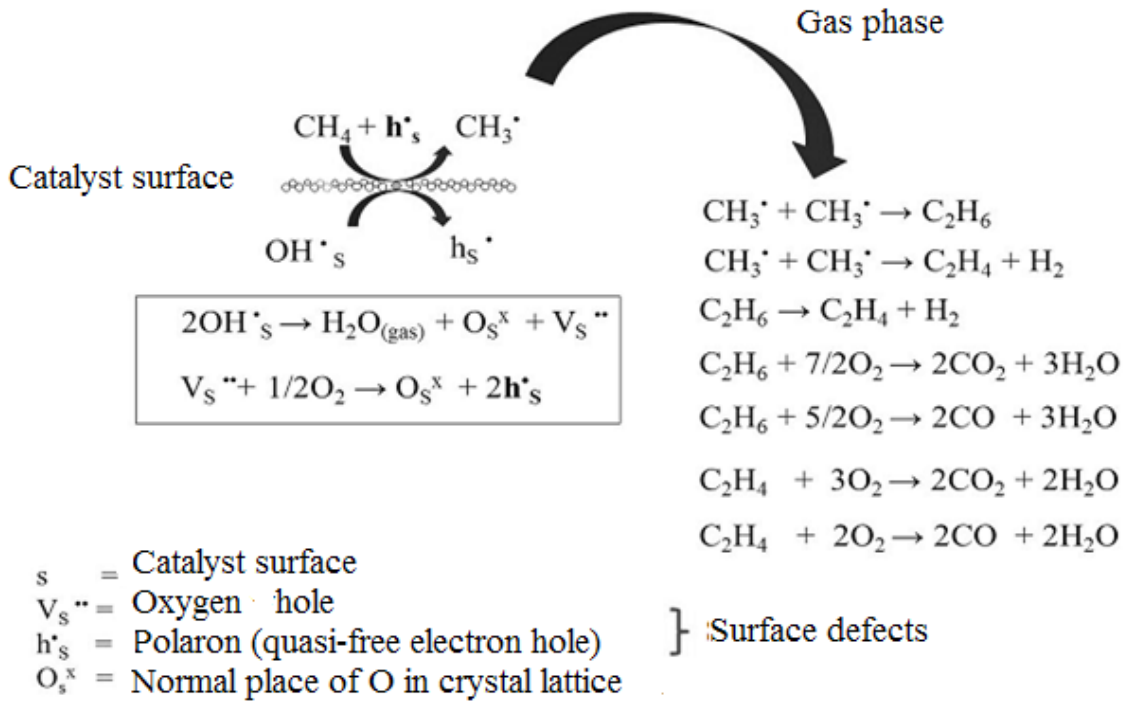

Schemes 2. Reaction path of oxycondensation reaction of methane

Ethylene formation from ethane takes place the temperature higher that 700 °C on the active site of the catalyst surface.

$$CH_4 \rightarrow [CH_3]_{ads} + 2[H]_{ads}$$
$$2[CH_3]_{ads} \rightarrow [C_2H_6]_{ads} + ads$$
$$[C_2H_6]_S + [O]_S \rightarrow [C_2H_5^{\bullet}]_S + [OH^{\bullet}]_S$$
$$[C_2H_5]_S + [O]_S \rightarrow [C_2H_4] + [OH^{\bullet}]_S$$
$$[C_2H_5^{\bullet}]_S + [O_2]_S \rightarrow [C_2H_4] + [OH^{\bullet}]_S$$
$$[C_2H_6]_S + [O_2]_S \rightarrow [C_2H_4]_S + 2[OH^{\bullet}]_S$$
$$[C_2H_5^{\bullet}] + CH_4 \rightarrow C_2H_6 + CH_3^{\bullet}$$
$$[C_2H_5^{\infty}]_S + [O_2]_S \rightarrow [C_2H_4] + [OH^{\bullet}]_S$$
$$[C_2H_6]_S + [O_2]_S \rightarrow [C_2H_4]_S + [H_2O]$$
$$[C_2H_6]_{ads} \rightarrow [C_2H_4]_{ads} + H_2$$

In presence of optimal catalyst with the content $(Mn_2O_3)_x \cdot (Na_2MoO_4)_y \cdot (ZrO_2)_z$ the kinetic laws of oxycondensation process of methane were studied partial pressures of reactants and at different temperatures at the differential reactor conditions, and the kinetic model of the process was developed. Oxycondensation of methane can be described using the following equations:

$$4CH_4 + O_2 \rightarrow 2C_2H_6 + 2H_2O \; w_1 = k_1 P_{O_2}$$
$$2C_2H_6 + O_2 \rightarrow 2C_2H_4 + 2H_2O \; w_2 = k_2 P_{C_2H_6} \cdot P_{O_2}$$
$$2CH_4 + O_2 \rightarrow C_2H_4 + 2H_2O \; w_3 = k_3 P_{O_2}$$
$$2C_2H_6 + 5O_2 \rightarrow 4CO + 6H_2O \; w_4 = k_4 P_{C_2H_6} \cdot P_{O_2}$$
$$2C_2H_6 + 7O_2 \rightarrow 4CO_2 + 6H_2O \; w_5 = k_5 \cdot P_{C_2H_6} \cdot P_{O_2}$$
$$C_2H_4 + 2O_2 \rightarrow 2CO + 2H_2O \; w_6 = k_6 \cdot P_{C_2H_4} \cdot P_{O_2}$$
$$C_2H_4 + 3O_2 \rightarrow 2CO_2 + 2H_2O \; w_7 = k_7 \cdot P_{C_2H_4} \cdot P_{O_2}$$

Kinetic studies and calculations give the following kinetic parameters:

$lgk_1 = 24{,}56 - 18020/T$;
$lgk_2 = 10{,}0 - 9997/T$;
$lgk_3 = 38{,}72 - 34073/T$;
$lgk_4 = 13{,}48 - 2855/T$;
$lgk_5 = 18{,}21 - 6104/T$;
$lgk_6 = 13{,}01 - 10904/T$;
$lgk_7 = 12{,}87 - 10114/T$;

where T – temperature, K.

Ethylene formation from oxycondensation of methane is one step process and takes place at normal atmospheric pressure. The process can be described using the following reactions:

$2CH_4 + 1/2O_2 \rightarrow C_2H_6 + H_2O\ \Delta H = -176.8$ kJ/mol
$2C_2H_6 + O_2 \rightarrow 2C_2H_4 + 2H_2O\ \Delta H = -105.5$ kJ/mol
$2CH_4 + O_2 \rightarrow C_2H_4 + 2H_2O\ \Delta H = -277.51$ kJ/mol
$C_2H_4 + O_2 \rightarrow 2CO + 2H_2\ \Delta H = -451.1$ kJ/mol
$C_2H_4 + 3O_2 \rightarrow 2CO_2 + 2H_2O\ \Delta H = -1329.7$ kJ/mol
$C_2H_6 + 7/2O_2 \rightarrow 2CO_2 + 3H_2O\ \Delta H = -1490.2$ kJ/mol
$CH_4 + 2O_2 \rightarrow CO_2 + 2H_2O\ \Delta H = -803.9$ kJ/mol
$CO_2 + H_2 \rightarrow CO + H_2O\ \Delta H = +412$ kJ/mol

The process takes place with the formation of ethane and its dehydrogenation forms ethylene. Taking into account all products, the following net reaction can be writtem:

$$400CH_4 + 259O_2 \rightarrow 90C_2H_6 + 70C_2H_4 + 64CO_2 + 374H_2O + 16H_2 + 16CO$$

$$\Delta H_{800^0C} = -514 \text{ kJ/mol}$$

The catalytic oxycondensation reaction of methane takes place at high temperature and the condensation can be described using the kinetic equation Langmuir-Hinshelwood mechanism. Taking into account abovementioned, the sorbtion process obeys to Langmuir isotherm, the kinetic equation for the catalytic oxycondensation reaction of methane the following Langmuir-Hinshelwood equations porposed:

$$W = \frac{k \cdot K_{CH_4} \cdot P_{CH_4} \cdot K_{O_2} \cdot P_{O_2}}{(1 + K_{CH_4} \cdot P_{CH_4} + K_{O_2} \cdot P_{O_2})} \quad (1)$$

$$W = \frac{k \cdot K_{CH_4} \cdot P_{CH_4} \cdot K_{O_2} \cdot P_{O_2}}{(1 + K_{CH_4} \cdot P_{CH_4} + K_{O_2} \cdot P_{O_2})^2} \quad (2)$$

$$W = \frac{k \cdot K_{CH_4} \cdot P_{CH_4} \cdot K_{O_2} \cdot P_{O_2}}{K_{CH_4} \cdot P_{CH_4} + K_{O_2} \cdot P_{O_2}} \quad (3)$$

It is eesential to test the adequacy of chosen eqautions (1–3) of experimental kinetic laws taken of differential reactor conditions. Taking into account of given equations and results of experiments, parameters of kinetic equations sum of quadratic deviation of experimental results must be minimally differ from the theoretically calculated results. Because of nonlinearity of proposed equations, their solution could be unlimited in mathematic way. In kinetics, solutions to equations are determined testing the adequacy for the range of the change of kinetic parameters based on the results of experiments. Thus, solutions of kinetic equations are determined using the rate constant *k* of the reaction, and adsorption coefficient of oxygen and methane (K_{O_2}, K_{CH_4}), partial pressures of oxygen and methane (K_{O_2}, K_{CH_4}), and experimental rate value (W). Checking the adequacy of equations were carried out based on the mean quadratic deviation (s) between the difference of experimental and theoretical results.

Based on given equations and experimental results, it was determined the paramaters of kinetic equation sum of quadratic deviation of experimental from the theoretically calculated value differs minimally. Basis of the adequacy of kinetic equation the fulfillment of the following condition was taken:

$$\sum_{i=1}^{n} (W_{amalia} - W_{nazarius})^2 \Rightarrow \min.$$

So, adequate kinetic equation for the oxycondensation reaction of methane in presence of $(Mn_2O_3)_x \cdot (Na_2MoO_4)_y \cdot (ZrO_2)_z \cdot (Mn_2O_3)_x \cdot (KCl)_y \cdot (ZrO_2)_z$ catalyst at differential reactor conditions were proposed and its adequacy was evaluated.

$$W = \frac{k \cdot K_{CH_4} \cdot P_{CH_4} \cdot K_{O_2} \cdot P_{O_2}}{(1 + K_{CH_4} \cdot P_{CH_4} + K_{O_2} \cdot P_{O_2})^2}$$

Based on constants of kinetic eqautions determined at different temperatures, the activation energy of the process (E_a = 33.8 kJ/mol) was calculated.

During the derivation of the kinetic equation of the oxycondensation reaction of methane limiting step was the rate of adsorption of oxygen and methane on the catalyst surface. The adsorption process on the catalyst surface is monomolecular, since oxygen and methane are adsorbed individually at active sites.

Conclusions

1. The internal diffusion retardation at the oxycondensation process of methane was analyzed.

2. Effect of different factors on the raction of ethylene formation from methane was studied.

3. The mechanis of ethylene formation from methane was proposed based on obtained results.

4. Kinetic equation characterizing the whole process was chosen and its adequacy was tested.

References:

1. Дедов А. Г., Локтев А. С., Тельпуховская Н. О., Пархоменко К. В., Геращенко М. В., Моисеев И. И. Окислительная конденсация метана в присуствии лантан-цериевых катализаторов: фундаментлаьный характер эффекта неаддитивности // Химия и технология топлив и масел. 2010.– Т. 46.– № 2.– С. 43–46.
2. Махлин В. А., Подлесная М. В., Дедов А. Г., Локтев А. С., Тельпуховская Н. О., Моисеев И. И. Окислительная димеризация метана: кинетика, математическое моделирование и оптимизация процесса на La/Ce катализаторах // Российский химический журнал. 2008.– Т. 52.– № 5.– С. 73–79.
3. Taheri Z., Seyed-Matin N., Safekordi A. A., Nazari K., Pashne S. Z. A comparative kinetic study on the oxidative coupling of methane over LSCF perovskite-type catalyst // Applied Catalysis. A: General. 2009. 354 (1).– P. 143–152.
4. Xin Y., Song Z., Tan Y. Z., Wang D. The directed relation graph method for mechanism reduction in the oxidative coupling of methane //Catalysis Today.2008. 131 (1) – P. 483–488.
5. Ломоносов В. И., Усманов Т. Р., Синев М. Ю., Бычков В. Ю. Закономерности окисления этилена в условиях реакции окислительной конденсации метана // Кинетика и катализ. 2014.– Т. 55.– № 4.– С. 498–505.
6. Ghose R., Hwang H. T., Varma A. Oxidative coupling of methane using cata-lysts synthe-sized by solution combustion method // Applied Catalysis A: General. 2013.– Vol. 452.– P. 147–154.
7. Kus S., Otremba M., Taniewski M. The catalytic performance in oxidative coupling of methane and the surface basicity of La_2O_3, Nd_2O_3, ZrO_2. // J. Fuel.2003. 82 (11).– P. 1331–1338.
8. Файзуллаев Н. И. Метандан этилен синтези реакторини моделлаштириш ва мақбуллаштириш // СамДУ илмий ахборотномаси. 2016.– № 5.– Р. 147–153.
9. Fayzullayev N. I. Catalytic Oxicondensation of Methane // International Journal of Chemical and Physical Science. 2015.– V. 4.– No. 2.– P. 49–54.
10. Махлин В. А., Магомедова М. В., Зыскин А. Г., Локтев А. С., Дедов А. Г., Моисеев И. И. Математическое моделирование кинетики окислительной конденсации метана: // Кинетика и катализ катализ. 2011.– Т. 52.– № 6.– С. 1–9.

Holnazarov Bakhodir Azamovich,
Senior Research Fellow,
Termez State University
E-mail: Baxodir.Xolnazarov@rambler.ru
Turaev Khayit Khudainazarovich,
Doctor of Chemical Sciences, Professor,
Termez State University
Dzhalilov Abdulakhat Turapovich,
Member of the Academy of Sciences of the Republic of Uzbekistan,
Professor, Doctor of Chemical Sciences,
Director of the Tashkent Research
Institute of Chemical Technology, Republic of Uzbekistan

SYNTHESIS OF STARCH, ACRYLAMIDE, ACRYLIC ACID AND MONTMORILLONITE-BASED SUPERABSORBENT POLYMER COMPOSITE

Abstract. This article studies the synthesis of a high swelling hydrogel based on starch, acrylamide, acrylic acid and montmorillonite. The reaction temperature and the effect of reaction time on the properties of the product are studied. The product of the copolymerization reaction was characterized by IR spectroscopy. The surface structures of the hydrogel were studied with an electron scanning microscope.

Keywords: Starch, acrylamide, acrylic acid, montmorlonite, superabsorbent hydrogel, binding agent, initiator, swelling kinetics.

Introduction: Hydrogels are three-dimensional hydrophilic polymeric networks capable of absorbing large amounts of water or biological fluids. They are widely used in gardening and agriculture. In agriculture, they are used for water retention [2], packaging materials, oil extraction, heavy metal absorbents and drug release carriers [3]. Starch-based hydrogels, copolymer of acrylic acid and acryamide, are widely used because of their high water absorption and low cost. However, these types of superabsorbent (SA) usually have a low salt tolerance and a slow rate of water absorption. In addition, after water absorption, they exhibit poor strength, dispersing and elastic properties of the gel. These disadvantages severely limit the quality of the product and the scope of this type of SA. To improve the properties of such a SA material, researchers used such methods as the formation of interpenetrating networks and mixing with inorganic clays [4]. These methods help to improve the mechanical properties of hydrogels. Adding inorganic clay is a relatively effective way to improve the properties of this type of hydrogel [5]. Montmorillonite, bentonite, kaolin are commonly used to modify hydrogel with high water absorption. The results showed that the addition of suitable amounts of inorganic clays can improve the mechanical strength and water-absorbing ability of the hydrogel [6]. The gel prepared by researchers [7] showed an improvement in salt tolerance and strength, which compared to a gel without kaolin and the addition of 5–10% kaolin to a composite hydrogel increases its water absorption coefficient by

20% and its ability to conserve water by 25%, which is the addition of modified montmorillonite not only increased the water absorption coefficient, but also improved the ability of the gel to conserve water.

Bentonite is a clay mineral whose main component is montmorillonite. Its crystal structure consists of two layers of an oxygen-silicon tetrahedron with one layer of an octahedral sheet of alumina. This clay has good properties of expansion, absorption and caking. Kaolin is a clay mostly composed of kaolinite. It has a relatively high ductility and sintering [8]. It is easily dispersed in water and has good fire resistance. Many researchers have recently reported compound hydrogels made from bentonite and kaolin. Researches have shown that bentonite and kaolin have a different effect on the properties of the hydrogel. Kaolin significantly increases the tensile strength and mechanical properties of composite gels, and bentonite significantly increases their water-absorbing ability [9]. To date, most studies have focused on the effect of one particular type of clay on the effectiveness of gels. However, it is not clear how the performance of a hydrogel changes when two different types of clay are added at the same time and whether two different types of gels can be synergistically applied to achieve a good effect.

Therefore, in this research, inorganic fillers starch, acrylic acid and acrylamide, bentonite were used as a water-absorbing monomers a, N, N'-methylene bisacrylamide (MBAm) as a crosslinking agent and potassium persulfate (KPS) as an initiator for the preparation of composite hydrogel based on starch, acrylic acid, acrylamide and bentonite. The effect of concentrations of initiator, crosslinking agent, bentonite on the water-absorbing ability of the hydrogel has been studied. In addition, the effect of the degree of neutralization of acrylic acid and the reaction temperature on the ability of the hydrogel to absorb water was also studied. The thermal stability, water-saving capacity, multiple water absorption and salt tolerance of the composite hydrogel were analyzed. The micromorphology and chemical structure of the gel were also analyzed.

Research objects and methods: The experiment used Golden Corn corn starch produced by the Tashkent starch factory, acrylamide (AA), acrylic acid (AAc), a crosslinking agent (CA) – N, N'-methylenebisacrylamide with main component content of 98% or more, potassium persulfate (KPS), sodium metabisulfite (initiator) and used montmorillonite (MT) from the Navbahor deposit (Uzbekistan).

Research objects and methods: In a four-necked round-bottomed flask with a mechanical stirrer, a reflux condenser, a thermometer and a nitrogen line, 8.1 g of dried potato starch was dispersed in 90 ml of distilled water. After purging with nitrogen for 10 minutes, dissolved oxygen was removed from the solution, the starch solution was heated to 80 °C in a water bath for 30 minutes with stirring to form a starch suspension. The ammonium persulfate initiator was added in amount of 0.5 to 1.5% to the starch suspension and the reaction was continued at 60 °C for 10 minutes. After that, in the process, a mixed solution of acrylamide, acrylic acid, crosslinking agent and mineral ultrafine powder was prepared by mixing acrylamide monomer – 7.1 g, acrylic acid – 3.5 ml, crosslinking agent N, N-methylenebisacrylamide in amount of 0.25 to 1%, distilled water – 30 ml and ultrafine mineral powder of 1 to 5% at room temperature and the reaction mixture is stirred for another 3 hours to ensure that the graft polymerization is completed. The nitrogen atmosphere was maintained throughout the reaction period. The graft copolymer was added to a 3% sodium hydroxide solution and left for the saponification reaction at 95 °C for 2 hours.

The saponified product was filtered and washed several times with distilled water to remove unreacted starting material, the monomer and washing were continued until the basic pH of the solution was equal to 7. The saponified product was dehydrated with methanol and the residual methanol was removed with anhydrous ethanol. The dehydrated sample was dried in vacuum at 60 °C until the weight of the sample

became constant. After grinding and subsequent filtration through a sieve, a powdered superabsorbent composite is obtained.

Results and discussion: IR spectra were used to identify the groups involved in the reaction, the spectra of montmorillonite (a) and SA (b) are shown in (Fig. 1).

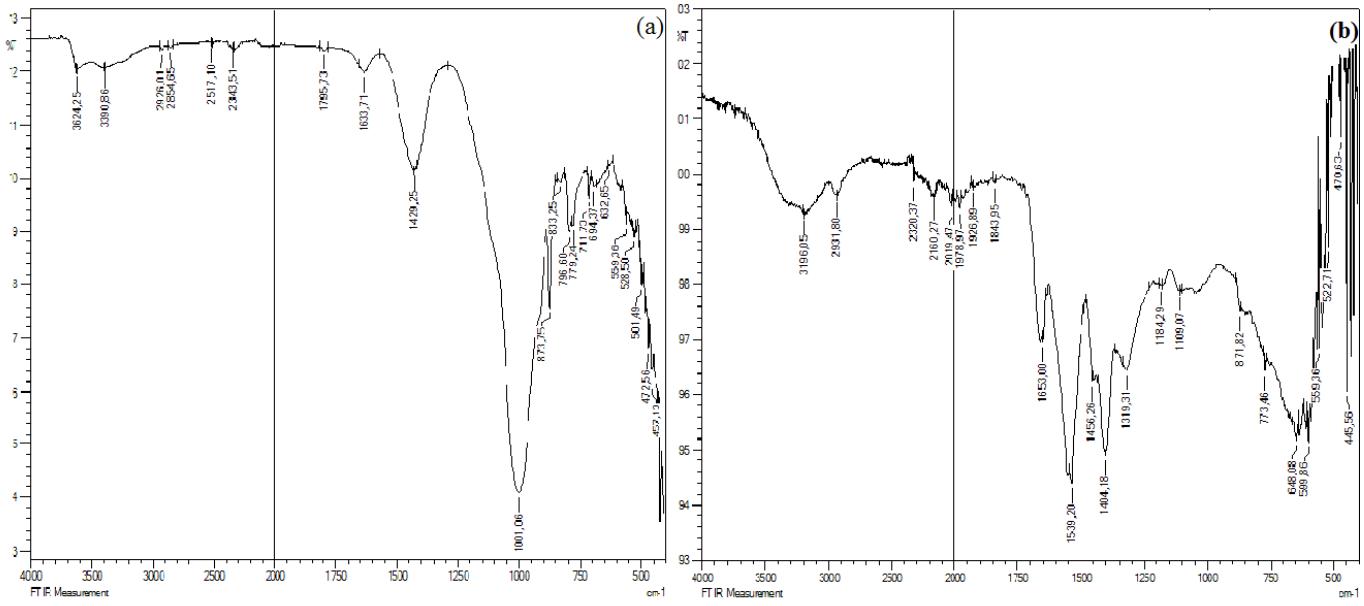

a) b)

Figure 1. Infrared Spectra (a) of montmorillonite, (b) starch/ copolymer based SA (AA-AAc /montmorillonite

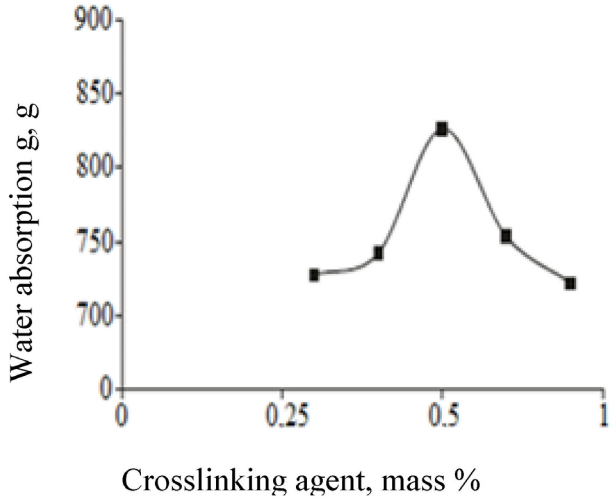

Figure 2. Effect of crosslinking agent concentration on hydrogel swelling

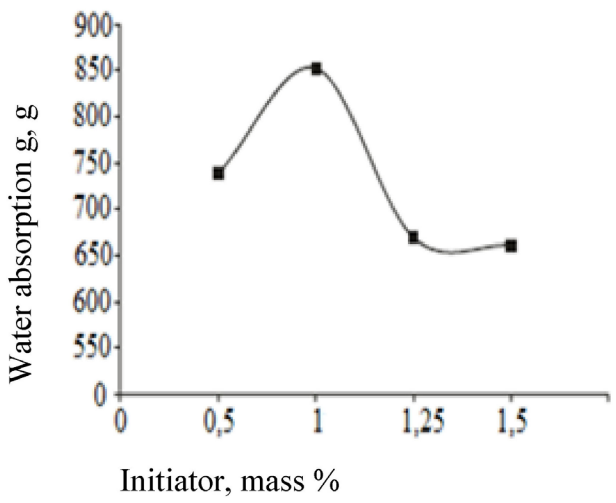

Figure 3. Effect of initiator concentration on hydrogel swelling

IR spectra of corn starch, acrylamide, acrylic acid montmorillonite obtained granulated highly swelling hydrogel were recorded on a Perkin Elmer Spectrum One FTIR using KBr. The IR spectrum of the highly swellable hydrogel shows absorption bands corresponding to the functional groups attached to

the monomeric units. In a layered silicate structure, OH groups can be absorbed at 3624–3390 cm^{-1}. The peak at 1001 cm^{-1}, due to the stretching of Si–O in MT, was not detected in nanocomposite MT hydrogels. The absorption bands in the regions 2931 cm^{-1} correspond to the asymmetric and symmetric stretching of the – CH2 groups. Stretching the –C= = acrylamide group and acrylic acid with a frequency of 1653 cm^{-1} manifests itself in all spectra of hydrogel composites. Absorption bands at 1404 cm^{-1} lead to symmetrical and asymmetric stretching of –COO-acrylate (acrylic acid, neutralized with NaOH).

The (Figure 2 (b)) shows the uniform distribution of the unreacted portions of montmorillonite in the polymer composite.

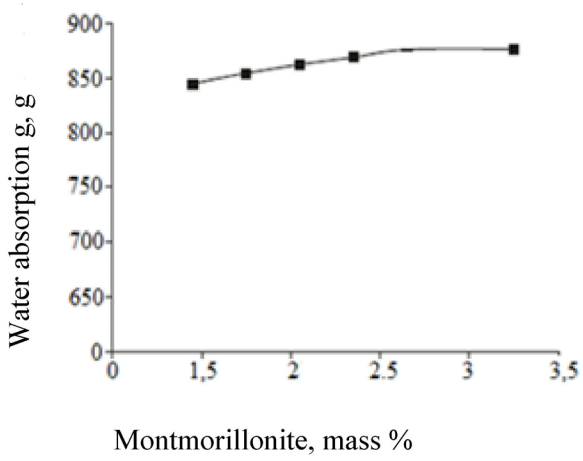

Figure 4. Effect of montmorillonite concentration on hydrogel swelling

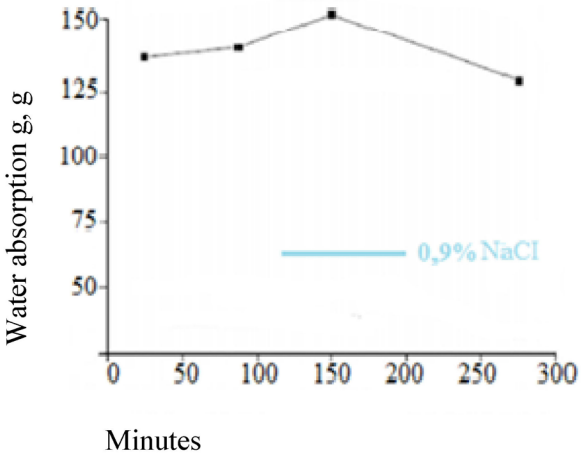

Figure 5. Effect of salt concentration on hydrogel swelling

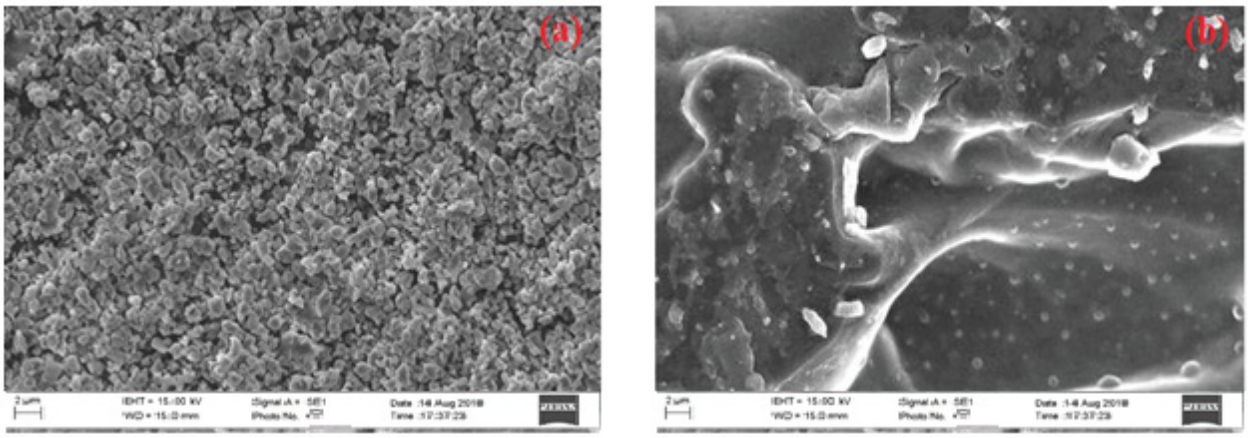

a) b)

Figure 6. SEM image showing surface structures of montmorillonite (a) and a starc /copolymer based SA (AA-AAc) of montmorillonite 3% (b)

Conclusion: In summary, the inclusion of hydrophilic substances containing hydrophilic groups, such as acrylic acid, polymers, such as starch, and clay, such as montmorillonite, in AA hydrogels can be sequentially obtained by a free-radical polymerization method. Multifunctional crosslinkers, such as IBA, were used in the polymerization process. Hydrogel systems based on starch, copolymer (AA-AAc) and montmorillonite showed high water absorption.

References:

1. Kamat M., Malkani R. Disposable diapers: A hygienic alternative. Indian J Pediatr. 2003;70(11):879–81.
2. Kuswandi B., Jayus Restyana A., Abdullah A., Heng L. Y., Ahmad M. A novel colorimetric food package label for fish spoilage based on polyaniline film. Food Control. 2012; 25(1): 184–9.
3. Alsabagh A. M., Abdou M. I., Khalil A. A., Ahmed H. E., Aboulrous A. A. Investigation of some locally water-soluble natural polymers as circulation loss control agents during oil fields drilling. Egypt J Petrol. 2014; 23(1): 27.
4. Chang C., Duan B., Cai J., Zhang L. Superabsorbent hydrogels based on cellulose for smart swelling and controllable delivery. Eur Polym J. 2010; 46(1): 92–100.
5. Tanaka Y., Kuwabara R., Gong J. P., Kurokawa T., Gong J. P., Osada Y. Determination of fracture energy of high strength double network hydrogels. J Phys Chem B. 2005; 109 (23): 11559–62.
6. Wang L., Zhang J. P., Wang A. Q. Removal of methylene blue from aqueous solution using chitosan-g-poly (acrylic acid) montmorillonite superadsorbent nanocomposite. Colloid Surface A. 2008; 322 (1–3): 47–53.
7. Gupta P., Vermani K., Garg S. Hydrogels: from controlled release to pH-responsive drug delivery. Drug Discov Today. 2002; 7(10): 569–79.
8. Холназаров Б. А., Тураев Х. Х., Ширинов Ш. Д., Джалилов А. Т. Исследование нового гидрогеля, синтезированного на основе крахмала, акриламида и бентонита // Universum: технические науки электронный научный журнал (Россия).–№. 4(61). 2019.
9. Ширинов Ш. Д., Джалилов А. Т. Исследование кинетики набухания синтезированных гидрогелей на основе гидролизованного полиакрилонитрила // Universum: химия и биология: электронный научный журнал.

Shermatov Bobomirza Eshbaevich,
Candidate of Technical Sciences, Senior Researcher,
A. Sultanov Uzbek Scientific Research Chemical and Pharmaceutical Institute.
Republic of Uzbekistan, Tashkent.
E-mail: bobomirza@mail.ru

Mansurova Malokhat Sagdullaevna,
Candidate of Chemical Sciences, Senior Researcher,
A. Sultanov Uzbek Scientific Research Chemical and Pharmaceutical Institute.
Republic of Uzbekistan, Tashkent.

Yalgashev Elmurod Yahshshaevich,
Research assistant,
A. Sultanov Uzbek Scientific Research Chemical and Pharmaceutical Institute
Republic of Uzbekistan, Tashkent
E-mail: chemyalgashev@mail.ru

Kurbanov Elmurod Narzullaevich,
Chief engineer OOO Limited liability company Mubarek Gas Processing Plant. Republic of Uzbekistan, Mubarek

Ismatov Dilmurat Nurullaevich,
Doctor of Technical Sciences, Professor,
Tashkent chemical – technological Institute,
Republic of Uzbekistan, Tashkent
E-mail: dilmurod.1958@mail.ru.

REGENERATION OF EXHAUSTED CARBON AT A PILOT PLANT

Abstract. The pilot plant is a rotating tube furnace with external gas heating. Exhausted carbon, in continuous flow enters the rotating tube, where oxidative regeneration with water vapor occurs at a temperature of 400–850 °C. The degree of regeneration of carbon depends on the technological parameters of the process (time, temperature, consumption of water vapor, etc.).

Keywords: exhausted carbon; technology; experienced industrial; camera; activity; coke; recovery; oxidizing agent.

Presently, activated carbons are widely applied in: drinking water and wastewater treatment; treatment of circulating water in enterprises; clarification of sugar syrups; gas cleaning and vapor recovery; medicines; purification of alcoholic water solutions and wines; catalysts and catalyst carriers; the gold industry to extract gold from working solutions. It should have (besides the high specific surface and adsorption capacity) regeneration ability, be capable of utilization and cheap. In the technological process of amine purification of natural gas from sulfur-containing components, high-boiling resinous substances and products

of oxidative decomposition of amines accumulate. High-boiling decomposition products of amines lead to foaming and loss of amine solution. For this reason, to remove resinous substances, amines are passed through columns filled with activated carbon (AG-3, SKT (Russia), HX-30 (China)). Contaminants penetrate the pores of activated carbon and are held there by weak chemical and physical forces and lead to a decrease in activity. Spent sorbents in gas processing (annual volume ~ 150–160 tons) due to the lack of regeneration plants in industrial conditions have not found their reuse in the national economy and is an actual scientific and technical problem. We conducted literary studies on the methods of regeneration of exhausted carbon shows the possibility of restoring activity and selectivity, as well as the economic benefits of the use of regenerated carbon. The existing methods of activated carbon regeneration were divided into 3 groups [1]:

1. Thermal regeneration – is carried out in special furnaces at a temperature of 500–1000 °C in an oxygen-free environment in a stream of inert gas or water vapor. In the process, decomposition of adsorbed substances occurs with the formation of low molecular weight volatile products (CO_2, NH_3, N_2 and NO_x) and the sorption capacity is restored to 100%.

2. Low-temperature thermal regeneration is performed at a temperature of 100–400 °C and is conducted with superheated water vapor directly in the system. Sorption capacity is restored by 25–50%, i.e. regeneration is incomplete.

3. Chemical regeneration – treatment of the sorbent with a gaseous or liquid organic or inorganic reagent at a temperature not exceeding 100 °C. The sorption capacity is restored to 80%, but the desorbate and chemical reagents must be completely recycled.

The process of regeneration of exhausted carbon proceeds in stages. At the beginning, moisture and water mixtures with organic and inorganic compounds are removed, after which intensive heating of the carbon to a predetermined temperature occurs to remove high molecular weight resinous substances.

In summary, the results of the experimental work [2] indicate that the regeneration of exhausted activated carbons using high-temperature treatment in the range of 750–850 °C leads to an effective restoration of the main sorption parameters: specific surface and sorption activity. The degree of restoration of the sorption properties of activated carbons depends on the temperature regime of regeneration: the higher the temperature, the higher the degree of regeneration of the sorption properties. At regeneration temperature of 850 °C, maximum recovery of the surface, pore structure, and sorbent activity is achieved. In the sorption technology for extracting gold and silver, a method is known for restoring the sorption properties of activated carbon by treating with mineral acids and alkaline solutions at elevated temperatures (150–200 °C) [3] and regenerating microwave (microwave) energy in the field of electromagnetic energy [4]. Each developed technology has its advantages and disadvantages.

As a result of many years of research and development, we have developed a new technology that allows restoration the original activity of activated carbons by 97–99%, while retaining all the physical and chemical parameters of sorbents [5]. Thermal-oxidative regeneration of exhausted carbon AG-3, BAU-A (Russia) and HX-30 (China) was carried out at the laboratory and pilot plant of the institute (two-section furnace with external heating) with a continuously moving layer of carbon, in the temperature range 450–800 °C, with the supply of water vapor 0.3–0.6 kg/kg of carbon for 30–55 minutes.

Due to the fact that every year the demand for activated carbon increases for natural gas desulfurization processes, clarification of technological solutions and the need arose to create a larger regeneration unit with a capacity of 500–1000 kg/day.

By studying the technical literature [6] devoted to chemical industry furnaces, a rotary kiln furnace was found and selected, which is a horizontal or slightly inclined drum, during rotation of which the material moves and provides high performance, continuous

operation and a simple design for the complete regeneration process. Therefore, the calculated length of the furnace is 9.5 m, diameter 0.319 m, capacity 20–50 kg/hour; the rotational speed of the furnace is 2–3 rpm, the furnace inclination is 2–5% to the length. The process of regeneration of waste carbon is carried out at a temperature of 450–8500 °C. The time of raw materials decomposition – 25–90 minutes. To implement this technology, a pilot industrial installation was designed and installed at OOO (Limited liability company) Mubarek Gas Processing Plant. Technical parameters are given in (table 1).

Table 1. – Technical parameters of the plant

№	Parameter name	Unit of measurement	Value
1.	Pipe length	m	9.5
2.	Inner diameter	mm	419.0
3.	Heat exchange area	m^2	12.5–13.0
4.	Pipe rotation frequency	rpm	4–15
5.	Number of heating zones	units	2
6.	The amount of gas supplied to the combustion	m^3/hour	10–15
7.	Chamber I temperature	°C	200–400
8.	Chamber II temperature	°C	450–850
9.	Type of heating		Gas
10.	Heating temperature control		TC

The machine is a rotating tubular furnace with external gas heating. The location of the burners and the regulation of the volume of gas supplied to the combustion allowing setting the desired temperature in two chambers. Exhausted carbon, poured into the hopper, auger feeder, driven by an electric motor, in a continuous stream enters the rotating tube, where it is regenerated.

In the first chamber, at a temperature of 200–400 °C, moisture removal and thermal desorption of strongly adsorbed substances mainly occurs. With further movement of activated carbon enters the 2nd zone of the furnace, heated to 850 °C. Heated water vapor at a rate of 0.1–0.6 kg/kg of carbon is fed into this zone through the lower part of the pipe. When water vapor interacts with residual organic impurities, oxidation and burnout occur with the formation of carbon dioxide and water.

Regenerated activated carbon enters the bunker, equipped with a water jacket, where it is cooled. From the bunker, activated carbon enters the vibrating screen for screening out dust particles, then it is packed in bags or iron barrels. Under these conditions, the degree of regeneration was 97.0–99.5%. Generating emissions from regeneration products are flared.

The optimal indicators of the technological parameters of the regeneration process of spent activated carbons AG-3, BAU-A and HX-30 are shown in (Table 2).

Table 2. – Technological parameters of the regeneration of exhausted AG-3, BAU-A and HX-30 carbon

Parameters of process	AG-3	BAU-A	HX-30
1	*2*	*3*	*4*
Temperature, °C Zone 1 Zone 2	 450 800	 450 800	 450 800
Water vapor consumption, kg/kg of carbon	0.3–0.6	0.1–0.3	0.2–0.5

1	*2*	*3*	*4*
Carbon speed, cm/min	7.0–11.5	15.5–25.6	12.5–15.5
Regeneration time, min.	30–55	15–25	25–35
Regeneration degree,%	97.0–98.5	98.2–99.0	98.5–99.5

As can be seen from the data of (Table 2) to achieve the degree of regeneration up to 97–98% for different carbons, the consumption of water vapor, the regeneration time is different.

To determine the degree of reduction or activity, a comparative test of fresh, exhausted and regenerated carbon was conducted on a dynamic unit. Test conditions: the height of the catbon loaded layer is 10 cm, the concentration of benzene in the vapor-air mixture is 30 mg/l, the linear velocity is 0.2 m/s, the adsorption temperature is 250 °C. The physicochemical characteristics and activities of the regenerated, exhausted and fresh activated carbon AG-3 have been comparatively studied. The test results are given in (Table 3).

Table 3-Physico-chemical parameters and activity of benzene
AG-3 fresh, exhausted and regenerated carbon

Parameters	**AG-3 fresh carbon**	**AG-3 exhausted carbon**	**AG-3 regenerated carbon**
Bulk density, g/dm ^{3}	550–552	565–568	550–554
Total pore volume by water absorption, cm^3/g	0.8–1.0	0.3–0.5	0.8–0.9
Specific surface, m^2/g	900–1100	300–400	900–950
Iodine activity,%	40–41	15–18	38–40
Dynamic benzene activity, g/dm^3	105.1–106.0	35.5–36.0	102.5–104.5
Benzene equilibrium activity, g/dm^3	126.5–127.0	48.4–50.0	122.7–124.5

AG-3 regenerated carbon according to its physicochemical characteristics, i.e. durability, activity is not inferior to fresh carbon, which allows us to recommend their reuse in this production. The cost of regenerated carbon produced by the thermo-oxidative method is 2–2.5 times cheaper than the cost of fresh carbon. The introduction of a pilot plant in the industry for the regeneration of exhausted carbon, shows a high degree of recovery of activity and selectivity, as well as the economic benefits of the use of regenerated carbon.

References:

1. Кузубова Л. И. Морозов С. В. Очистка нефтсодержащих сточных вод: аналит.обзор/СО РАН ГПНТБ, НИОХ.– Новосибирск, 1992.– 72 с.
2. Калашникова Л. И., Калашникова А. А., Привалова Н. М., Процай А. А. Метод восстановления активности сорбентов // Современные наукоемкие технологии. 2007.– № 1.– С. 62–63.
3. Барченков И. И. Как восстановить сорбционные свойства активированного угля / Золотодобыча, – № 221, Апрель, 2017.
4. Патент RU. № 2109828, 1998. //Способ регенерации активированных углей. Елшин В. В., Леонов С. Б., Голодков., Коновалов Н. П., Решенко.
5. Шерматов Б. Э., Мансурова М. С., Ялгашев Э. Я., Курбонов Э. Н., Исматов Д. Н. Термоокислительной регенерации отработанных углей // Журнал Наука среды нас., 3(7). 2018.– С. 76–82.
6. Исламов Ш. М. Пуск и наладка печей химических заводов. Изд-ва Химия,– Л. 1980.

Eshmuratov Bakhodir Beshimovich,
cand. tech. sciences, Tashkent Scientific Research Institute
of Chemical Technology of the Republic of Uzbekistan, Tashkent
E-mail: bbeshmuratov@mail.ru

Karimov Masud Ubaydulla ugli,
doc. tech. sciences, Tashkent Scientific Research Institute
of Chemical Technology of the Republic of Uzbekistan, Tashkent
E-mail: adler_219@mail.ru

Jalilov Abdulakhat Turapovich,
academician, doc. chem. Sciences, prof.,
Tashkent Scientific Research Institute of Chemical Technology
of the Republic of Uzbekistan, Tashkent
E-mail: a.t.djalilov@mail.ru

SYNTHESIS AND STUDY OF DEMULSIFIERS BASED ON POLYCARBOXYLATE ETHERS

Abstract. The article presents the relevance of the use of demulsifiers in oil production. The results of studies of the obtained demulsifier using IR spectroscopy are shown, and the results of the study of the kinetics of the approximate and refined effective dosage of the demulsifier DE-1 in different fields are presented.

Keywords: demulsifier, IR spectroscopy, approximate and refined effective, polycarboxylate ethers.

Demulsification is the destruction of the emulsion in the oil and water phases. From a technological point of view, oil producers are interested in two aspects of de-emulsification: the speed at which destruction occurs and the amount of water remaining in the crude oil after preparation. Extracted oil should usually comply with the specifications of the company and pipeline transport; therefore, the oil is desalted and dehydrated beforehand in the oil fields. A low content of water and chlorides in the oil is required to reduce the corrosive effects and salt deposits. At refineries, the main task is to remove inorganic salts (mainly chloride) from crude oil before they cause corrosion or other harmful effects on refining equipment. When this salt is removed from the crude oil by washing with fresh water on the ELOU.

Extracted oil emulsions have a degree of kinetic stability due to the formation of interfacial films surrounding water droplets. In order to separate the emulsion into oil and water, the interfacial film must be destroyed, resulting in coalescence of the droplets and separation of the aqueous phase. Therefore, the destabilization of emulsions is very closely related to the destruction of this interfacial film. Factors affecting the phase boundary and, consequently, the stability of emulsions were discussed earlier (the dispersive properties of formation water and oil, water content, natural emulsifiers, particulate matter, etc.) [1–6].

We obtained polycarboxylate ethers based on polyacrylonitrile.

After processing of polyacrylonitrile with sulfuric acid and ethyl alcohol, followed by neutralization, some changes in the structure of the raw materials are manifested. These changes can be seen in the IR spectrum of (Fig. 1).

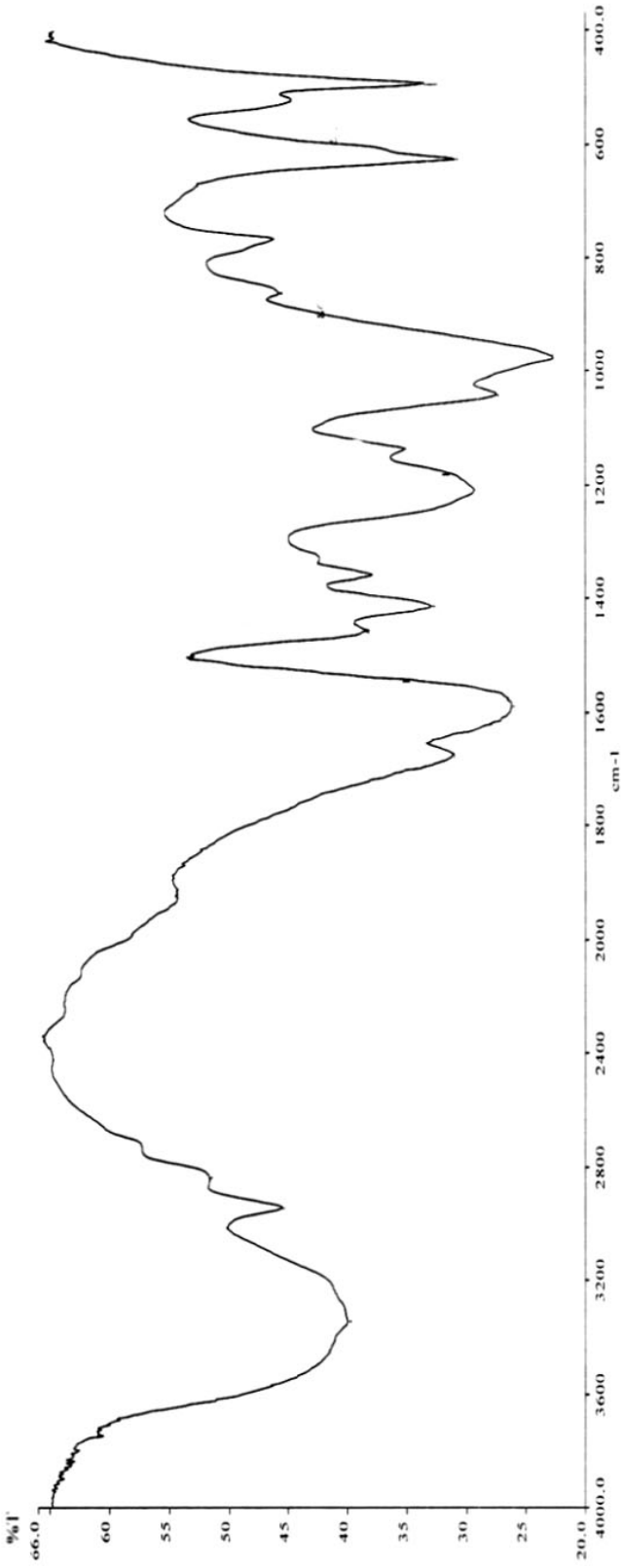

Figure 1. IR – spectrum of the synthesized demulsifier

After processing, the absorption bands in the region of 3000–3200 cm^{-1} disappeared and new absorption bands appeared in the region of 3346 cm^{-1}. This shows that the functional group – $CONH_2$ has changed its structure to – CONH-chemical bonds. This shows that the absorption bands are asymmetric to the valence vibrations in the region of 1150––1260 cm^{-1}, and the absorption bands characteristic of symmetric stretching vibrations manifest themselves in the region of 1010–1080 cm^{-1}.

Used glue, as a raw material for the production of the demulsifier, has in its structure hydrophilic (– COONa,– $COOC_2H_5$ -$CONH_2$) and -C – C chemical bonds.

In (tab. 1–4) shows the results of the study of the kinetics of water excretion of the tested demulsifiers in the conditions of the field Toshli. The analysis of laboratory studies showed that the oil field selected from the well and the gas-measuring unit is homogeneous: it is similar in chemical composition and properties to paraffin type (average 3.7% wt.), High resin (average 19% wt.) according to the sulfur content – high-sulphurous, according to chloride salts and mechanical impurities belong to the third group.

According to the test results (Table 1), it can be seen that when introduced into the initial water-oil emulsion in the amount of 240 g/t, there is no negative effect on the preparation process, dehydration and desalting of oil: the degree of dehydration is 60.11%, and the residual content of chloride salts 2.51 g/l.

The results of the study (Table 2) show that the demulsifier, when introduced into the oil-water emulsion, shows a high demulsifying ability. With a maximum specific consumption of 300 g/t, the degree of dehydration is 29.32%, the residual water content in oil is 70.68%. The content of chloride salts in oil decreased from 5.94 to 3.39 g/l. When a demulsifier is introduced into the water-oil emulsion, the released water does not become cloudy, there is no clear phase interface, adhesion to the tube walls is present, there is no intermediate layer, no precipitate forms.

Table 1.– The results of the study of the kinetics of the approximate and refined effective dosage of the obtained demulsifier at a test temperature of 90 °C for Western Toshli oil

№	Product	Dosage, g / t	The amount of released water,% Time, min											The degree of dehydration,%	Residual water content,%	Content of chloride salts, mg/l
			5	10	15	20	30	40	50	60	75	90	12			
Estimated efficiency, the value of bound water – 44.6%																
1.	Blank test	0	0.00	0.00	0.00	0.00	0.00	0.41	0.82	0.82	1.64	3.28	4.10	9.19	90.81	8090.9
2.	obtained demulsifier	150	0.00	2.34	11.69	17.14	21.03	21.81	22.59	23.37	24.93	25.71	25.71	57.64	42.36	2625.99
3.	obtained demulsifier	200	0.00	3.71	11.12	16.30	21.49	21.49	22.23	22.97	23.71	24.45	24.45	54.83	45.17	2827.49
4.	obtained demulsifier	240	0.00	2.37	11.83	19.71	23.66	25.23	26.02	26.02	26.81	26.81	26.81	60.11	39.89	2314.87
5.	obtained demulsifier	300	0.00	3.04	12.92	18.24	21.28	23.56	24.32	25.08	25.84	25.84	25.84	57.94	42.06	2515.70
Estimated efficiency, the value of bound water – 42%																
1.	Blank test	0	0.00	0.00	0.00	0.00	0.00	0.80	0.80	0.80	1.20	1.60	2.40	5.71	94.29	13045.9
2.	obtained demulsifier	220	0	7.60	12.92	15.20	18.24	20.52	21.28	21.28	21.28	22.04	22.80	54.29	45.71	12393.61
3.	obtained demulsifier	260	0	7.79	13.24	16.36	19.48	21.03	21.81	22.59	23.37	23.37	23.76	56.57	43.43	6003.15

Table 2.– The results of the study of the kinetics of the estimated effective dosage of the obtained demulsifier at a test temperature of 90 °C for East Tashli oil (the value of bound water is 55.6%)

№	Product	Dosage, g/t	The amount of released water,% Time, min											The degree of dehydration,%	Residual water content,%	Content of chloride salts, mg/l
			5	10	15	20	30	40	50	60	75	90	120			
1.	Blank test	0	0.00	0.00	0.00	0.00	0.00	0.00	0.00	0.00	0.00	0.80	3.20	5.76	94.24	5940.9
2.	obtained demulsifier	150	0.00	0.00	0.08	1.52	4.56	6.84	7.60	9.88	12.16	14.44	17.48	31.44	68.56	3033.83
3.	obtained demulsifier	200	0.00	0.00	0.08	3.75	6.75	9.01	9.76	12.01	13.51	14.26	17.26	31.05	68.95	3106.12
4.	obtained demulsifier	240	0.00	0.00	0.08	5.32	9.12	11.40	14.44	15.20	17.48	19.76	22.04	39.64	60.36	2458.03
5.	obtained demulsifier	300	0.00	0.00	0.15	5.48	7.56	10.08	11.64	12.23	13.49	15.11	16.30	29.32	70.68	3387.70

Table 3. – Results of the study of the kinetics of the approximate and refined effective dosage of the obtained demulsifier at a test temperature of 90 °C for northern shurtan oil

№	Product	Dosage, g/t	The amount of released water,%											The degree of dehydration,%	Residual water content,%	Content of chloride salts, mg/l
			Time, min													
			5	10	15	20	30	40	50	60	75	90	120			
Estimated efficiency, the value of bound water – 54%																
1.	Blank test	0	0.00	0.00	0.00	0.00	0.00	0.00	0.00	0.00	0.80	1.60	2.40	4.44	95.56	7118.3
2.	obtained demulsifier	150	0.00	0.00	2.19	5.85	8.05	17.56	23.41	26.33	28.53	29.26	29.99	67.25	32.75	2133.32
3.	obtained demulsifier	200	0.00	0.00	3.00	7.51	18.01	24.77	28.52	29.27	30.02	30.77	30.77	68.99	31.01	2034.24
4.	obtained demulsifier	240	0.00	0.00	2.22	7.41	12.60	25.19	28.16	28.90	29.64	30.38	31.12	69.78	30.22	1994.81
5.	obtained demulsifier	300	0.00	0.00	2.34	9.35	21.03	27.27	28.82	30.38	31.94	32.72	32.72	73.36	26.64	1936.86
Estimated efficiency, the value of bound water – 42%																
1.	Blank test	0	0.00	0.00	0.00	0.00	0.00	0.80	0.80	0.80	1.20	1.60	2.40	5.71	94.29	5940.9
2.	obtained demulsifier	220	0.00	6.84	10.64	12.92	15.20	18.24	19.00	19.76	20.52	20.52	21.28	50.67	49.33	2014.67
3.	obtained demulsifier	260	0.00	6.23	9.35	13.24	15.58	17.92	18.70	20.25	20.25	21.03	21.03	50.08	49.92	2639.58

Table 4. – The results of the study of the kinetics of the approximate and refined effective dosage of the demulsifier DE-1 at a test temperature of 90 °C for the North Pamuk oil

№	Product	Dosage, g/t	The amount of released water,%											The degree of dehydration,%	Residual water content,%	Content of chloride salts, mg/l
			Time, min													
			5	10	15	20	30	40	50	60	75	90	120			
1	*2*	*3*	*4*	*5*	*6*	*7*	*8*	*9*	*10*	*11*	*12*	*13*	*14*	*15*	*16*	*17*
Estimated efficiency, the value of bound water – 44%																
1.	Blank test	0	0.00	0.00	0.16	2.40	3.20	4.00	4.80	4.80	5.60	6.40	7.20	16.36	83.64	6749.2
2.	obtained demulsifier	150	0.08	4.50	8.26	11.26	14.26	20.26	21.76	24.02	24.77	24.77	24.77	56.29	43.71	2334.15
3.	obtained demulsifier	200	0.00	2.34	5.45	9.35	13.24	19.48	21.03	23.37	23.37	24.15	24.93	56.65	43.35	2248.65
4.	obtained demulsifier	240	0.15	3.80	6.84	9.88	14.44	17.48	20.52	22.80	23.56	24.32	25.08	57.00	43.00	1054.22
5.	obtained demulsifier	300	0.04	3.12	7.01	10.91	16.36	22.59	25.71	26.49	27.27	27.27	28.04	63.74	36.26	688.75

1	*2*	*3*	*4*	*5*	*6*	*7*	*8*	*9*	*10*	*11*	*12*	*13*	*14*	*15*	*16*	*17*
Estimated efficiency, the value of bound water – 42%																
1.	obtained demulsifier	0	0.00	0.00	0.00	0.00	0.00	0.80	0.80	0.80	1.20	1.60	2.40	5.71	94.29	5940.9
2.	obtained demulsifier	220	0.00	6.84	12.92	15.96	19.76	21.28	22.04	22.80	22.80	22.80	22.80	54.29	45.71	1478.39
3.	obtained demulsifier	260	0.00	7.79	13.24	15.58	20.25	22.59	22.59	23.37	24.15	24.15	24.15	57.50	42.50	1038.73

As a result, the efficiency evaluation from the obtained demulsifier line was continued to clarify the optimal effective dosage.

With the introduction of obtained demulsifier (tab. 3) at a dose of 240 and 300 g/t to the oil emulsion, a decrease in the chloride salts content (from 7.12 to 1.94 g/t

l) more than three times is observed. The degree of dehydration reaches a maximum value at 300 g/t and is 73.36%, while the same effect is achieved when using 240 g/t of base reagent. Commercial (separated) water does not grow cloudy, there is a clear phase boundary, there is no intermediate layer, no precipitate is formed and adhesion to the walls of the tube is not established.

The results of the obtained demulsifier, are presented in (table 4) show that with the introduction of it into the oil-water emulsion, a significant decrease in chloride salts to 0.69 g/l is observed. With other things being equal, the obtained demulsifier compared to two other obtained demulsifiers from the same line) at a dosage of 300 g/t is more effective, the degree of dehydration reaches a maximum value of 63.74%. Compared to the base, the demulsifier does not provide sufficiently good dehydration at a specific consumption of 240 g/t.

With the introduction of the demulsifier into the water-oil emulsion, the released water does not become cloudy, there is a clear phase boundary, there is no intermediate layer, adhesion to the walls of the tube is not formed, but visually present in a small amount of sediment.

Thus, it was established that when preparing Western Toshli and Toshli oil, the consumption rate of the developed demulsifier is 2–1.5 times less than for the known and amounts to 5 and 10 g/t of oil, respectively. It is noted that the rate of separation of water-oil emulsion when using a new demulsifier is higher.

References:

1. Kasparyants K. S. Oil field preparation / K. S. Kasparyants.– M.: Nedra, 1973.– 376 p.
2. Levchenko D. N. Oil emulsions with water and methods for their destruction / D. N. Levchenko, N. V. Bergstein, A. D. Khudyakova, N. M. Nikolaev.– M.: Chemistry, 1967.– 200 p.
3. Pozdnyshev G. N. Stabilization and destruction of oil emulsions / G. N. Pozdnyshev.– M.: Nedra, 1982.– 224 p.
4. Dehydration and desalting of oil: Chemical encyclopedia / F. M. Khutoryansky.– M.: Scientific. ed. Great Russian Encyclopedia.– V. 3. 1992.– P. 608–610.
5. Levchenko D. N. Oil desalting technology at oil refineries / D. N. Levchenko, N. V. Bergstein, N. M. Nikolaev.– M.: Chemistry, 1985.– 168 p.
6. Khutoryansky F. M. A comprehensive program for the preparation of oil and chemical-technological corrosion protection of condensation-refrigeration equipment of primary oil refining plants / F. M. Khutoryansky and others // World of petroleum products.– M. 2002.– No. 3.– P. 17–22.

Section 5. Power industry

Pham Hoang Nam,
Tran Dinh Dung,
Doan Van Phuc Uoc,
Vinh University, Vietnam
E-mail: namph@vinhuni.edu.vn, dungtd@vinhuni.edu.vn;
doanuoc1751999@gmail.com

BUILDING THE PRACTICE MODEL OF POWER SUPPLY FOR AN APARTMENT

Abstract. It can be seen that the more modern life is indispensable to the presence of electrical and electronic devices. These devices are ubiquitous and serve all human interests, from living to production. Therefore, Electrical Engineering (Electrical and Electronic Engineering) is always an important discipline in the field of engineering. In this report, we introduce our study on the construction of a practical power supply model for an apartment. The research results are used to develop practical exercises for the "Power supply practice", to serve the training and improvement the quality of practice for students; To help students access to reality as well as improve suitable skills that the recruitment market demands.

Keywords: Power supply, Electrical system for buildings, civil electric circuits.

1. Introduction

In the training of Electrical and Electronic Engineering Technology, the practice of supplying electricity to buildings plays a very important role, it not only plays a role in forming career skills but also helps students apply their knowledge and skills in everyday life. The subject of practical power supply will equip the students with basic knowledge- and hone the necessary skills in civil and industrial electrical installation. Studying an applicable subject, students can solve practical problems by themselves, which is essential for any worker or technical staff working in electricity industry. These skills include repairing, installing electric houses, installing automatic water pumping circuits, and at a more advanced level, students can operate, control modern distribution cabinets, automatic low voltage compensation cabinets. Students will be completely confident when approaching reality.

Currently, to meet the practical needs of power supply for a building, there have been many models available by domestic and foreign facilities. The models designed specifically for the practical installation of electrical systems in civil will train students with the following skills: Cable twisting skills; Pipe bending skills; Pipe coupling skill with wiring box; Skills of installing common electrical equipment.

However, these models still have many shortcomings. Despite using practical electrical equipment, these models have only applicable on principle diagrams; practical devices mounted on flat shelves, there have been no specific apartment models to

simulate apartments in reality, thus not ensuring the visual properties.

In order to overcome this, we have carried out research and built a practical model of power supply for an apartment. This model is built in accordance with the design drawings to supply enough electricity for an apartment, with the size being wide enough for easy operation and installation of electrial wires thus ensuring the visual properties. In particular, this apartment model is constructed from small blocks so we can practice electricity supply with many different apartment models.

2. Fabrication and practice on power supply practice models

2.1. Power supply premises for apartments

We manufacture the power supply practice set as follows:

Figure 1 Describes the premises of the apartment and designs the power supply for the apartment. The apartment has an area of 80 m^2, including: 02 bedrooms, 01 living room, 01 kitchen, and 02 bathrooms. Power supply requirements are as follows: power supply for lighting, sockets, water heater, air conditioning, etc.

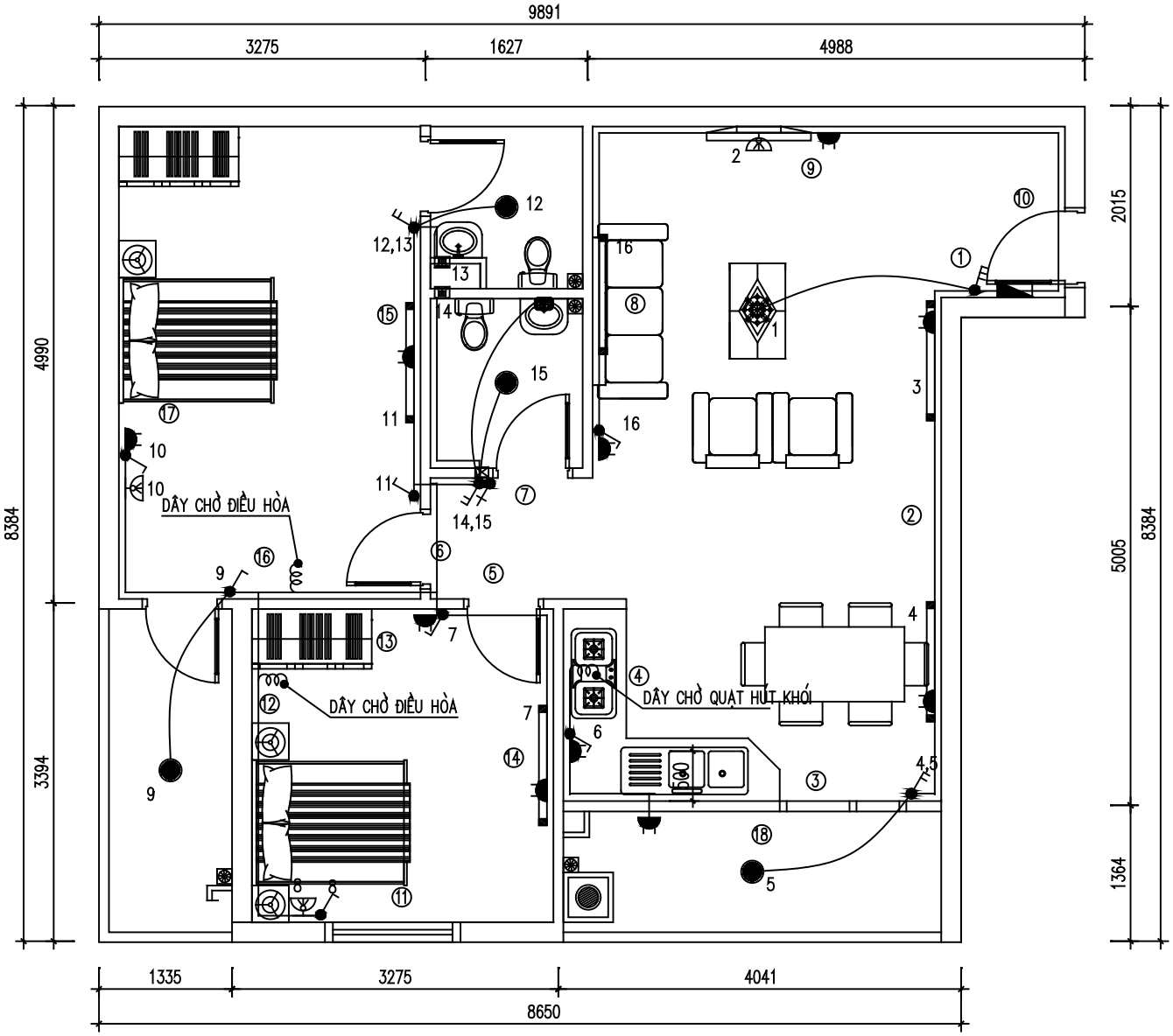

Figure 1. Power supply premises for apartments

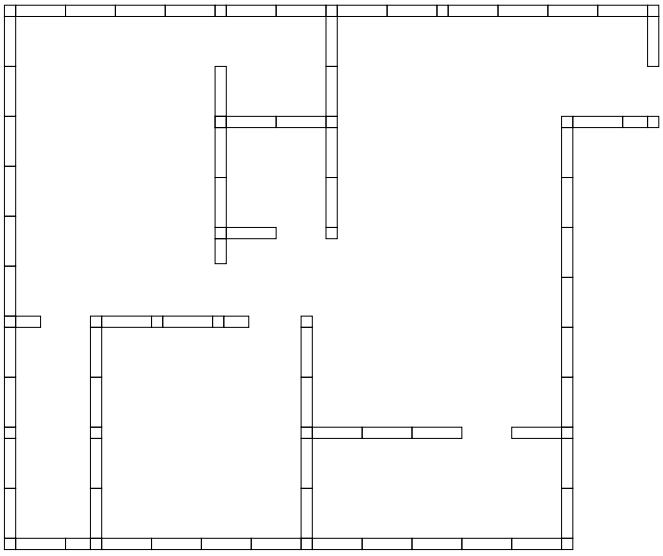

Figure 2. Flat design apartment

2.2. Design of apartment model

Figure 2 Description of the design of the blocks are made of 12 mm- thick-MDF boards and blocks with holes to catch threaded companies (Figure 3).

Figure 3. MDF board, ty lace and bolt 8 mm

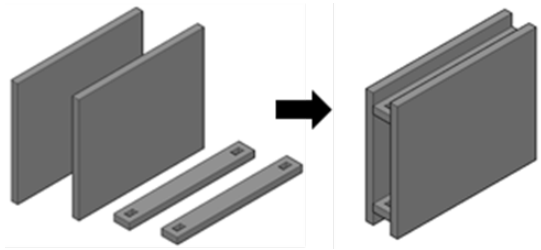

Figure 4. Block structure details 200 mm × 240 mm

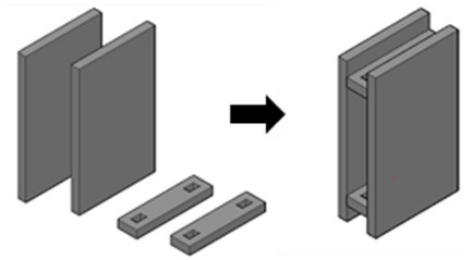

Figure 5. Detail of block structure 200 mm × 120 mm

Three main composite blocks are as follows: 200 mm × 240 mm (Figure 4), 200 mm × 54 mm (Figure 5), 200 mm × 120 mm (Figure 6).

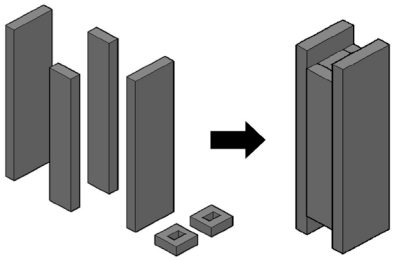

Figure 6. Details of block structure 200 mm × 54 mm

The upper blocks are slotted and the soles are installed to install the power (Figure 7):

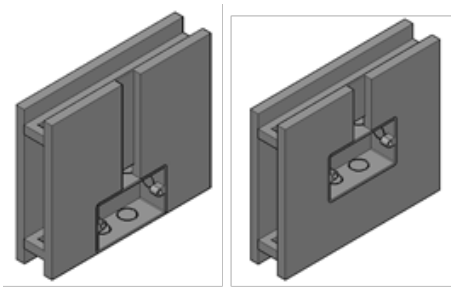

Figure 7. Block structure details contain negative bases

In addition, there are paired models to link blocks (Figure 8), small blocks of 200 mm × 54 mm fitted with right angles (Figure 9), small blocks of 200 mm × × 54 mm fitted with T-shaped blocks (Figure 10).

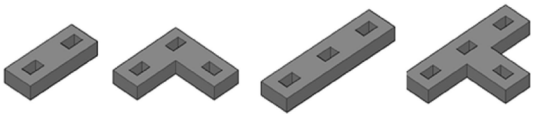

Figure 8. The detailed construction of the pairing patterns

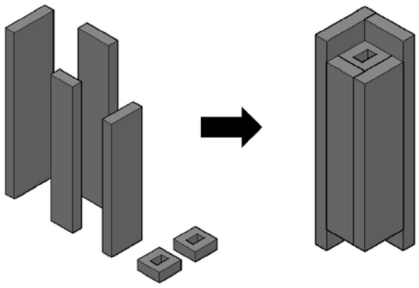

Figure 9. Detailed structure of two perpendicular blocks

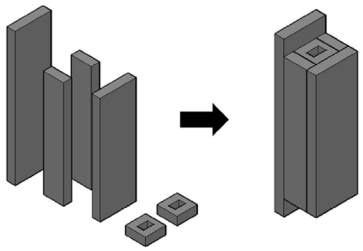

Figure 10. Details for placing two T-shaped blocks

2.3. Installation of the apartment model

Apartment installed from small blocks (Figure 11, Figure 12, Figure 13) consist of three floors; to install the apartment, we install each apartment floor one by one (Figure 14). The height of the apartment after installation is 600 mm. With this height, students can easily move inside the apartment to perform the installation of electrical systems for the apartment.

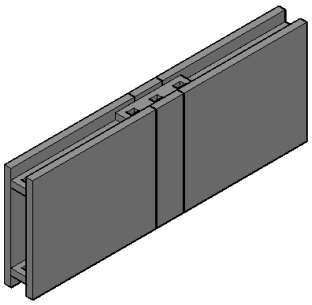

Figure 11. Detail of two straight blocks

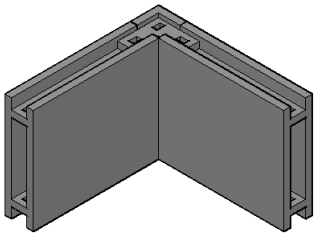

Figure 12. Details of placing two perpendicular blocks

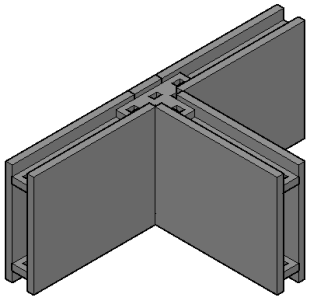

Figure 13. Details of placing two T-blocks

2.4. Practical installation of apartment electrical systems

Figure 14 Pictures of students performing the installation of electrical systems for the apartment model.

3. Conclusions

We have successfully built practical power supply models for apartments. This practical model helps students to install and run an electrical system for an apartment well and thorougly as in practice. With models made up of small blocks, we can install different models of apartments every year for students to practice. Experiments show that through practice on this model, students will be more confident in installing electrical systems for actual apartments.

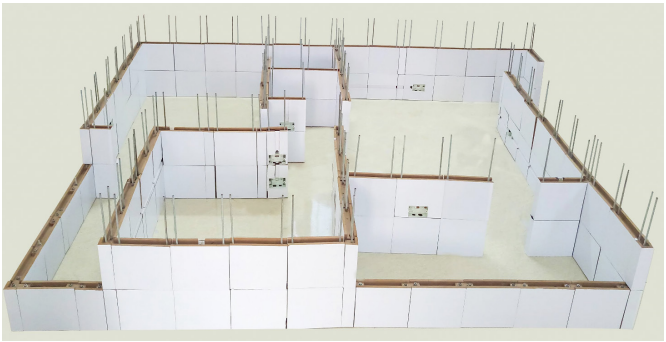

Figure 14. Installation of the second floor of the apartment model

References:

1. Nguyen Xuan Phu, Nguyen Cong Hien, Nguyen Boi Khue. Electricity Supply, Science and Technology Publishing, Hanoi (2005).
2. Ngo Hong Quang, Vu Van Tam. Electrical design, Scientific and technical publishing, Hanoi (2003).
3. Nguyen Cong Hien, Nguyen Manh Hoach. Power supply system of urban industrial enterprises and high-rise buildings, Science and Technology Publishing, Hanoi (2005).

4. Phan Thi Thanh Binh and other authors. Electrical installation guide According to IEC international standards, Science and Technology Publishing, Hanoi (2009).
5. Tran Quang Khanh. Power Supply Curriculum, Educational Publisher, (2010).

Contents